REDOX-PHOTOSENSITIZED REACTIONS OF AN NAD^+/NADH MODEL AND RELATED COMPOUNDS BY Ru(II) AND Re(I) 2,2′-BIPYRIDINE COMPLEXES

1987

OSAMU ISHITANI

REDOX-PHOTOSENSITIZED REACTIONS OF AN NAD^+/NADH MODEL AND RELATED COMPOUNDS BY Ru(II) AND Re(I) 2,2′-BIPYRIDINE COMPLEXES

(Ru(Ⅱ)およびRe(Ⅰ)2,2′-ビピリジン錯体による
NAD^+/NADHモデル化合物の
レドックス光増感反応)

1987

OSAMU ISHITANI

PREFACE

The work presented in this thesis has been carried out under guidance of Professor Setuo Takamuku at Osaka University during 1982-1987.

Osamu Ishitani

Department of Chemical Process Engineering
Faculty of Engineering
Osaka University
Yamada-oka, Suita,
Osaka 565,
Japan

January, 1987

LIST OF PUBLICATIONS

(1) Formation of a Novel Type of Adduct between an NADH Model and Carbonyl Compounds by Photosensitization Using $Ru(bpy)_3^{2+}$

Ishitani, O.; Pac, C.; Sakurai, H. J. Org. Chem. **1983**, 48, 2941.

(2) Redox-Photosensitized Reactions. 11. $Ru(bpy)_3^{2+}$-Photosensitized Reactions of 1-Benzyl-1,4-dihydronicotinamide with Aryl-Substituted Enones, Derivatives of Methyl Cinnamate, and Substituted Cinnamonitriles: Electron-Transfer Mechanism and Structure-Reactivity Relationships

Pac, C.; Miyauchi, Y.; Ishitani, O.; Ihama, M.; Yasuda, M.; Sakurai, H. J. Org. Chem.,**1984**, 49, 26.

(3) Redox-Photosensitised Reductions. Part 12. Effects of Magnesium(II) Ion on the $[Ru(bpy)_3]^{2+}$-Photomediated Reduction of Olefins by 1-Benzyl-1,4-dihydronicotinamide: Metal-ion Catalysis of Electron Transfer Processes Involving an NADH Model.

Ishitani, O.; Ihama, M.; Miyauchi, Y.; Pac, C. J. Chem. Soc., Perkin Trans. I, **1985**, 1525.

(4) Redox-Photosensitized Reactions. 13. $Ru(bpy)_3^{2+}$-Photosensitized Reactions of an NADH Model, 1-Benzyl-1,4-dihydronicotinamide with Aromatic Carbonyl Compounds and Conparison with Thermal Reactions.

Ishitani, O.; Yanagida, S.; Takamuku, S.; Pac, C. J. Org. Chem. in contribution.

(5) Redox-Photosensitized Reactions. XIV. Photochemistry of 4-Alkylated NADH Models,1-benzyl-4-(1-hydroxyalkyl)-1,4-dihydronicotinamides

Ishitani, O.; Yanagida, S.; Takamuku, S.; Pac, C. Bull. Chem. Soc. Jpn. in press.

(6) Redox-Photosensitized Reactions. XV. Photosensitized and Direct Photolytic Isomerizations of the Tetrahydro Dimers of 1-Benzylnicotinamide.

Ishitani, O.; Yanagida, S.; Takamuku, S.; Pac, C. Bull. Chem. Soc. Jpn. in contribution.

(7) Photochemistry of $Ru(bpy)_3^{2+}$ and Their Derivatives in the Presence of Aliphatic Amines.

Ishitani, O.; Takada, K.-I.; Wada, Y.; Yanagida, S.; Takamuku, S.; Pac, C. in preparation.

(8) Photochemistry of fac-$Re(bpy)(CO)_3Br$ with Triethylamine.

Ishitani, O.; Namura, I.; Yanagida, S.; Takamuku, S.; Pac, C. in preparation.

List of Supplementary Papers

(1) $Ru(bpy)_3^{2+}$-Photosensitized Reduction of an NAD^+ Model by Amines - A Mechanism Involving a Non-Emissive Excited State

Pac, C.; Wada, Y.; Ishitani, O.; Sakurai, H. Proc. The Fifth International Conference on Photochemical Conversion and Storage of Solar Energy, Osaka, **1984**, p. 308.

(2) Mechanistic Significance of Ligand Substitution in $Ru(bpy)_3^{2+}$-Photosensitized Reduction of NAD^+ Model by Triethylamine

Ishitani, O.; Wada, Y.; Takada, K.-I.; Pac, C.; Sakurai, H. Proc. XIIth International Conference on Photochemistry, Tokyo, **1985**, p. 301.

(3) Visible-Light Induced Reduction of Water and Carbonyl Compounds by the Use of Poly(p-phenylene) as Photocatalyst

Yanagida, S.; Ishitani, O.; Kabumoto, A.; Shibata, T.; Pac, C. The Sixth Inter-national Conference on Photocchemical Conversion and Strage of Solar Energy, Paris, **1986**, p. C-35.

(4) Photochemical Formation of a Catalyst for a Novel Type of Reaction of an NAD^+ Model from $Ru(bpy)_3^{2+}$ and Triethylamine

Ishitani, O.; Takada, K.-I.; Yanagida, S.; Pac, C. XI IUPAC Symposium on Photochemistry, Lisboa, **1986**, p. 396.

CONTENTS

GENERAL INTRODUCTION

Photosynthesis is the only way to achieve chemical conversion and storage of solar energy in nature through the following essential process; (1) the photosensitized process accuring in the reaction center, (2) electron transfer from the water-oxidation site to the $NADP^+$-reduction site, (3) ATP synthesis during the electron transfer in the photosynthetic membrance, and (4) multi-electron redox processes for both the water oxidation and the $NADP^+$ reduction.

In a great number of studies mimiking photosynthesis for solar energy utilization,[1] major aims have been directed to design systems that can realize multi-electron redox reactions induced by visible light. It is, however, very difficult to achieve photochemical multi-electron redox reactions since only a single electron can be transfered upon absorption of one photon. Although photoelectron-transfer reactions utilizing heterogeneous interfaces have been regarded to be a possible way for the accumulation of electrons or charges,[2] it should be pointed out that the achievement of photochemical multi-electron redox reactions in homogeneous solution would provide important information to construct photosynthesis-mimicking systems as well as to develop new synthetic methods.

In photosynthesis, the electrons pumped up from water by solar energy are eventually used to reduce $NADP^+$ to NADPH. the $NAD(P)^+/NAD(P)H$ couples are the redox coenzymes present in widespread biological systems, which have unique capabilities in undergoing specific two-electron redox reactions (Scheme 1).[3] If chemical behaviors of the co-enzymes in one-electron transfer processes can be clarified, therefore, one can obtain important information to understand what requirements should be met to design photo-

chemical two-electron redox systems. Photoelectron transfer should be the best way to realize single electron transfer without the occurrence of other complicated reactions. In this work, therefore, 1-benzylnicotinamide (BNA^+) and 1,4-dihydro compound (BNAH) were employed as models of the NAD^+/NADH couple, chemical behavior of which were explored by using photosensitized electron transfer.

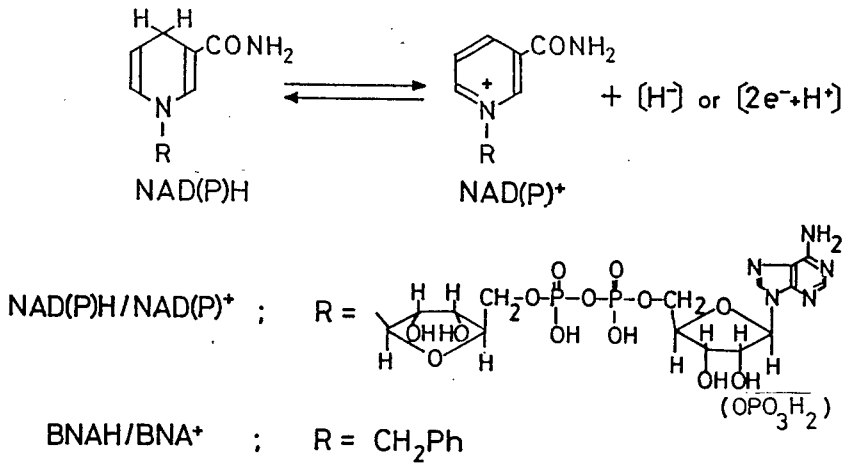

Scheme 1

Another essential subject for mimicking photosynthesis is what sensitizers should be used to cause efficient electron transfer by visible light. Transition-metal complexes have been well studied as visible-light photosensitizers, which can induce photoelectron transfer.[4] The complexes are also known to undergo ligand exchange upon photoexcitation.[5] Such ligand exchange may give new catalysts capable of undergoing multi-electron redox reactions or a novel type of catalyses. With these views, $Ru(bpy)_3^{2+}$ and fac-$Re(bpy)(CO)_3Br$ (bpy = 2,2'-bipyridine) are used as the photosensitizers.

Chapter 1 deals with the photosensitized reactions of some selected olefins with BNAH by $Ru(bpy)_3^{2+}$. The mecha-

nism and the structure-reactivity relationships in the reduction of olefins will be discussed.

Chapter 2 is concerned with the $Ru(bpy)_3^{2+}$-photosensitized reactions of several aromatic ketones and aldehydes with BNAH. On the basis of the comparison between the photosensitized and thermal reactions , the mechanism of the two types of reactions will be also discussed .

In chapter 3, Effects of magnesium (II) ion on the $Ru(bpy)_3^{2+}$-photosensitized reduction of some olefins by BNAH will be discussed on the basis of the kinetic results.

Chapters 4 and 5 describe the photochemical behaviors of some 4-alkylated 1-benzyl-1,4-dihydronicotinamide and the tetrahydrodimers of 1-benzylnicotinamide, respectively.

Chapters 6 and 7 described fac-$Re(bpy)(CO)_3Br$-photosensitized and $Ru(bpy)_3^{"+}$-photoinduced redox reactions of 1-benzylnicotinamide in the presence of triethylamine. Photoreactions of these complexes with triethylamine were also discussed.

REFERENCES

[1] "Photochemical Conversion and Strage of Solar Energy"; Cannolly, J. S., Ed.; Academic Press: New York, 1981. "Solar Energy: Chemical Conversion and Strage"; Hautala, R. R.; King, R. B., Eds.; Humana Press: New Jersey, 1979. Julliard, M; Chanon, M. Chem. Rev. **1983**, 83, 425.

[2] "Interfacial Photoprocess: Energy Conversion and Storage"; Wrighton, M. S., Ed.; American Chemical Society: Washington, D. C., 1980.

[3] Bruce, T. C.; Benkovic, S. J. "Bioorganic Mechanisms", Vol 2; W A Benjamin: New York, 1966; pp 343 - 349.

[4] Sutin, N.; Creutz, C. J. Chem. Edc. **1983**, 60, 809.

[5] Endicott, J. F. J. Chem. Edc. **1983**, 60, 824.

Chapter 1

$Ru(bpy)_3^{2+}$-PHOTOSENSITIZED REACTIONS OF 1-BENZYL-1,4-DIHYDRONICOTINAMIDE WITH OLEFINS

1-1 INTRODUCTION

The reduction of carbon-carbon double bonds by 1,4-dihydronicotinamides (Eq. 1) is of biological interest as a model for enzymatic reductions of steroidal enones[1] and unsaturated fatty acids[2] involving the pyridine nucleotide coenzymes. However, nonenzymatic reduction by usual NADH

$$\underset{1}{R^1R^2C{=}CR^3X} + NADH + H^+ \rightarrow \underset{2}{R^1R^2CHCHR^3X} + NAD^+ \quad (1)$$

models mostly requires relatively high temperatures or activated substrates. Diethyl 1,4-dihydro-2,6-dimethyl-pyridine-3,5-dicarboxylate, the Hantzsch ester, can reduce maleic and fumaric acids, their esters, and related electron-deficient olefins only at > 100 °C.[3] The reduction of 1-phenyl-4,4,4-trifluoro-2-buten-1-one can be achieved by the Hantzsch ester but not at all by 1-benzyl-1,4-dihydro-nicotinamide (BNAH), a more suitable model.[4] More activated olefins such as benzylidenemalonate, α-cyanocinnamate, and

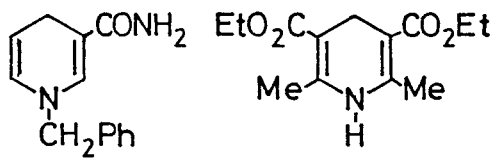

BNAH Hantzsch ester BNA^+

benzylidenemalononitrile are reduced by BNAH or related models,[5-7] though the facile reduction requires the presence of acetic acid or magnesium ion. Zinc or magnesium ion is

again essential for the reduction of 2-cinnamoylpyridine by BNAH or the Hantzsch ester.[8]

Although mechanisms are still unknown, it has been proved that hydrogen is transferred directly from the C-4 position of NADH models to the carbon atom β to the electron-deficient group (X).[4,5,8] Therefore, an ECE mechanism involving sequential electron-proton-electron transfer (Eq. 4) is pointed out to be unfavorable for the reduction of enones.[8] A suggested mechanism involves direct hydride transfer (Eq. 2)[4,5,8] or electron transfer followed by hydrogen atom transfer (Eq. 3).[8] However, general applicability of the suggested mechanisms has not been demonstrated because of the restrictions of the available reaction systems. Therefore, either direct hydride

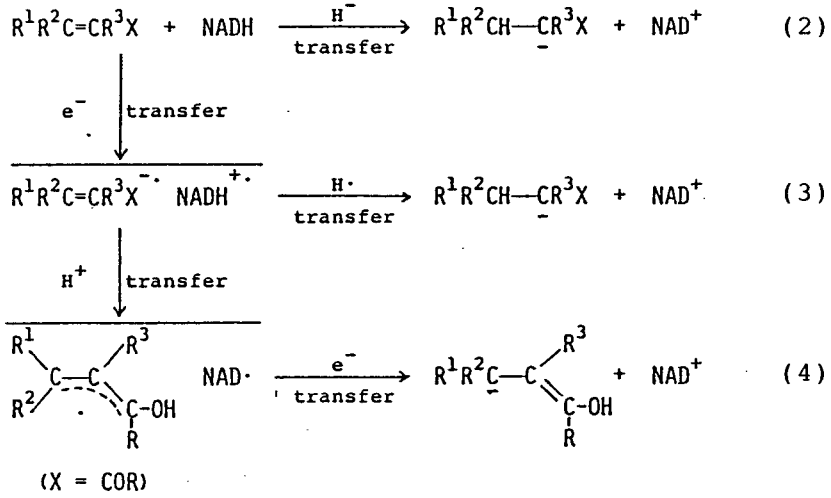

transfer[4,5,8] or a stepwise mechanism involving electron transfer[7,8] may be true only for pertinent specific reaction systems; mechanistic pathways would depend on the substituents.

This chapter deals with a systematic study on the

$Ru(bpy)_3^{2+}$-photosensitized reactions of BNAH with olefins which are unreactive with 1,4-dihydronicotinamides in the dark at room temperature.

1-2 RESULTS

Reduction of Dimethyl Fumarate and Dimethyl Maleate. All the photosensitized reactions were carried out by visible-light irradiation of methanolic or 10:1 pyridine-methanol solutions containing an olefin (50 mM), BNAH (0.1 M), and $Ru(bpy)_3^{2+}$ (1 mM) at < 20 °C. It was confirmed that no reaction occurs in the dark in any case. The progress of the reactions was followed by VPC. The products were **2a(b)**, **4a(b)**, and **5** (Scheme II and Table I), which were determined from their spectroscopic properties and elemental composition data (Experimental Section).

Reduction of Aromatic Enones. The enones used can be classified into two groups, one capable of being reduced to **2** and another undergoing no two-electron reduction but undergoing other reactions. Table II shows the results of the photosensitized reactions of the former group (**1c-e**). The reduction of **1c** and **1d** was efficient and favored in 10 : 1 pyridine-methanol solvent more than methanol. On the other hand, no significant solvent effect was observed in the reduction of **1e** which was slow and not completed even on irradiation for much longer time.

In cases of **1f-j**, the photosensitized reactions did not give **2** but complex mixtures, from which **3f**, **3i**, **4f-j**, and **5** (Scheme II) could be isolated; such reduced dimers as **3f** and **3i** could not be obtained in other cases. Column chromato-

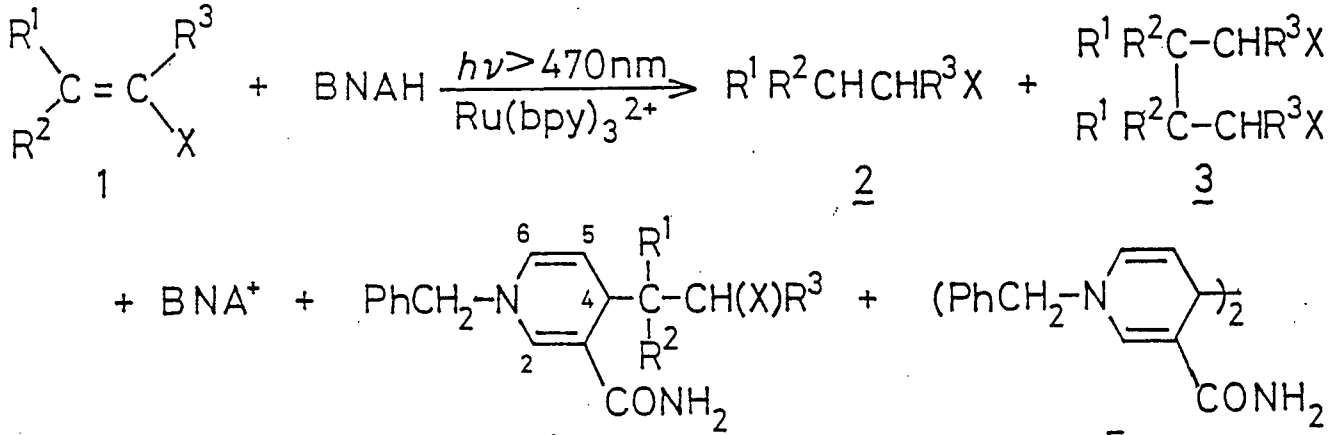

1 2 3 4 5

4a(4b) 4h

Scheme 2

Table I. $Ru(bpy)_3^{2+}$-Photosensitized Reactions of BNAH with 1a,b[a]

	1				$-E_{1/2}$[b]/V	Solvent[c]	Yield[d]/%		
	R^1	R^2	R^3	X			2[e]	4[f]	5[g]
a	CO_2Me	H	H	CO_2Me	1.72	10:1 py-MeOH	68	tr	34
						DMF	20		
						MeOH	9	29	21
b	H	CO_2Me	H	CO_2Me	1.88	10:1 py-MeOH	96	0	35
						DMF	90		
						MeCN	47		18
						MeOH	36	14	19

[a] For solutions containing BNAH (0.1 M), **1** (50 mM), and $Ru(bpy)_3^{2+}$ (1 mM). [b] Polarographic half-wave reduction potentials in volts vs. $Ag/AgNO_3$ in MeCN by using a dropping mercury electrode and Et_4NClO_4 (0.1 M) as a supporting electrolyte. [c] py = pyridine, MeOH = methanol, DMF = N,N-dimethylformamide, and MeCN = acetonitrile. [d] At 100% conversion of **1**. [e] VPC or NMR yields based on **1** used. [f] Isolated yields based on **1** used. [g] Isolated yields based on BNAH used.

Table II. $Ru(bpy)_3^{2+}$-Photosensitized Reactions of 1c-e to 2c-e by BNAH[a]

	1[b]			$-E_{1/2}$/V	Convn. of 1[c]/%	Yields of 2[c,d]/%
	R^1	R^2	R^3			
c	p-C_6H_4CN	H	C_6H_5	1.76	95 (55)	89 (40)
d	p-$C_6H_4CO_2Me$	H	C_6H_5	1.82	95 (80)	90 (50)
e	C_6H_5	C_6H_5	H	2.00	40 (55)	25 (30)

[a] For 3-mL solutions containing 1c-e (50 mM), BNAH (0.1 M), and $Ru(bpy)_3^{2+}$ (1 mM) irradiated at > 470 nm for 1 h. [b] X = COMe in all cases. [c] Determined by VPC for 10:1 pyridine-methanol solutions. In parentheses are values for methanol solutions. [d] Based on the 1c-e used.

Table III. $Ru(bpy)_3^{2+}$-Photosensitized Reactions of BNAH with 1f-j

	1[b]			$-E_{1/2}$/V	Yields/%		
	R^1	R^2	X		3[c]	4[c]	5[d]
f	C_6H_5	H	COPh	1.78	4(5)	15(16)	13(3)
g	p-C_6H_4Cl	H	COMe	1.92		13(10)	13(tr)
h	C_6H_5	H	COMe	2.02		37(38)	15(9)
i	C_6H_5	C_6H_5	COMe	2.04	2(2)	4(9)	12(7)
j	p-C_6H_4OMe	H	COMe	2.12		10(18)	18(4)

[a] For 100-mL solutions containing 1f-j (50 mM), BNAH (0.1 M), and $Ru(bpy)_3^{2+}$ (1 mM) irradiated at > 470 nm until 1f-j had been completely consumed. [b] R^2 = H in all cases. [c] Isolated yields based on the 1f-j used for 10:1 pyridine-methanol solutions and for methanolic solutions (in parentheses). [d] Based on the BNAH used.

graphy on basic alumina was found to be convenient for isolation of compounds **4** and **5** except for **4h**; rapid elution gave several fractions of mixtures from which **4** and **5** was crystallized out upon adding cold methanol. On the other hand, **4h** was directly obtained by adding cold methanol to condensed photolysates. Each product isolated is one of the possible diastereomers. Compounds that were supposed to be the diastereoisomers of **4f-j** were detected by NMR spectra of mixtures containing **4f-j**. However, repeated column chromatography of the mixtures caused only substantial losses of materials without separation of any definite compound. Table III shows isolated yields of **3f**, **3i**, **4f-j**, and **5**. The assigned structures of the isolated products are in accord with the spectroscopic properties. Table IV shows major fragment peaks in the

Table IV. Mass Spectral Data of 3f and 3i

Compd.	MS m/e	Assignment (Rel. Intens.)
3f	418	M^+ (10)
	299	$C_6CHCH(C_6H_5)CH_2COPh^+$ (41)
	298	$C_6H_5CHC(C_6H_5)CH_2COPh^+$ (26)
	209	$(M/2)^+$ (100)
3i	446	M^+ (4)
	313	$C_6H_5CHCH(C_6H_5)CH(C_6H_5)COMe^+$ (53)
	269	$C_6H_5CHC(C_6H_5)CHC_6H_5^+$ (21)
	223	$(M/2)^+$ (13)
	180	$C_6H_5CHCHC_6H_5^+$ (100)
	134	$C_6H_5CHC(OH)Me^+$ (24)
	133	$C_6H_5CHCOMe^+$ (14)

mass spectra of **3f** and **3i** which demonstrate the β,β' dimer structures. Moreover, the ^{1}H NMR spectrum of **3i** exhibits resonances at δ 3.96 - 4.30 as multiplets for unequivalent methine protons but none for methylene protons. The common 4-substituted 1,4-dihydronicotinamide structures of **4f-j** are easily assignable from similar spectroscopic features involving strong UV absorption maxima at 338 - 345 nm, the basic fragment peak at m/e 213 in the mass spectra, and characteristic ^{1}H NMR signals for the C-2, C-4, C-5 and C-6 protons of the dihydropyridine ring; Table V summarizes the rmajor spectroscopic properties of **4f-j**.

Reduction of Substituted Cinnamates and Cinnamonitriles. Table VI shows the results of photosensitized reactions with **1k-u**. No attempt was made for isolation and identification of other products. In cases of **1n** and **1t**, the reactions were slow and not completed even by irradiation for much longer time. The photoreduction of **1s** was accompanied by *E,Z* isomerization, while the geometric isomerization was exclusive in case of **1m** (Eq. 5).

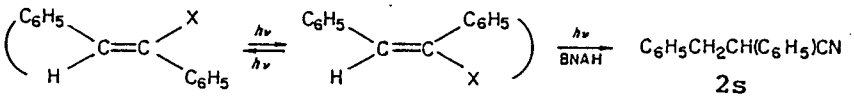

1m, X = CO_2Me
1s, X = CN

(5)

Table V. Spectroscopic Properties of 4f-j

Compd.	Chemical Shifts in ^{1}H NMR spectra[a] (J/Hz)										λ_{max}[b]/nm	MS/m/e[c]
	H-2[d]	H-4	H-5	H-6	NCH_2	$CONH_2$	COMe	R^1R^2C[d]	$R^3CH(X)$	Others	(ε/M^{-1} cm^{-1})	(M^+)
4f	6.50	3.16-3.84	4.66 (5, 8)	5.60 (2, 8)	3.09	6.37		3.16-3.84	3.16-3.84	6.95-8.03	344 (4800)	422
4g	6.64	3.68 (3, 5)	6.68 (5, 8)	5.68 (2, 8)	4.00	6.38	2.16	3.38	2.56 (3, 18)	6.91-7.40	338 (5300)	393
4h	6.60	3.70 (3, 5)	4.68 (5, 8)	5.65 (2, 8)	4.00	6.25	2.21	3.42	2.66(3, 18) 3.18(11, 18)	6.92-7.40	345 (5000)	360
4i	6.58	3.88[d]	4.81 (5, 8)	5.72 (2, 8)	3.93	6.38	2.19	3.86	4.38(12)	6.92-7.40	339 (4500)	436
4j[e]	6.64	3.67 (3, 5)	4.67 (5, 8)	5.66 (2, 8)	4.03	6.32	2.18	3.38	2.60(3, 18) 3.10(11, 18)	6.70-7.40	338 (6500)	390

[a] For $CDCl_3$ solutions in parts per million from Me_4Si. [b] Absorption maxima in CH_3CN. [c] A basic peak commonly appears at m/e 213. [d] Multiplet. [e] A sharp singlet for OCH_3 appears at δ 3.80.

Table VI. $Ru(bpy)_3^{2+}$-Photosensitized Reduction of 1k-u by BNAH

	1				$-E_{1/2}$	Time[b]	Convn. of	Yields of
	R^1	R^2	R^3	X	V	h	of 1[c]/%	of 2[c,d]/%
k	p-C_6H_4CN	H	H	CO_2Me	1.80	0.8	100(70)	100(40)
l	p-$C_6H_4CO_2Me$	H	H	CO_2Me	1.87	1.0	75(50)	60(25)
m	C_6H_5	H	C_6H_5	CO_2Me	2.14	1.0	e	
n	C_6H_5	C_6H_5	H	CO_2Me	2.18	2.0	17(23)	9(20)
o	C_6H_5	H	H	CO_2Me			No reaction	
p	p-C_6H_4CN	H	H	CN		f	∿80(∿50)	∿60(∿25)
q	H	p-C_6H_4CN	H	CN		f	∿80(∿60)	∿70(∿30)
r	p-$C_6H_4CO_2Me$	H	H	CN		1.0	58	33
s	H	C_6H_5	C_6H_5	CN	1.95	2.0	100(100)	33[g](13[h])
t	C_6H_5	C_6H_5	H	CN	2.14	4.0	22	10
u	C_6H_5	H	H	CN			No reaction	

[a] For 3-mL solutions containing 1k-u (50 mM), BNAH (0.1 M), and $Ru(bpy)_3^{2+}$ (1 mM) irradiated at > 470 m. [b] Irradiation time. [c] Determined by VPC for 10:1 pyridine-methanol solutions and for methanolic solutions (in parenthesis). [d] Based on the 1k-u used. [e] No reduction but exclusive *E,Z* isomerization. [f] For 100-mL solutions irradiated for 1.5 h. Both conversions and yields were determined by NMR. [g] The *Z* isomer was formed in 35% yield. [h] The *Z* isomer was formed in 85% yield.

1-3 DISCUSSION

Photochemical Electron-Transfer Process.

The incident light at > 470 nm can excite only $Ru(bpy)_3^{2+}$; no photoreaction took place in the absence of the ruthenium complex. The luminescence of $Ru(bpy)_3^{2+}$ was quenched by BNAH while the olefins are poor quenchers with a few exceptions (Table VII). It is probable that the efficient

Table VII. Rate Constants for Quenching of $Ru(bpy)_3^{2+}$ Luminescence[a]

Quencher	Solvent	τ[b] / μs	$k_q\tau$ / M^{-1}	k_q / $M^{-1}s^{-1}$
BNAH	MeOH	0.80	120	1.5×10^8
	MeCN	1.00	294	2.9×10^8
	DMF[c]	0.93	184	2.0×10^8
	py-MeOH[d]	0.96	358	3.7×10^8
5	py-MeOH		1700	1.8×10^9
DMT[e]	MeOH		820	9.9×10^8
1i	MeOH		1	1.1×10^7
1m	MeOH		920	1.2×10^9
1s	MeCN		210	2.1×10^8
Other olefins	MeCN		< 5	$<< 10^7$

[a] Determined by Stern-Volmer plots of the luminescence quenching for deaerated solutions by 550-nm excitation. [b] Observed lifetimes of the $Ru(bpy)_3^{2+}$ luminescence. [c] N,N-Dimethylformamide. [d] 10:1 pyridine-methanol solvent. [e] N,N-Dimethyl-p-toluidine.

luminescence quenching by **1m** and **1d** arises from triplet energy transfer from excited $Ru(bpy)_3^{2+}$ to the olefins possessing the stilbene chromophore, which results in the *E,Z* isomerization.[9] On the other hand, it is now well-known that quenching of the $Ru(bpy)_3^{2+}$ luninescence generally involves electron transfer.[10-12] The observed rate constant for the luminescence quenching by BNAH in acetonitrile falls on a value predicted for electron transfer from an electron donor to $Ru(bpy)_3^{2+}$ in the luminescent excited state according to the Rehm-Weller's treatment[13] using Eqs. 6-9,[11] where A = $Ru(bpy)_3^{2+}$, D = BNAH, $E(D/D^{+\cdot})$ =

$$A^* + D \underset{k_{2,1}}{\overset{k_{1,2}}{\rightleftharpoons}} [A^* \quad D] \underset{k_{3,2}}{\overset{k_{2,3}}{\rightleftharpoons}} [A^{-\cdot} \; D^{+\cdot}] \xrightarrow{\alpha k_{3,0}} A^{-\cdot} + D^{\cdot +} \qquad (6)$$
$$\xrightarrow{(1-\alpha)k_{3,0}} A + D$$

$$k_q^{calcd} = \frac{k_{1,2}}{1 + \frac{k_{1,2}}{\Delta V k_{3,0}}\left[\exp\left(\frac{\Delta G_{2,3}^{\ddagger}}{RT}\right) + \exp\left(\frac{\Delta G_{2,3}}{RT}\right)\right]} \qquad (7)$$

$$\Delta G_{2,3}^{\ddagger} = G_{2,3}/2 + [(\Delta G_{2,3}/2)^2 + (\Delta G^{\ddagger}(0))^2]^{1/2} \qquad (8)$$

$$\Delta G_{23} = -E(A^*/A^{-\cdot}) + E(D/D^{+\cdot}) \qquad (9)$$

0.76 V vs. SCE in acetonitrile,[14] $E(A^*/A^{-\cdot})$ = 0.7 V vs. SCE in acetonitrile,[11,15] ΔG (0) = 4 kcal/mol,[11] $\Delta V k_{3,0}$ = 8 x 10^{11} $M^{-1}s^{-1}$,[11] $k_{1,2}$ = 10^{10} $M^{-1}s^{-1}$, and T = 293 K. The caluculated value (k_q^{calcd}) is 2.4 x 10^8 $M^{-1}s^{-1}$, very close to the observed rate constant. Therefore, it is strongly suggested that electron transfer is the primary process responsible for the photosensitized reactions. The quantum yields (α) for the net electron transfer giving the reactive

redox intermediates appear to be greater than 0.44 in methanol and 0.55 in 10:1 pyridine-methanol as the solvent, the highest obseved quantum yields for the disappearance of the olefins in the respective solvents (vide infra).

Alternatively, $Ru(bpy)_3^{2+}$ in a nonluminescent excited state would abstract a hydrogen atom from a solvent molecle to generate $Ru(bpy)_3H^{2+}$, a mechanism suggested by Kellog et al.[16] for the $Ru(bpy)_3^{2+}$-photosensitized reaction of activated sulfonium salts by NADH models of structures similar to the Hantzsch ester. The mechanistic argument is based on the observation that no apparent quenching of the $Ru(bpy)_3^{2+}$ luminescence occurred at $< 10^{-3}$ M in the NADH model. Recently the population of a nonluminescent d-d state by crossing from the charge-transfer luminescent state has been demonstrated to become significant in the absence of quenching of the latter state and especially at higher temperatures.[17] A major chemical consequence from the d-d state is, however, ligand substitution (Eq. 10).[17,18]

$$Ru(bpy)_3^{2+*}_{^3CT} \rightleftharpoons Ru(bpy)_3^{2+*}_{^3d\text{-}d} \xrightarrow{2L} Ru(bpy)_2L_2^{2+} + bpy \qquad (10)$$

In the present photoreactions, however, the involvement of a nonluminescent state is very unlikely since the reactions were conducted at 0.1 M in BNAH where the luminescence of $Ru(bpy)_3^{2+}$ was completely quenched. In fact, neither the consumption of $Ru(bpy)_3^{2+}$ nor the formation of free bpy was observed in any case even after the photosensitized reactions had reached the maximum conversions. Generally speaking, mechanistic arguments based on lumines-

cence quenching by inefficient quenchers at low concentrations should be examined with care since pertinent photosensitized reactions usually employ high concentrations of quenchers. Complete or dominant quenching of the $Ru(bpy)_3^{2+}$ luminescence can be easily achieved even by inefficient quenchers since lifetimes of the luminescent state are very long. Moreover, low values of k_q are not necessarily associated with net low yields of electron transfer but indicate only the endergonic nature of the electron-transfer process. It was reported that net quantum yields of photochemical electron transfer are moderate (0.2 - 0.3) in cases of some ruthenium (II) complex-aliphatic amine pairs where k_q's are low ($\sim 10^8$ M^{-1} s^{-1}).[19]

Mechanistic Pathways and Reactive Species in Olefin Reduction. In order to obtain insights into the mechanism, deuteration experiments were performed by using BNAH-4,4-d_2, methanol-O-d, or methanol-d_4 in the photomediated reduction of **1a** and **1b**. The results shown in Table VIII demonstrate that hydroxylic protons of methanol are predominantly involved in the reduction pathway,[20] i.e., direct hydrogen transfer from BNAH to the olefins is negligible. In these reactions there was observed neither stereomutation of **1a** and **1b** nor deuterium incorporation in the recovered olefins even 50 - 80% conversions. Moreover, an identical deuterium isotopic distribution in the reduced product was obtained with either methanol-d_4 or methanol-O-d. These observations unambiguously eliminate the possibilities that the half-reduced species of the olefins would disproportionate or abstract a hydrogen atom from methanol or BNAH to give the reduced product. Therefore we conclude that the

Table VIII. **Deuterium Isotopic Distribution in the Reduction Product from $Ru(bpy)_3^{2+}$-Mediated Photoreactions of Dimethyl Fumarate and Maleate**

1	Deteration Reagent	Yield[a,b]/% 2-d_0	2-d_1	2-d_2
a	BNAH-4,4-d_3	94	6	0
	CH_3OD	3	38	59
b	BNAH-4,4-d_2[c]	99	1	0
	CH_3OD	4	37	59
	CD_3OD	4	37	59
	CH_3OD[d]	0	22	78

[a] Determined by VPC-mass analyses. [b] Unless otherwise specified, the photoreactions were carried out in 10:1 pyridine-methanol (or deuterated methanol) by using $Ru(bpy)_3Cl_2 \cdot 6H_2O$. [c] The isotopic purity was over 98%. [d] The ruthenium complex and BNAH were used after single recrystallization from D_2O and CH_3OD, respectively.

photomediated reduction of **1a** and **1b** occurs as a consequence of sequential two-electron transfer from BNAH to the olefins (Eq. 11); a similar mechanism should operate in the reduction of the other olefins.

Table IX. Quantum Yields for Disappearance of 1 and Formation of 2

1	R^1	R^2	R^3	X	$-E_{1/2}$/V	Φ_{-1}[a,b]	Φ_2[a,c]
a	CO_2Me	H	H	CO_2Me	1.72	0.44(0.44)	0.33(0.029)
b	H	CO_2Me	H	CO_2Me	1.88	0.20(0.13)	0.20(0.060)
c	p-C_6H_4CN	H	C_6H_5	COMe	1.76	0.26(0.20)	0.25(0.066)
d	p-$C_6H_4CO_2Me$	H	C_6H_5	COMe	1.82	0.28(0.18)	0.28(0.078)
e	C_6H_4	C_6H_5	H	COMe	2.00	0.053(0.056)	0.030(0.038)
k	p-C_6H_4CN	H	H	CO_2Me	1.80	0.55(0.25)	0.55(0.18)
l	p-$C_6H_4CO_2Me$	H	H	CO_2Me	1.87	0.37(0.10)	0.31(0.079)

[a] Determined by the irradiation at 520 nm for deaerated 10:1 pyridine-methanol solutions and for methanolic solutions (in parentheses) containing 1 (50 mM), BNAH (0.1 M), and $Ru(bpy)_3^{2+}$ (2.7 mM). [b] Quantum yields for the disappearance of 1. [c] Quantum yields for the formation of 2.

$$MeO_2CCH{=}CHCO_2Me \xrightarrow[D^+]{e^- \ (Ru(bpy)_3{}^{+})} MeO_2C\text{-}C(D)H\text{-}\dot{C}H\text{-}CO_2Me \xrightarrow[D^+]{e^- \ (BNA^{\bullet})} MeO_2C\text{-}CH(D)CH(D)\text{-}CO_2Me \quad (11)$$

The reduction potential of $Ru(bpy)_3{}^{2+}$ (- 1.69 V) is more positive than but similar to those of the olefins. The polarographic reduction waves of the olefins are probably due to reversible one-electron transfer since reversibility in one-electron reduction of enones has been proved by cyclic voltammetry.[21] The electrochemical data can therefore be used to estimate free-energy changes for electron transfer from $Ru(bpy)_3{}^{2+}$ to the olefins which are positive by 1 - 10 kcal mol^{-1}. As predicted by the Marcus equation[22] or the related empirical modifications,[13,23] a linear free energy relationship may hold for such an endergonic process. Table IX lists quantum yields for the disappearance of **1** (Φ_{-1}) as well as for the formation of **2** (Φ_2) for some olefins. As is shown in Scheme III and Eq. 12, Φ_{-1} can serve to show the dependence of k_e on $E_{1/2}$, provided that regeneration of **1** from $\mathbf{1}^{-\bullet}$ and $^{\bullet}\mathbf{1}$-H is not important.

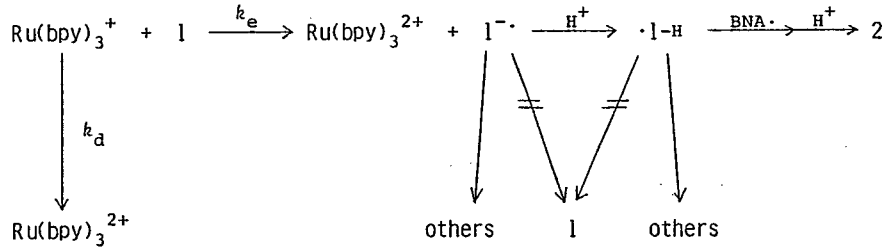

Scheme 3

$$\Phi_{-1}/(\alpha - \Phi_{-1}) = k_e/k_d \qquad (12)$$

Eventually log $[\Phi_{-1}/(1 - \Phi_{-1})]$ was plotted against $E_{1/2}$ since α is unknown. A linear correlation in Figure 1 demonstrates that the disappearance of **1** involves one-electron transfer in a rate-detemining step.

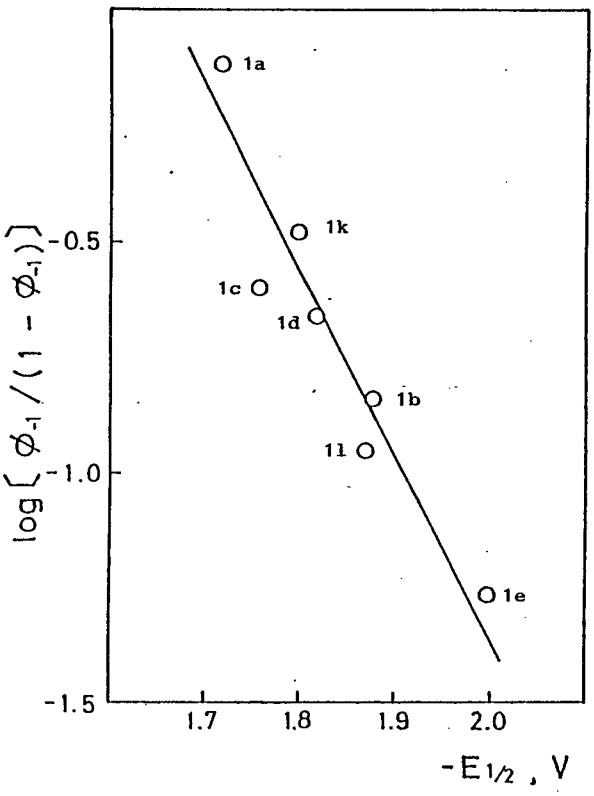

Figure 1. Plot of log$[\Phi_{-1}/(1 - \Phi_{-1})]$ vs. reduction potentials ($E_{1/2}$) for the photosensitized reactions of methanolic solutions. For the abbreviations of olefins see Table I, II, III, and VI.

A key species in the one-electron reduction of •1-H is BNA• that is readily formed by the loss of a proton from the cation radical of BNAH ($BNAH^{+\bullet}$, Eq. 13). In the absence of

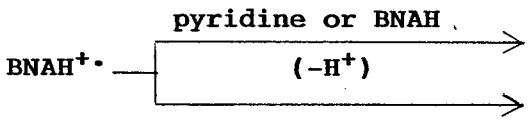

(13a)

(13b)

an added base, BNAH can act as a base to receive a proton from $BNAH^{+\bullet}$ in competition with other reactions.[24] In 10:1 pyridne-methanol solvent, however, the deprotonation process predominates over other pathways, thus giving BNA• in higher steady-state concentration. This is in line with the observations that Φ_2's and yields of 5 remarkably increase upon changing solvent from methanol to 10:1 pyridine-methanol in most cases. Since electron transfer from BNA• to $Ru(bpy)_3^{2+}$ and neutral molecules of 1 appears to be very slow because of relatively high endothermicity of this process, BNA• might survive long enough to undergo follow-up processes. On the other hand, the participation of $Ru(bpy)_3^{+}$ in the reduction of •1-H to 2 is not important since this species is probably scavenged by large excess of neutral molecules of 1.

With regard to the two-electron-reduction capabilities of BNAH, it should be noted that neither N,N-dimethyl-p-toluidine (DMT) nor 5 can be used as a two-electron reductant instead of BNAH, though the luminescence of $Ru(bpy)_3^{2+}$ is quenched by DMT and 5 at 9.9×10^8 and 1.7×10^9 $M^{-1}s^{-1}$ in methanol, respectively. The $Ru(bpy)_3^{2+}$-photosensitized reactions of **1c** with DMT in methanol or 10:1 pyridine-methanol solvent resulted in no or little (< 5%) reduction of **2c**, but each gave complex mixtures. In the case of **1b**

no reduction but dominant formation of complex mixtures again occurred in the photosensitized reactions with DMT in methanol as well as with 5 in N,N-dimethylformamide. Unique reactivities of BNAH capable of donating two electrons to a substrate molecule seem to originate from facile formation of BNA· after the first one-electron transfer as well as from the relatively low oxidation potential of the radical intermediate. Scheme 4 delineates the reaction pathways of the photosensitized reactions.

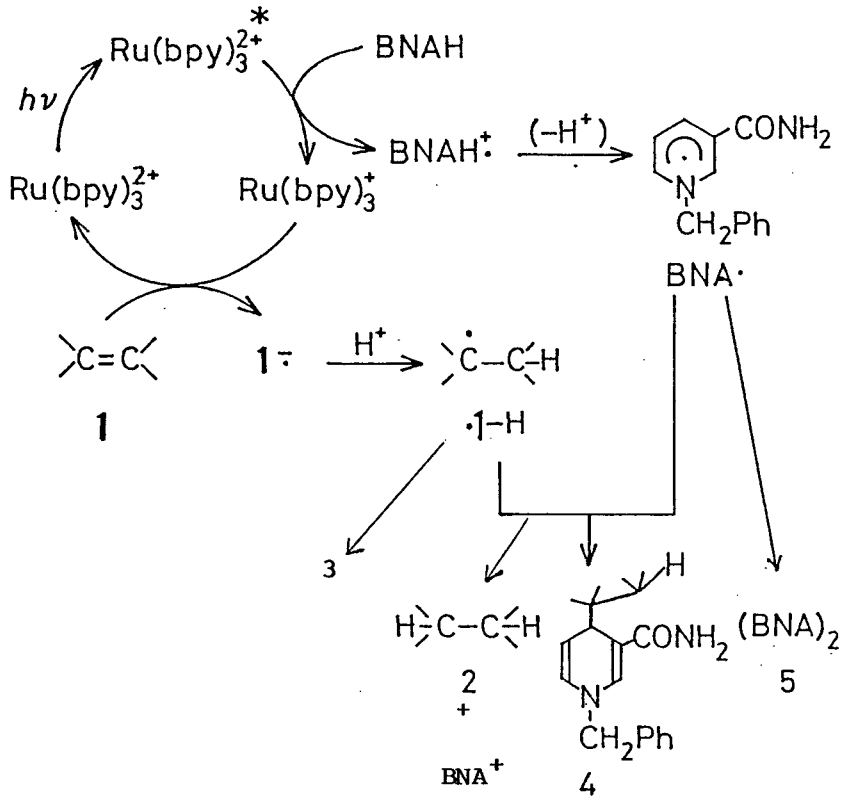

Scheme 4

Stracture-Reactivity Relationships in Two-Electron Reduction and Adduct Formation. The two-electron reducrtion can occur in cases where R^1 = p-C_6H_4CN or p-$C_6H_4CO_2Me$ and R^2 = H or R^1 = R^2 = C_6H_5 irrespective of X. On the other hand, the enones that contain neither such an extra electron-withdrowing group nor the two phenyl groups at the position β to X are not reduced to **2** but give **4**. These reactivity differences associated with R^1 and/or R^2 suggest that a prefered structure of •**1**-H should be •**1**-H(A) rather than •1-H(B), a structure assignment supported by the strctures of **3f,i** and **4f-j**.

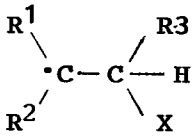

•**1**-H(A)

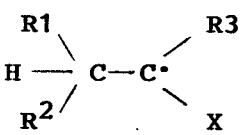

•**1**-H(B)

Reduction potentials of •**1**-H(A) should depend on R^1 and R^2 but not on R^3 and X. In cases where R^1 = p-C_6H_4CN or p-$C_6H_4CO_2Me$, the strong electron-withdrawing nature of the substituents certainly enhances the electron-accepting power of the radicals. On the other hand, •**1**-H(A), which contains no such extra electron-withdrawing group but only one aryl substituent at the beta position, does not have a reduction potential enough positive to be reduced by BNA•, thus undergoing dimerization and radical-coupling reactions to give **3** and **4**. The substitution of the two phenyl groups at the β position appears to make the radicals capable of receiving an electron from BNA• to some extent, probably by combined inductive effects of the two phenyl groups as well as by an extended cross section for electron transfer due to greater delocalization of an odd electron; these effects

appear not to be large since the Φ_2 values are very small for the pertinent reaction systems. Moreover, steric hindrance of the two phenyl groups that prevents radical-coupling reactions should be taken into account as an additional effect allowing slow electron transfer from BNA• to •**1**-H to ensue.

It should be stressed that the above discussion is valid only for •**1**-H(A). In cases where R^1 and/or R^2 = aryl and R^3 = H, •**1**-H(A) is certainly more stable than •**1**-H(B) because of greater resonance stabilization by the aryl group(s). However, the reverse may happen when R^3 = C_6H_5; i.e., •**1**-H(B) is more stable. The radical intermediates from **1i,m** and **1s** would fit the case. The one-electron reduction of •**1**-H(B) by BNA• may occur since the strong electron-withdrawing group (X) directly attaches to the free-radical center.

In contradiction to the expectation, **1i** was not reduced to **2i**, and the structures of the isolated products (**3i** and **4i**) demonstrate that •**1**-H(A) is formed as a reactive intermediate (Eq. 14). According to the reported ESR studies on

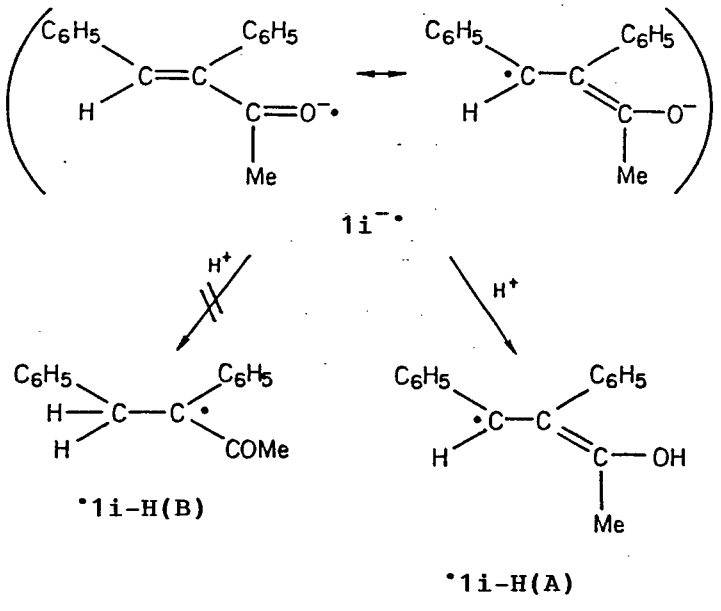

(14)

the anion radicals of enones,[21,25] about half of the unpaired electron density is located at the β carbon atom and the other half at the carbonyl group with little or no spin density at the α carbon atom. Therefore, it is probable that the carbonyl oxygen of the anion radical of enones is selectively protonated to leave the spin density at the β carbon atom irrespective of R^3; no reduction of **1i** to **2i** can thus be expected since •**1**-H(A) is a benzylic radical with no extra electron-withdrowing substituent.

On the other hand, since the photosensitized reduction of **1s** to **2s** occurs (Eq. 15), it is suggested that the anion

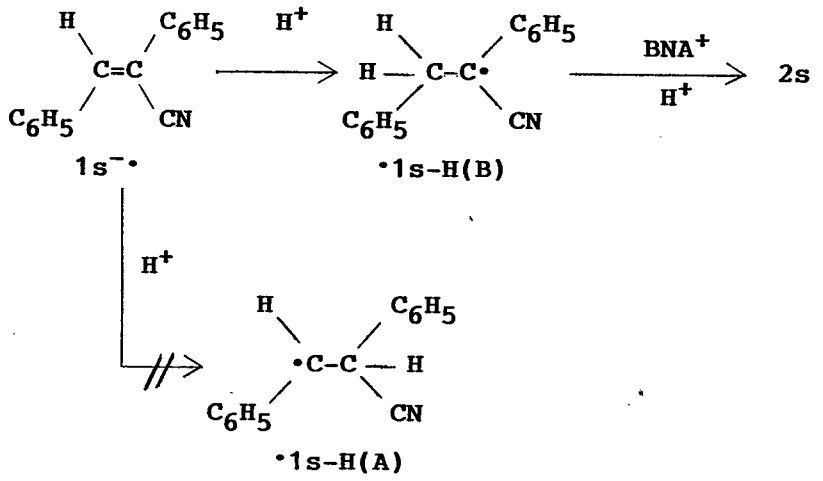

(15)

radical of **1s** is protonated at the β carbon atom to yield a more stable radical •**1s**-H(B). It is highly probable that this radical is capable of being reduced by BNA• because of a strong electron-withdrowing effect of the nitrile group. In contrast, protonation at the α carbon atom would afford less stable radical •**1s**-H(A) which should be incapable of receiving an electron from BNA• as expected from the electronic structure very similar to those of •**1i**-H(A) and related benzylic radicals with no strong electron-with-

drawing substituent. In case of **1m** which is a carboxylate analogue of **1i** and **1s** (i.e., X = CO_2Me), unfortunately, nothing can be discussed with respect to the structures and reactivities of •1-H since the *E,Z* isomerization exclusively occurs without redox reactions.

Mechanistic Implications for Thermal Reduction of Carbon-Carbon Double Bonds by NADH Models. The present results clearly demonstrate that BNAH and probably other similar NADH models are capable of donating two electrons to a molecule of olefin via ECE processes. Therefore, an ECE mechanism is a possible, but not obligatoly, choice for thermal reduction of carbon-carbon double bonds by NADH models. Since reduction of some olefins in the dark involves direct hydrogen transfer to the carbon atom β to X,[4,5,8] however, this mechanism may hold only in cases where •1-H(B) is formed (Scheme 5). If so, it is evident that thermal reduction of enones does not fit the case since the intervention of •1-H(A) appears to be an inevitable consequence of sequential electron-proton transfer to enones as discussed in the previous section.

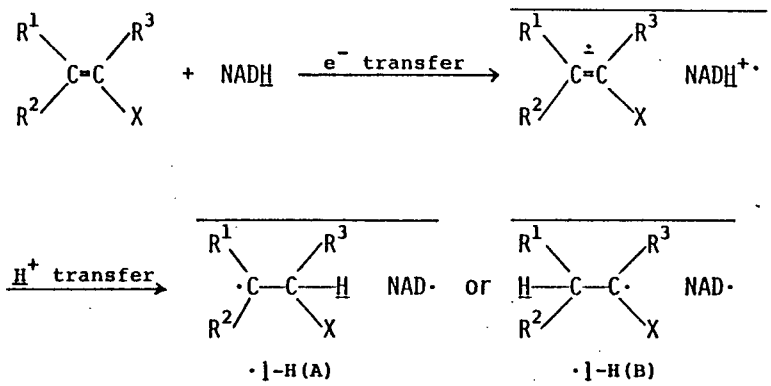

Scheme 5

In order to obtain further insights into mechanistic aspects of thermal reduction of enones, $Ru(bpy)_3^{2+}$-photosensitized reactions were compared with thermal reactions by using (*E*)-2-cinnamoylpyridine (**1v**) and (*Z*)-1-(2-pyridyl)-2-phenyl-1-buten-3-one (**1w**). Thermal reactions were conducted in the presence of Mg^{2+} in methanol at 20 °C since no reaction occured in the absence of Mg^{2+} even upon heating. In case of **1v**, the Mg^{2+}-catalyzed reduction was very efficient as reported,[8] while the photosensitized reaction did not give **2v** at all but complex mixtures (Eq. 16). In contrast, the reduction of **1w** in the dark was inefficient, unlike the efficient photosensitized reduction (Eq. 17).

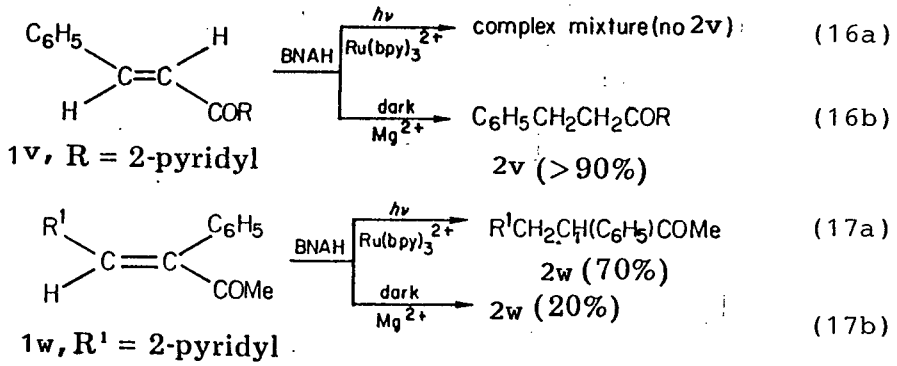

The different behaviors of **1v** and **1w** in photosensitized reactions are strictly in line with those of **1f-j** and **1c-e**, respectively, demonstrating again the intermediacy of •**1**-H(A) in these photosensitized reactions. On the other hand, it is highly improbable that similar mechanisms involving •**1**-H(A) are operative in both the photosensitized

and thermal reactions of either **1v** or **1w**, since no correlation was observed between them. Especially, the facile reduction of **1v** by catalysis of Mg^{2+} in the dark disagrees with a simple ECE mechanism, unless specific interactions of Mg^{2+} with **1v** would allow the intervention of **·1**-H(B) as a consequence of electron-proton transfer.

On the other hand, thermal reduction of cyanated olefins may proceed via ECE processes in cases where **·1**-H(B) is more stable than **·1**-H(A); alkylidenemalononitriles which are reduced by NADH models[5] fit the case. Although mechanistic aspects of thermal reduction of unsaturated carboxylic acids and their derivatives remain unsolved, it is of interest to note that the dark reaction of maleic anhydride with an NADH model affords a 1:1 adduct of a structure very similar to those of **4** (Eq. 18),[26] a result implying the involvement of electron-proton transfer from the model to the substrate. Unfortunately, no further discussion can be made since any other example of the adduct formation in the dark has not appeared.

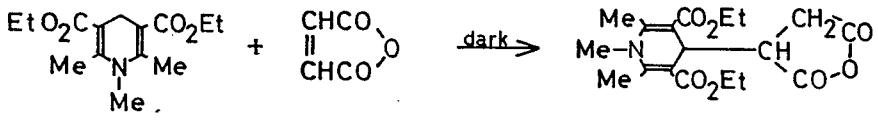

(18)

1-4 EXPERIMENTAL SECTION

Materials. Methanol was distilled from magnesium methoxide. Pyridine was refluxed over anhydrous potassium hydroxide and then distilled before use. BNAH[27] and $Ru(bpy)_3Cl_2 \cdot 6H_2O$[28] were prepared and purified according to the literature methods. **1a,b,f,h,o,** and **1u** were reagent grade (Tokyo Kasei). The following known olefins were prepared according to published methods: **1e,** bp 200 - 205 °C (15 mmHg) [lit.[29] bp 103 - 105 °C(0.01 mmHg)]; **1g,** mp 56 - 57.5 °C (lit.[30] mp 59 - 59.5 °C); **1i,** mp 54 - 56 °C (lit.[31] mp 56 °C); **1m,** mp 73 - 74 °C (lit.[32] mp 76 °C); **1s,** mp 86 - 87 °C (lit.[33] mp 88 °C); **1t,** mp 48 - 49 °C (lit.[34] mp 49 - 50 °C); **1v,** mp 67 - 69 °C (lit.[35] mp 71 - 72 °C). Procedures employed for the preparation of **1i**[31] were adopted to obtain **1c** (mp 97 - 99 °C), **1d** (mp 103 - 105 °C), and **1w** (mp 32 - 33 °C); a benzene solution (35 mL) containing phenylacetone (23 mmol), an aromatic aldehyde (22 mmol), and piperidine (0.5 g) was refluxed for 12 h with the use of a Dean-Stark water separator and then evaporated to give solids, which were recrystallized from a mixture of hexane and benzene. p-Methoxybenzalacetone (**1j,** mp 66 - 67 °C) was prepared by a condensation reaction of p-methoxybenzaldehyde with acetone in the presence of sodium hydroxide according to the method employed for the preparation of **1g.**[30] Methyl p-cyanocinnamate (**1k,** mp 125 - 126 °C) was prepared by the esterification of the parent carboxylic acid which was obtained from p-cyanobenzaldehyde and malonic acid.[36] An identical method in which p-(methoxycarbonyl)benzaldehyde was used in place of p-cyanobenzaldehyde was employed for the preparation of **1l** (mp 119 - 121 °C). Methyl β-phenyl-

cinnamate (**1n**, bp 195 - 198 °C) was obtained by the esterification of the corresponding acid chloride prepared from 1,1-diphenylethylene and oxalyl chloride.[37] The preparation of **1p**, **1q**, and **1r** was carried out as follows. A 2:1 toluene-pyridine solution (15 mL) of p-cyanobenzaldehyde or p-(methoxycarbonyl)benzaldehyde (50 mmol), cyanoacetic acid (60 mmol), and ammonium acetate (0.16 g) was refluxed for 8 h, and then volatile materials were evaporated to dryness in vacuo. Sublimation of the residue gave crystalline materials which were subjected to column chromatography on silica gel (70 - 230 mesh, Merck) to separate the olefins: **1p**, mp 183 - 185 °C; **1q**, mp 138.5 - 139 °C; **1r**, mp 144 - 145 °C.

Analytical Methods. Melting point were taken on a hot stage and are uncorrected. VPC was performed on a Shimadzu GC-3BF dual column instrument with flame-ionization detectors and a 2 m x 4 mm column packed with 2% OV-17 on Shimalite W. HPLC was carried out on a JAILC-09 by using an LS-225 ODS column. ^{1}H NMR spectra were recorded on a JEOL JNM-PS-100 spectrometer, IR spectra on a Hitachi 260-10 spectrometer, UV and visible absorption spectra on a Hitachi 220-A spectrometer, and mass spectra on a Hitachi RMU-6E.

Reduction potentials were mesured for N_2-saturated dry acetonitrile solutions (1 mM) vs. an $Ag/AgNO_3$ reference electrode at 20 ± 0.1 C by using a dropping mercury electrode and a Yanagimoto P-1000 potentiostat. Tetraethylammonium perchlorate (0.1 M) was used as the supporting electrolyte. Luminescence-quenching experiments were performed on a Hitachi MPF-4 spectrofluorometer equipped with a data processor (Type 612-0085), and solutions were

deaerated by passing a gentle stream of Ar through solutions for 20 min. The ruthenium complex (0.25 mM) was excited at 550 nm, and intensities of the luminescence were monitored at 610 nm. The luminescence lifetimes were determined by the use of an N_2 laser with a pulse width of 1 ns.

Quantum yields were determined for thoroughly degassed solutions containing an olefin (50 mM), BNAH (0.1 M), and $Ru(bpy)_3^{2+}$ (2.7 mM) by using Reinecke's salt as an actinometer. The incident light at 520 nm was isolated from a xenon lamp by using a Hitachi MPF-2A monochromator, and the intensity was determined to be 2.57×10^{17} photons/min. All the procedures were performed in a dark room with a safety lamp. Both the disappearance of **1** and the formation of **2** were analyzed by VPC and plotted against time. Quantum yields were calculated from the slopes of initial linear portion of the plots.

Photosensitized Reactions of 1c-e and 1k-w. The light source was a Matushita tungsten-halogen lamp (300 W) immersed in a quartz well, outside of which was placed a double-cylindrical Pyrex vessel with a 1-cm space filled with a filter solution. This filter solution which was made by dissolving potassium chromate (20 g/L), sodium nitrate (200 g/L), and sodium hydroxide (6.7 g/L) in distilled water can completely cut off the light below 470 nm and was able to be used throughout the present investigation without any change in absorbance. The light source and the filter solution were set in the center of a "merry-go-round" apparatus immersed in a water bath with circulation of cold water.

Methanolic or 10:1 pyridine-methanol solutions con-

taining an olefin (50 mM), BNAH (0.1 M), and $Ru(bpy)_3Cl_2 \cdot 6H_2O$ (1 mM) were bubbled with a gentle stream of Ar for 15 min and then irradiated. The irradiation was carried out for 3-mL solutions in Pyrex tubes (8 mm i.d.) by using the merry-go-round apparatus under cooling with water except for the reactions of **1p** and **1q**, and the progress of the reactions was followed by VPC. The reactions of **1p** and **1q** were carried out on a greater scale and analyzed by ^1H NMR, since almost identical retention times of **1p, 1q,** and **2p, 2q** did not allow VPC analyses. A double-cylindrical Pyrex vessel filled with a reactant solution (100 mL) was placed just outside of the filter-solution vessel and then irradiated for 1.5 h. After removal of the solvent in vacuo, the residue was chromatographed on silica gel. Elution with 500 mL of diethyl ether gave a mixture of the starting olefin, **2p (2q)**, and BNAH as shown by ^1H NMR. The results are summarized in Table II and VI.

General Procedure for Isolation of 4 and 5. The irradiation was carried out for 100-mL solutions as described above. The complete disappearance of **1** required the irradiation for 3 - 5 h. After removal of the solvent from the photolysate, chloroform (20 mL) was added to the residue to make a homogeneous solution, which was then added to 5 g of basic alumina (70 - 230 mesh, Merck Art 1076). After gentle evaporation of the chloroform with a rotary evaporator under reduced pressure, the alumina-supported photolysate was added to the top of a column of basic alumina (50 g) and then eluted with mixtures of methanol and diethyl ether. Elution with 500 mL of 10% methanol in diethyl ether gave unreacted BNAH (10 - 70 mg), whereas

mixtures containing **4** were eluted with 20 - 50% methanol in diethyl ether. To the mixtures were added minimal volumes of methanol to make homogeneous solutions, which were combined and then stored in a refregerator. Pale yellow solids were precipitated and filtered to give **4**. Further elution with methanol gave red-brown materials to which a minimal volume of methanol was added, and then the mixture was cooled on an ice bath. A pale yellow solid was precipitated and filtered to give **5**. The isolation of **4a(b)** and **4h** was performed without the use of column chromatography as follows. After removal of the solvent from the irradiated solution, methanol (10 mL) was added to the residue to make a homogenoeus solution, which was then cooled on an ice bath. Pale yellow solids were precipitated and filtered to give **4a(b)** or **4h**. The filtrates were subjected to column chromatography to isolate **5** as described above. The isolated yields are listed in Table I and III. The products were recrystallized from ethanol, and the spectroscopic properties of **4f-j** are summarized in Table V.

For **4a(b)**: mp 232 - 235 °C dec.; UV λ_{max} (CH_3OH) 363 nm (ε 23000); ^1H NMR (CD_3SOCD_3) δ 3.43 (s, 2H), 3.59 (s, 3H), 5.21 (s, 2H), 6.77 (d, J = 7.4 Hz, 1H), 7.37 (br s, 5H), 7.50 (dd, J = 1.6 and 7.4 Hz, 1H), 8.47 (dd, J = 1.6 and 2 Hz, 1H), 10.72 (br s, 1H); ^{13}C NMR (CD_3SOCD_3) δ 29.12, 51.15, 58.36, 95.45, 110.68, 113.01, 127.03 - 128.61 (4C), 135.70, 135.88, 140.45, 141.62, 162.36, 164.12, 171.50; mass spectrum, m/e 324 (M+). Anal. ($C_{18}H_{16}N_2O_4$) C, H, N.

For **4f**: mp 183 - 185 °C dec. Anal. ($C_{28}H_{26}N_2O_2$) C, H, N.

For **4g**: mp 173 - 175 °C dec. Anal. ($C_{23}H_{23}ClN_2O_2$) C, H, N.

For **4h**: mp 206 - 207 °C dec. Anal. ($C_{23}H_{24}N_2O_2$) C, H, N.

For **4i**: mp 216 - 220 C dec. Anal. ($C_{29}H_{28}N_2O_2$) C, H, N.

For **5**: mp 173 - 174 C dec.; ^{1}H NMR (CD_3SOCD_3)[39] δ 3.20 (d, J = 5 Hz, 1H), 4.32 (dd, J = 5.8 Hz, 1H), 4.33 (s, 2H), 5.95 (dd, J = 2.8 Hz, 1H), 6.85 (br, s, 2H), 7.15 (m, 1H), 7.23 (m, 5H); mass spectrum, m/e 213 ($M^+/2$); UV (MeOH) λ_{max} 356 nm (ε 6900). Anal. ($C_{26}H_{26}N_4O_2$) C, H, N.

Isolation of 3f. The irradiation of a 100-mL methanolic or 10:1 pyridine-methanol solution for 3 or 4 h resulted in the complete disappearance of **1f**. In case of the 10:1 pyridine-methanol solution, the solvent was mostly evaporated in vacuo, and then methanol (10 mL) was added. While solids were precipitated upon cooling and then filtered to give **3f** (42 mg). The irradiated methanolic solution was condensed in vacuo to one-tenth of its volume to give **3f** (52 mg). This compound was recrystallized from a mixture of methanol and benzene: mp 273 - 276 C; ^{1}H NMR ($CDCl_3$) δ 2.82 - 3.83 (m, 3H), 7.02 - 7.80 (m, 10 H); IR (KBr) 1670 cm^{-1}. Anal. ($C_{30}H_{26}O_2$) C, H.

Isolation of 3i. After evaporation of the 100-mL methanolic or 10:1 pyridine-methanol solution (irradiated for 5 h) chloroform (30 mL) was added, and then the mixture was washed with diluted hydrochloric acid, saturated sodium bicarbonate, and brine. Evaporation of chloroform left a small amount of brownish oil, to which methanol (3 mL) was added, and then the mixture was cooled on an ice bath to give **3i** (5 mg) as a white solid: mp 254 - 255 C (from methanol-benzene); ^{1}H NMR ($CDCl_3$) δ 1.78 (s, 3H), 3.96 - 4.30 (m, 4H), 6.70 - 7.20 (m, 10H); IR (KBr) 1700 cm^{-1}. Anal. ($C_{32}H_{30}O_2$) C, H.

1-5 REFERENCE AND NOTES

[1] Pandit, U. K.; Mas Gabre, F. R.; Gase, R. A. J. Chem. Soc., Chem. Commun. **1974**, 627. Gase, R. A.; Pandit, U. K. Ibid. **1977**, 480.

[2] Lynen, F. Angew. Chem. **1965**, 77, 929.

[3] Braude, E. A.; Hannah, B. J.; Linstead, S. R. J. Am. Chem. Soc. **1960**, 3257.

[4] Nocross, B. E.; Klinedinst, P. E.; Westheimer, F. J. J. Am. Chem. Soc. **1962**, 84, 797.

[5] Wallenfels, K.; Ertel, W.; Friedrich, K. Justus Liebigs Ann. Chem. **1973**, 1663.

[6] Shinkai, S.; Kusano, Y.; Ide, T.; Sone, T.; Manabe, O. Bull. Chem. Soc. Jpn. **1978**, 51, 3544.

[7] Ohnishi, Y.; Kagami, M.; Numakunai, T.; Ohno, A. Chem. Lett. **1976**, 915.

[8] Gase, R. A.; Pandit, U. K. J. Am. Chem. Soc. **1979**, 101, 7059; J. Chem. Soc., Chem, Commun. **1977**, 480.

[9] Wrighton, M. S.; Morse, D. L.; Pdungsap, L. J. Am. Chem. Soc. **1975**, 97, 2073. Wrighton, M. S.; Markham, J. J. Phys. Chem. **1973**, 77, 3042.

[10] Wrighton, D. G. Acc. Chem. Res. **1980**, 13, 83.

[11] Ballardini, R.; Varani, G.; Indelli, M. T.; Scandola, F.; Balzani, V. J. Am. Chem. Soc. **1978**, 100, 7219.

[12] Back, C. R.; Connor, J. A.; Gutierrez, A. R.; Meyer, T. J.; Whitten, D. G.; Sullivan, B. P.; Nagle, J. K. J. Am. Chem. Soc. **1979**, 101, 4815.

[13] Rehm, D.; Weller, A. Isr. J. Chem. **1970**, 8, 259.

[14] Martens, F. M.; Verhoeven, J. W.; Gase, R. A.; Pandit, U. K.; Boer, T. J. D. Tetrahedron **1978**, 34, 443.

[15] (a) Although a slightly different value (0.77 V) has

been reported, [14,17b] we employ 0.7 V since the parameters used for the calualation of k_q are from ref 13. (b) Anderson,C. P.; Salmon, D. J.; Meyer, T. J.; Young, R. C. J. Am. Chem. Soc. **1977**, 99, 1980.

[16] van Bergen, J. J.; Hendstrand, D. M.; Kruizinga, W. H.; Kellog, R. M. J. Org. Chem. **1979**, 44, 4953.

[17] Durhan, B.; Caspar, J. V.; Nagle, J. K.; Meyer, T. J. J. Am. Chem. Soc. **1982**, 104, 4803.

[18] van Houten, J.; Watts, R. J. J. Inorg. Chem. **1978**, 17, 3381. Haggard, P. E.; Porter, G. B. J. Am. Chem. Soc. **1978**, 100, 1457.

[19] Monserrat, K.; Foreman, T. K.; Grätzel, M.; Whitten, D. G. J. Am. Chem. Soc. **1981**, 103, 6667.

[20] In the deuteration experiments with methanol-O-d and -d_4, $Ru(bpy)_3Cl_2 \cdot 6H_2O$ and BNAH both of which have exchangeable protons were used without thorough H-D exchange for convenience, thus giving significant amounts of **2a**-d_0 and-d_1. In fact, the formation of **2a**-d_2 was remarkably improved when the ruthenium complex and BNAH obtained by single recrystallization from deuterium oxide and methanol-O-d, respectively, were used.

[21] Bowers, K. W.; Giese, R. W.; Grimshaw, J.; House, H. O.; Kolodny, N. H.; Kronberger, K.; Roe, D. K. J. Am. Chem. Soc. **1970**, 92, 2783.

[22] Markus, R. A. J. Chem. Phys. **1956**, 24, 966; Discuss. Farady Soc. **1960**, 29, 21.

[23] Scandola, F.; Balzani, V.; Schuster, G. B. J. Am. Chem. Soc. **1981**, 103, 2519.

[24] Blaedel, W. J.; Haas, R. G. Anal. Chem. **1970**, 42, 918.

[25] Russel, G. A.; Stevenson, G. R. J. Am. Chem. Soc. **1971**, 93, 2432.

[26] Sims, A. F. E.; Smith, P. W. G. Proc. Chem. Soc. **1958**, 282.

[27] Mauzarall, D.; Westheimer, F. M. J. Am. Chem. Soc. **1955**, 77, 2261.

[28] Fujita, I.; Kobayashi, H.; Ber. Busenges. Phys. Chem. **1972**, 70, 115.

[29] Wilson, W.; Kyi, Z.-Y. J. Chem. Soc. **1952**, 1321.

[30] Lutz, R. E.; Marten, T. A.; Codington, J. F.; Amacker, T. M.; Allison, R. K.; Leake, N. H.; Rowlet, R. J., Jr.; Smith, J. D.; Wilson, J. W., III. J. Org. Chem. **1949**, 14, 993

[31] Zimmerman, H. E.; Singer, L.; Thyagarajan, B. S. J. Am. Chem. Soc. **1958**, 81, 108.

[32] Müller, E.; Gawlick, H.; Kreutzmann, W. Justus Liebigs ann. Chem. **1935**, 515, 97.

[33] Wawzoneck, S.; Smolin, E. M. "Organic Syntheses"; Willey: New York, 1973; Collect Vol. III, p 715.

[34] Lettre, H.; Wick, K. justus Liebigs Ann. Chem. **1957**, 603, 189.

[35] Marvel, C. S.; Coleman, L. E., Jr.; Scott, G. P. J. Org. Chem. **155**, 20, 1785.

[36] Davies, W.; Holmes, B. M.; Kefford, J. F. J. Chem. Soc. **1939**, 357.

[37] Kharasch, M. S.; Kane, S. S.; Brown, H. C. J. Am. Chem. Soc. **1942**, 64, 333.

[38] Wegner, E. E.; Adamson, A. W. J. Am. Chem. Soc. **1966**, 88, 394.

[39] The ^{1}H NMR spectrum is identical with that of one of the diastereomeric 4,4'-dimers: Ohnishi, Y.; Kitami, M. Bull Chem. Soc. Jpn. **1979**, 52, 2674.

Chapter 2

$Ru(bpy)_3^{2+}$-PHOTOSENSITIZED REACTIONS OF AN NADH MODEL, 1-BENZYL-1,4-DIHYDRONICOTINAMIDE, WITH AROMATIC CARBONYL COMPOUNDS AND COMPARISON WITH THERMAL REACTIONS

2-1 INTRODUCTION

As described in chapter 1, electron-transfer induced reactions of BNAH with olefins are efficiently photosensitized by $Ru(bpy)_3^{2+}$ to yield the two-electron reduction products of olefins and 1:1 adducts of the reactants as shown in Scheme 1. The $Ru(bpy)_3^{2+}$-photosensitized reactions can therefore exemplify chemical behaviors of BNAH in electron-transfer processes, being thus diagnostic to test controversial mechanisms of electron transfer[1-4] or hydride transfer[5-8] in thermal reactions of NADH models in the dark. Furthermore, the adduct formation is of synthetic and pharmacological interest since preparation of 4-alkyl-1,4-dihydronicotinamide is relatively difficult and since the unique structure of the adducts is reminiscent of 4-arylated Hantzsch esters which are known to be pharmacologically active.[9] However, isolated yields of the adducts are low or, at best, moderate because of difficulties of the isolation; only one isomer of the possible diastereoisomers was obtained in each case. On the other hand it was found that the $Ru(bpy)_3^{2+}$-photosensitized reactions with aromatic carbonyl compounds give 1:1 adducts in high yields, a finding of synthetic and mechanistic interest. This chapter deals with details of the photosensitized reactions of BNAH with several aromatic ketones and aldehydes.

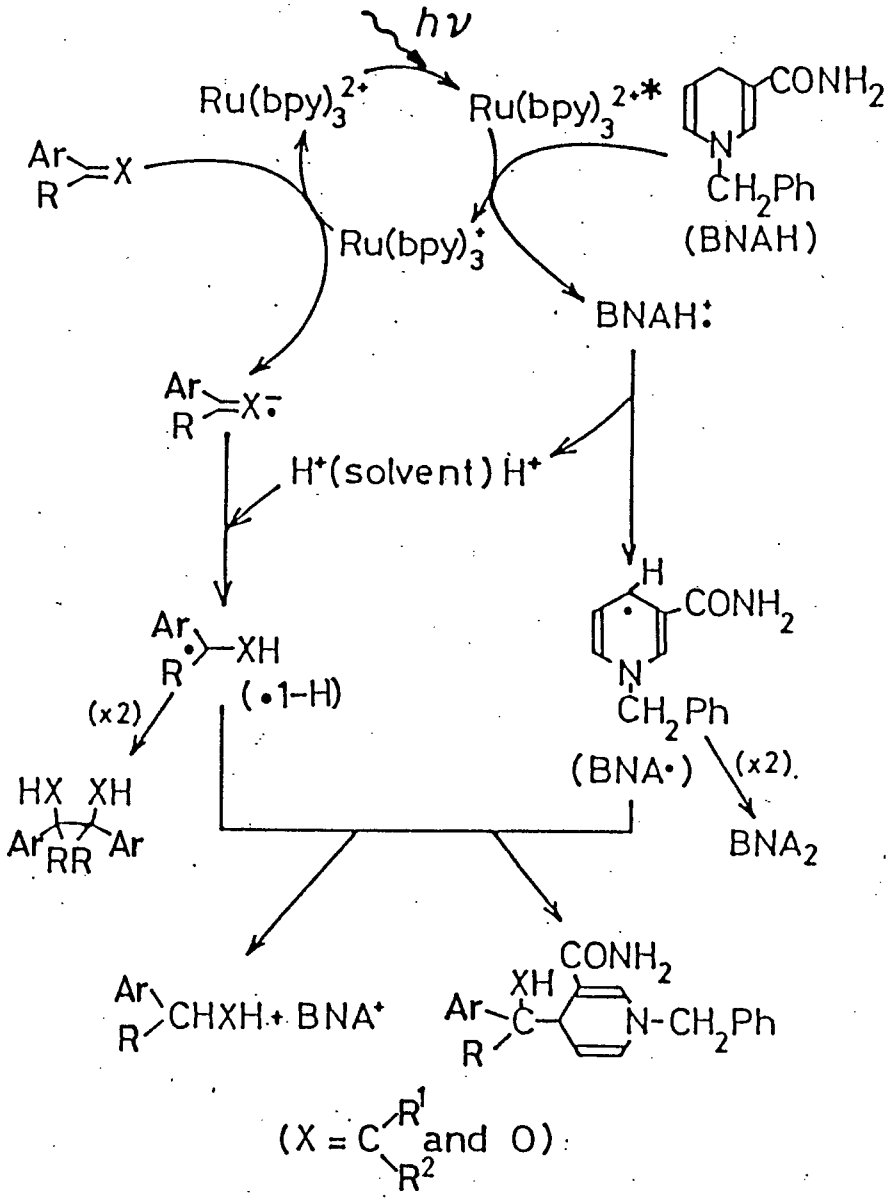
hν
Ru(bpy)3 2+
Ru(bpy)3 2+*
Ru(bpy)3 +
CONH2
N
CH2Ph
(BNAH)
Ar
R
X
BNAH:
X-
H+(solvent) H+
H
(•1-H)
(x2)
HX XH
Ar RR Ar
(BNA•)
BNA2
CHXH + BNA+
XH
N-CH2Ph
(X = C R1 R2 and O)

Scheme 1

2-2 RESULTS

Photosensitized Reactions. Methanolic solutions of $Ru(bpy)_3^{2+}$ (∿ 0.27 mM), BNAH (∿ 0.1 M), and **1a-f** (∿ 50 mM) were irradiated at > 470 nm. Equation 1 shows the products formed, yields of which are summarized in Table I.

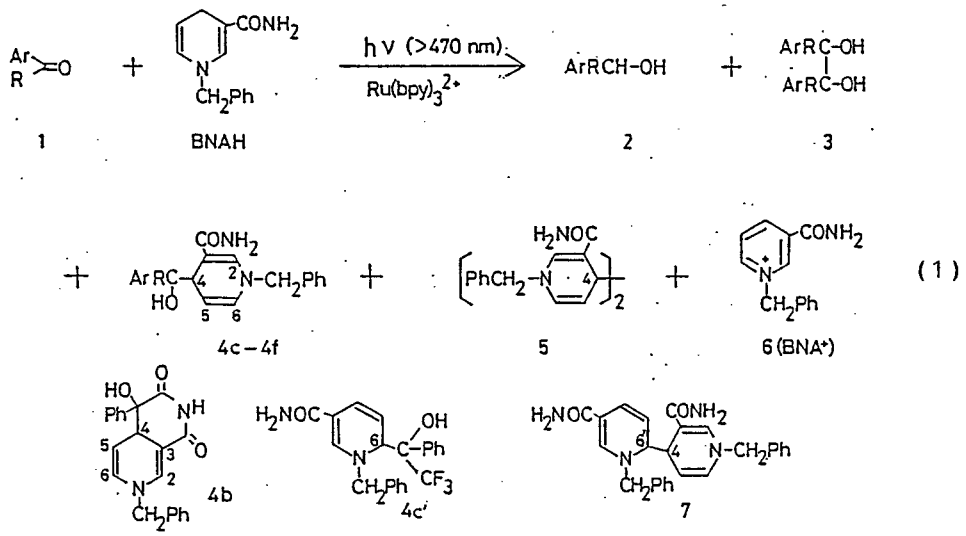

(1)

In the case of di(2-pyridyl) ketone (**1a**), the reduction to the corresponding alcohol (**2a**) quantitatively occurred with no formation of any adduct. The photosensitized reaction of methyl benzoylformate (**1b**) mainly gave an adduct as a single isomer of a condenced cyclic imide (**4b**) along with a smaller amount of **2b**. In the other cases 1:1 diastereomeric mixtures of 4-hydroxyalkyl-1,4-dihydronicotinamides (**4c-f**) were mainly formed, which were separated into each isomer by column chromatography on basic alumina.

Table I. $Ru(bpy)_3^{2+}$-Photosensitized Reactions of 1 with BNAH[a]

	1		Time	Conversion	Yield,[b] %		
	Ar	R	h	%	2	4[c]	5
a	2-Pyridyl	2-Pyridyl	2	79	95	0	10
b	C_6H_5	$COOCH_3$	7	100	18	60[d]	9
c	C_6H_5	CF_3	6	97	4[e]	86[f]	<1
d	2-Pyridyl	H	2	99	12	55	4
e	p-C_6H_5CN	H	3	97	5	63	6
f	C_6H_5	H	15	85	0	85	<1

[a] For methanolic solutions containing of 1 (∿ 50 mM), BNAH (∿ 0.1 M), and $Ru(bpy)_3^{2+}$ (∿ 0.27 mM) irradiated at > 470 nm under cooling with water. [b] Isolated yields based on the 1 consumed unless otherwise noted. [c] Mixtures of two diastereoisomers. [d] A single isomer. [e] GLC yield. [f] Total yield of **4c** and **4c'**.

In the case of **1c**, the diastereomeric 6-hydroxyalkyl-1,6-dihydronicotinamides (**4c'**) were isolated in very small amounts by HPLC while no indication was obtained for the formation of the positional isomers of **4d-f**. Although a half-oxidized dimer of BNAH (**5**) was isolated in a 10% yield in the case of **1a**, controll runs showed that 5 and an isomer of 5 (**7**) were not detected at an early stage of the photoreaction but only after substantial consumption of **1a**. In

the cases of **1b-f**, on the other hand, HPLC demonstrated that **5** and **7** were primary products.

In either case of 2-pyridinecarboxyaldehyde (**1d**) or p-cyanobenzaldehyde (**1e**), the corresponding alcohol (**2d** or **2e**) was formed in a significant amount at the completion of the photoreaction. However, the alcohol formation can be attributed to the consequences of secondary reactions since an induction period was observed as shown in Figure 1.

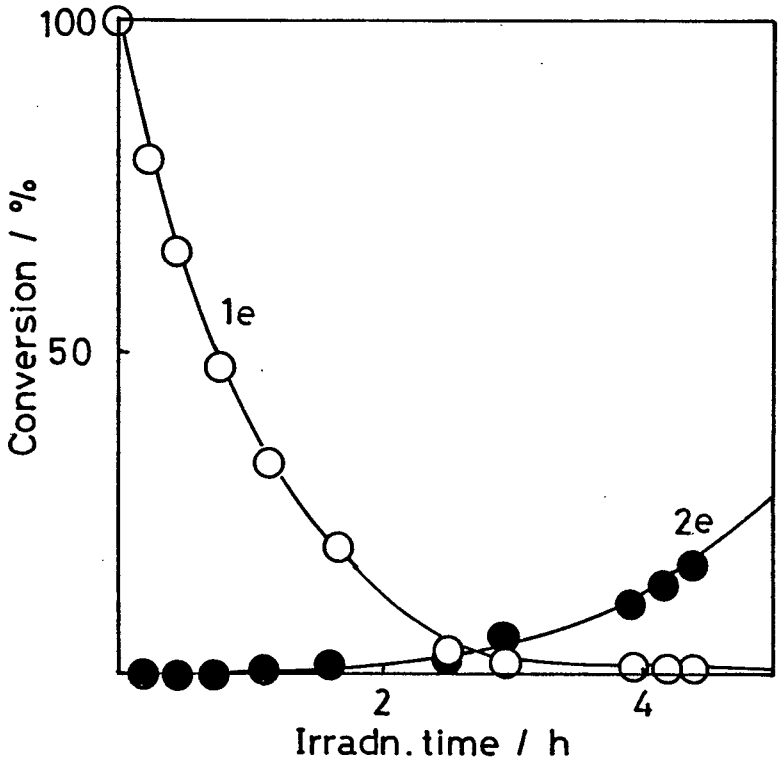

Figure 1. Time-conversion plots for the disappearence of **1e** (—○—) and for the formation of **2e** (—●—) by irradiation of a methanolic solution of **1e** (50 mM), BNAH (0.1 M), and $Ru(bpy)_3Cl_2 \cdot 6H_2O$ (1 mM) at >470 nm.

It was indeed found that irradiation of a methanolic solution of **4d** or **4e** (25 mM) in the presence of BNAH (25 mM) and $Ru(bpy)_3^{2+}$ (1 mM) gave **2d** or **2e** each in 40 - 50% yield described in chapter 4. On the other hand, either **2a** or **2b** was confirmed to be a primary photoproduct. In the case of trifluoroacetophenone (**1c**), the yield of **2c** in the photosensitized reaction was lower than that in a thermal reaction at room temperature, suggesting that the alcohol formation mostly occurs by a thermal reaction.

It was confirmed by VPC that 1,2-diphenyl-1,2-ethanediol (**3f**) was formed in 13% yield in the photosensitized reaction of **1f**. In the other cases, unfortunately, the corresponding diols (**3b-e**) which had been prepared by the $TiCl_4$-Zn reduction[14] of **1b-e** revealed no peak in VPC, probably due to decompositions. Furthermore, HPLC analyses of **3b-e** again encountered severe difficulties since the diol peaks were hidden by the huge peak of BNAH or the adduct.

Thermal Reactions. Heating of methanolic solutions of **1a-f** and BNAH at 60 ± 0.5 C in the dark resulted in the reduction to **2a-e** while 1f was not reduced to **2f** at all. In any case, neither the 1:1 adducts nor the half-oxidized dimers of BNAH could be detected at all. Table II summarizes the results.

Table II. Thermal Reacions of BNAH with 1 in the Dark[a]

1			Time	Conversion	Yields of 2[b]
	Ar	R	h	%	%
a	2-Pyridyl	2-Pyridyl	22	15	70
b	C_6H_5	$COOCH_3$	20	39	53
c	C_6H_5	CF_3	10	33	67
d	2-Pyridyl	H	8	40	5
e	p-C_6H_4CN	H	22	35	9
f	C_6H_5	H	20	0	0

[a] Methanolic solutions were heated at 60 C in the dark.

[b] Based on the 1 consumed.

2-3 DISCUSSION

Isolation and Identification of the Adducts (4b-f and 4c'). Column chromatography on basic alumina was found to be convenient for the isolation of relatively pure, diastereomeric 1:1 mixtures of **4c-f** in good yields as well as for separation of the diastereoisomers in amounts enough for various spectroscopic measurements. Analytically pure samples were thus obtained for the both diastereoisomers of **4c** and for the (RR + SS) isomers of **4e** and **4f** whereas the (RS + SR) isomers of the latter could not be made free from the contamination of very small amounts of the other isomers. In the case of **4d**, the both isomers could not be purified enough for elemental analysis because of decompositions occurring during isolation-purification procedures. However, all the compounds isolated were found to be sufficiently pure for spectroscopic purposes. In the case of **4b**, partial evaporation of an irradiated solution resulted in efficient precipitation of solids which were then recrystallized to give an analytically pure sample. Either the precipitate or the purified sample of **4b** revealed only a single HPLC peak unlike diastereomeric mixtures of **4c-f**, even though methanol-water mixtures in different ratios were used as the moving phase. Moreover the ^{1}H NMR spectra show homogeneous resonances independently of solvents. These observations demonstrate that **4b** is homogeneous in the diastereochemistry.

All the isolated adducts commonly reveal similar spectroscopic features characteristic of the 4-substituted 1,4-dihydronicotinamide structure. However, the UV absorption maximum of **4b** (377 nm) is significantly longer

than those of the other adducts (335 - 343 nm), thus reflecting the more conjugated, bicyclic imide structure. Moreover **4b** shows no ^{1}H NMR signal assignable to the CH_3O protons but a broad singlet of imide NH at δ 10.4. The absolute structures of (RR + SS)-**4e** and (RR + SS)-**4f** were unambiguously determined by X-ray crystallographic studies; an ORTEP drawing of (RR + SS)-**4e** is shown in Figure 2.

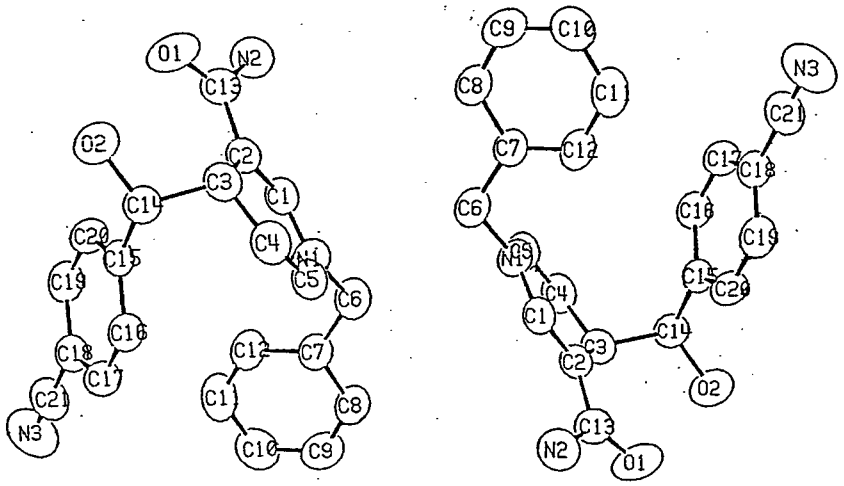

Figure 2. An ORTEP drawing of (RR + SS)-**4e** showing the atomic numbering scheme.

A preliminary X-ray crystallographic analysis of an isomer of **4c** (**4c**-A) gave a strong support to the assignment of the (RS + SR) configuration, which was also made on the basis of ^{1}H NMR analysis (vide infra). Further refinement of data is now in progress. In cases of the other adducts, however, all attempts failed to obtain crystals suitable for crystallographic measurements.

A notable observation for the structure assignment of **4c** is that H-5 of an isomer (**4c**-A) shows the ^{1}H NMR resonance at δ 3.88, a chemical shift much higher than that

of the other isomer (**4c**-B) (δ 4.9). Molecular models of **4c** show that conformations at the two chiral centers are almost freezed because of the remarkable steric bulkiness of the $PhCH(OH)CF_3$ group independently of the configurations. With regard to the conformational freezing, it should be noted that the OH proton of the both isomers shows the ^1H NMR signals at very low fields in either $CDCl_3$ or CD_3SOCD_3 (δ 8 - 9) compared with those of the other adducts (δ 5.6 - 6.5), an observations demonstrating the formation of relatively strong hydrogen bonding between OH and $CONH_2$ associated with conformational rigidity. With the (RS + SR) configuration, therefore, H-5 should be strongly shielded by the phenyl ring at the quarternary chiral center while such a shielding effect on H-5 can not be expected with the (RR + SS) configuration, as shown in Figure 3. On the basis of these arguments, we assign the (RS + SR) configuration to **4c**-A and the (RR + SS) one to **4c**-B.

With regard to the configuration of **4b**, it should be noted that the chemical shift of H-5 (δ 3.92) is very similar to that of (RS + SR)-**4c** but much higher than that of the (RR + SS)-**4c**. According to molecular models, **4b** is again conformatioally freezed so that H-5 is shielded by the phenyl ring at the quarternary chiral center with the (RS + SR) configuration but not at all with the (RR + SS) one, as shown in Figure 3. Therefore the (RS + SR) configuration is attributable to **4b**. On the other hand the diastereomeric configurations of **4d** are left unidentified since the diastereoisomers reveal very similar spectroscopic properties, perhaps due to free rotation of the ArCH(OH) group.

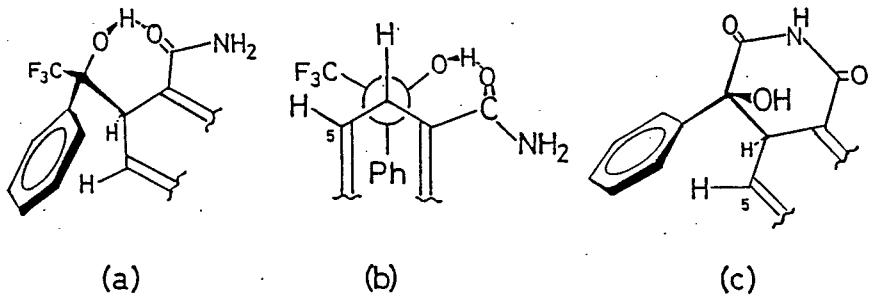

Figure 3. (a) A perspective illustration of (RS + SR)-**4c** in the most stable conformation; H-5 is located just over the shielding region of the phenyl ring. (b) The Newman projection formulas of the (RR + SS) configuration of **4c**; the phenyl ring can not take any conformation for shielding of H-5. (c) A perspective illustration of (RS + SR)-**4b**.

The other minor isomers of **4c** (**4c'**-A and **4c'**-B) show IR and mass spectra very similar to each other as well as to those of **4c**. In ^{1}H NMR the benzylic methylene protons of either **4c'**-A or **4c'**-B show an AB quartet which should be the consequence of diastereotopic splitting, thus demonstrating that the minor adducts are the diasteromeric 6-substituted 1,6-dihydronicotinamides. Similar diastereotopic splitting occurs for the benzylic protons of the 4,6'-bonded half-oxidized dimers of BNAH (**7**).[11] Significantly **4c'**-A reveals the ^{1}H NMR resonance of the benzylic methylene protons at a much highter field (δ 3.33) than either **4c'**-B (δ 4.63) or the diastereomers of **7** (δ 4.38 and 4.42).[11] On the contrary H-5 of **4c'**-B shows the signal at δ 5.98, a higher field compared with the H-5 resonance of **4c'**-A which is overlapped with the aromatic resonances at δ 6.5 - 7.8. Molecular models reveal that conformations of these adducts

are again freezed to allow specific shielding effects of the phenyl ring on the benzylic methylene protons with the (RR + SS) configurations or on H-5 with the (RS + SR) cofiguration as shown in Figure 4. These arguments enable us to assign the (RR + SS) configuration to **4c'**-A and the (RS + SR) configuration to **4c'**-B.

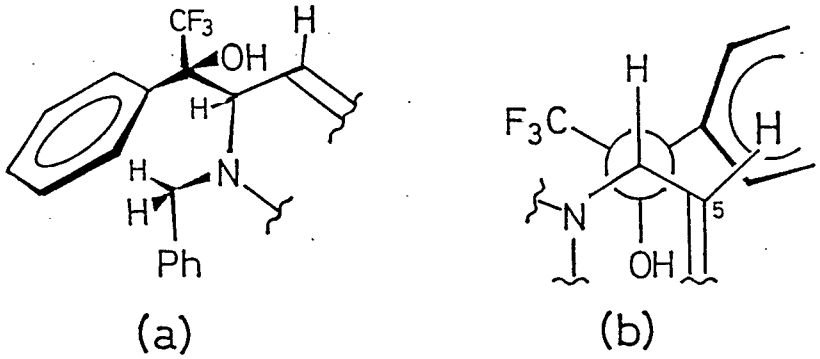

Figure 4. (a) A perspective illustration of (RR + SS)-**4c'** in the most stable conformation; the benzylic protons are strongly shielded. (b) The Newman projection formulas of (RS + SR)-**4c'** which shows the shielding of H-5 by the phenyl ring in the most stable conformation.

Mechanism. In chapter 1, it was previously demonstrated that the photosensitized reactions of olefins with BNAH by $Ru(bpy)_3^{2+}$ proceed via indirect electron-proton transfer from BNAH to olefins of $E_{1/2}^{red} > -2.2$ V vs. Ag/Ag^+, a unique mechanistic sequence arising from the facile generation of the azacyclohexadienyl radical, BNA·, by the proton loss from very acidic $BNAH^{+\cdot}$ (pKa < 1)[12] following photochemical electron transfer. This radical may undergo electron transfer or radical coupling with the half-reduced olefin radicals depending on the substituents of olefins as shown in Scheme I. This mechanism can reasonably describe the present photosensitised reactions. It was confirmed that the luminescence of $Ru(bpy)_3^{2+}$ is not quenched by **1a-f** at all while the luminescence quenching by BNAH efficiently occurs as described in chapter 1. Moreover no photosensitized reaction occurred with acetophenone and benzophenone that have $E_{1/2}^{red} < -2.2$ V, probably the limit for the occurence of electron transfer from $Ru(bpy)_3^+$ to carbonyl compounds as well as to olefins.

According to this mechanism, reduction potentials of the half-reduced species, ·**1**-H, should be primarily essential in determining the choice of the electron transfer or the radical-coupling reaction with BNA·. Figure 5 shows the polarographic behaviors of **1b** in which the first reduction wave grows at the expense of the second one being accompanied by positive shifts upon addition of methanol to an acetonitrile solution of **1b** . The two reduction waves in acetonitrile have similar diffusion-current constants (I_d), probably corresponding to the reversible, sequential two-electron-transfer processes (eq 2 and 3).[13] The effect of methanol on the polarographic behaviors can be reasonably

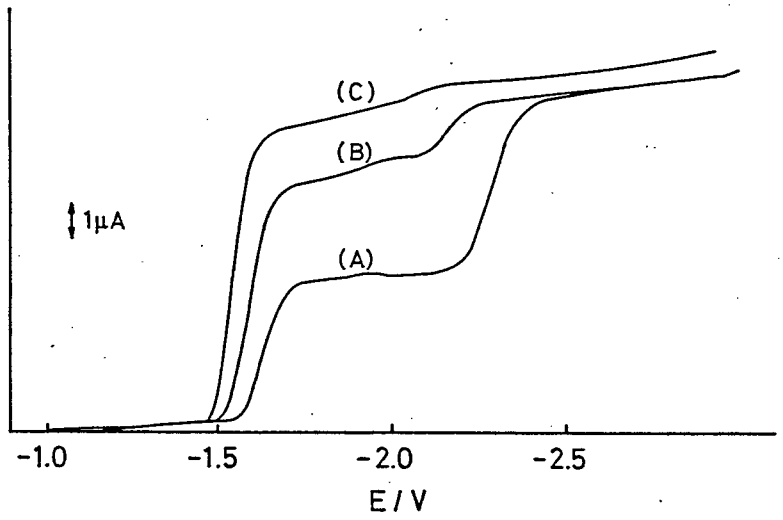

Figure 5. Polarograms of deaerated acetonitrile solutions of **1b** (1.15 mM) (A) in the absence of methanol and in the presence of (B) 1.0 vol% methanol and (C) 3.0 vol% methanol vs. an $Ag/AgNO_3$ reference electrode; $[Et_4NClO_4]$ = 0.1 M; Scan Rate 10 mV s^{-1}.

interpreted in terms of the ECE processes (eq 4 and 5) occurring in the first reduction wave as discussed for the electrochemical reduction of benzophenone in the presence of a proton donor.[14,15] In other words, the potential of this reduction wave in the presence of methanol is certainly diagnostic for qualitative estimation of the reduction potential of **·1b-H**. Table III lists the polarographic reduction potentials of **1a-f** in either methanol or acetonitrile together with quantum yields for the disappearance of **1a-f** and for the formation of **2a,b**. The single waves of **1a** and **1d** in methanol should be due to the ECE processes whereas the second waves of **1e** and **1f** might correspond to eq 5.[16-18]

$$\mathbf{1} + e^- \rightleftharpoons \mathbf{1}^{-\cdot} \qquad (2)$$

$$\mathbf{1}^{-\cdot} + e^- \rightleftharpoons \mathbf{1}^{2-} \qquad (3)$$

in acetonitrile

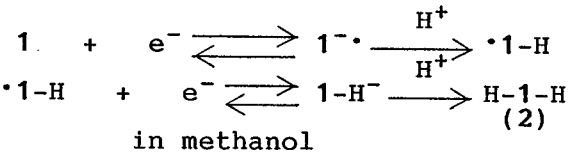

in methanol

The reduction wave of BNA^+ in methanol appears at - 1.445 V vs. Ag/Ag^+ certainly due to the one-electron reduction process. Although this potential does not necessarily equal the oxidation potential of BNA•, it is significant to note that this value is not far from the estimated oxidation potentials of BNA• and related species in acetonitrile (- 1.0 ∿ - 1.4 V vs. Ag/Ag^+)[19] as well as from the redox potential of the $NAD^+/NAD•$ couple in a buffer solution at pH 9.1 (- 1.155 V vs. SCE).[20] The observed reduction potential of BNA^+ is very similar to that of the reduction wave of **1a** in methanol and only slightly positive than that of **1b**, while the reduction potentials of **1d-f** corresponding to eq 5 are much more negative. Namely, BNA• can undergo electron transfer to •**1a**-H in a high efficiency and also to •**1b**-H (eq 6) competitively with the radical coupling (eq 7), while the latter reaction predominantly occurs with the other half-reduced radicals. The essential role of BNA• in the two-electron reduction is demonstrated by the complete lack of the reduction of **1a** to **2a** in the $Ru(bpy)_3^{2+}$-photosensitized reaction of **1a** using a potential one-electron donor, N,N-dimethyl-p-toluidine, in place of BNAH.

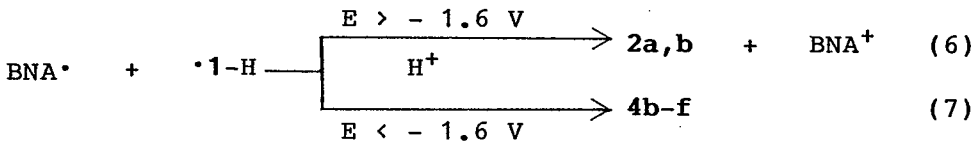

Table III. Polarographic Data of 1a-f and Quantum Yields for the Disappearance of 1 (Φ_{-1}) and the formation of 2 (Φ_2)

1		$-E^{red}_{1/2}$, V[a] (I_d, μA $mM^{-1}mg^{2/3}s^{-1/2}$)[b]					
Ar	R	Methanol[d]		Acetonitrile[e]		Φ_{-1}[c]	Φ_2[c]
a 2-Pyridyl	2-Pyridyl	1.46 (4.4)		∿1.8 (3.9)	∿1.9 (2.9)	0.20	0.20
b C_6H_5	$COOCH_3$	∿1.5 (3.8)	∿1.6 (2.4)	1.64 (3.6)	2.41 (3.6)	0.49	0.14
c C_6H_5	CF_3	1.83 (0.5)		1.71 (4.5)	2.38 (3.5)	0.14	0
d 2-Pyridyl	H	1.71 (5.4)		1.91 (2.4)	2.48 (0.7)	0.44	0
e p-C_6H_4CN	H	1.52 (3.3)	1.94 (3.0)	1.70 (2.9)	2.28 (0.7)	0.49	0
f C_6H_5	H	1.86 (3.2)	∿2.1 (1.7)	2.17 (3.8)		0.05	0

[a] Polarographic half-wave potentials in volts vs. $Ag/AgNO_3$ using a dropping mercury electrode and $NaClO_4$ (0.1 M) in methanol or Et_4NClO_4 (0.1 M) in acetnitrile as the supporting electrolyte. [b] Diffusion current constant, $I_d = i_d/Cm^{2/3}t^{1/6}$. [c] At 520 nm for deaerated methanolic solutions containing a carbonyl compound (50 mM), BNAH (0.1 M), and $Ru(bpy)_3^{2+}$ (2.7 mM). [d] Capillary with $m^{2/3}t^{1/6}$ of 1.13 $mg^{2/3}s^{-1/2}$ and a drop time of 0.5 s (pulse interval) at a 67 cm-pressure. [e] Capillary with $m^{2/3}t^{1/6}$ of 1.15 $mg^{2/3}s^{-1/2}$ and a drop time of 0.5 s (pulse interval) at a 67 cm pressure.

Interestingly the cross coupling between BNA• and •**1**-H (eq 7) is highly regioselective in a sharp contrast to the nonselective dimerization of BNA•.[21] This can be explained by assuming important roles of hydrogen bonding between the hydroxyl group of •**1**-H and carbamoyl carbonyl of BNA• in bringing the radicals favorably for the predominant coupling at C4 of BNA•. In the case of •**1c**-H, however, steric bulkiness of this radical would weaken the hydrogen bonding to allow the competitive coupling at C6 even to a minor extent. According to this interpretation, the low-yield formation of the C4-bonded 1:1 adducts in the photosensitized reactions of olefins with BNAH would be , at least in part, due to the consequences of nonselective radical-coupling reactions arising from the lack of such specific hydrogen bonding as well as from steric repulsions in the relevant pathway. By the same reason, such hydrogen bonding might be also kinetically effective to facilitate either electron transfer or the cross coupling between BNA• and •**1**-H predominating over the homo coupling reaction of each radical.[22] Concerning the formation of **1b**, on the other hand, no significant data are available for a reasonable interpretation of mechanistic details, though interactions of the methoxycarbonyl group of •**1b**-H and the carbamoyl substituent of BNA• are presumed to play important roles in the stereoselective cross coupling of the radicals.

Comparisons between Thermal and Photosensitized Reactions. The thermal reactions of **1a-f** with BNAH in methanol did not give at all the 1:1 adducts (**4b-f**) nor the half-oxidized dimers of BNAH (**5** and **7**), thus revealing quite different behaviors from the $Ru(bpy)_3^{2+}$-photosensitized reactions. It is therefore implied that the photo-

sensitized reactions provide a useful synthetic tool for the preparation of **4b-f**. Moreover, there is little parallelism in the "two-electron" reduction of the carbonyl compounds between the two types of reactions. In particular the efficient reduction of **1c** to **2c** in the dark shows a sharp contrast to the lack of the reduction in the redox-photosensitized reactions.

A mechanistic implication of the entire different behaviors of the thermal reactions is that a simple ECE mechanism involving discrete radical intermediates is probably inadequate to describe the hydride-equivalent transfer from BNAH to **1a-e** in the dark, since the redox-photosensitized reactions indeed involve indirect electron-proton transfer as has been discussed in the previous section. Moreover, the ECE mechanism again disagrees with specific transfer of the C4 deuterium label of NADH models to carbonyl carbon of carbonyl compounds in the dark,[23] unless specific interactions between ion-radical pairs in a solvent cage would operate to allow unique reactions entirely different from those of free ion radicals in which protonation does occur at carbonyl oxygen of **1a-f**. Alternatively sequential transfer of an electron and a hydrogen atom would be another possible candidate for the mechanism of the thermal reduction of **1a-e**. If this were the case, the hydrogen-atom transfer following the initial electron transfer from BNAH to **1a-e** should be much faster than the proton transfer from very acidic $BNAH^{+\cdot}$[12] to the very basic anion radical of **1a-e**. Therefore a mechanism involving hydride transfer may be the best choice.

2-4 CONCLUSIONS

The $Ru(bpy)_3^{2+}$-photosensitized reactions of BNAH with **1b-f** provides a useful synthetic method for the preparation of the 4-hydroxyalkylated 1,4-dihydronicotinamides, **4b-f**, a new class of compounds which can not be obtained by direct thermal reactions in the dark. The two-electron reduction of carbonyl compounds is predicted to occur upon redox photosensitization by $Ru(bpy)_3^{2+}$ in cases where polarographic reduction waves in methanol appear at more positive potentials than - 1.6 V vs. Ag/Ag^+, a formal limit for electron transfer from BNA$^\bullet$ to $^\bullet$**1**-H to occur. On the other hand, electron-transfer mechanisms involving discrete radical intermediates can not reasonably interpret chemical behaviors of thermal reactions of BNAH with **1a-e**.

2-5 EXPERIMENTAL SECTION

Melting points were taken on a hot plate and are uncorbrected. Vapor-phase chromatography (VPC) was performed on a Shimadzu GC-7A dual column instrument using a 0.5 m x 3.2 mm glass column packed with 5% UCON LB550X on Shimalite W, a 1 m x 3.2 mm column packed with 5% PEG 20M on Shimalite W, a 2 m x 3.2 mm column packed with 3% OV-17 on Chromosorb W, and a 1 m x 3.2 mm column packed with 5% OV-1 on Celite 545. HPLC was carried out on a Toyosoda CCPD dual pump and a Yanaco M-315 spectromonitor using 25 cm x 4.6 mm column packed with Chemicosorb 7-ODS-H; the mobile phase was 40% methanol in NaOH-KH_2PO_4 buffer solution (pH 7) at a flow rate of 0.8 mL/min, and the wavelength of the spectromonitor was set at 355 nm. ^1H NMR spectra were recorded on a JEOL JNM-PMX-100 spectrometer, ^{13}C NMR spectra on a JEOL FX-100, IR spectra on a Hitachi 220-10 spectrometer, UV and visible absorption spectra on a Hitachi 220-A spectrometer, and mass spectra on a Hitachi RMU-6E. Luminescence spectra were recorded on a Hitachi 850 spectrofluorometer for deaerated solutions of $Ru(bpy)_3^{2+}$ (0.25 mM) after correction of instrument responses.

All data sets ($I = > 30 (I)$) in X-ray crystallographic analysis were measured by the ω-2θ method on an Enraf-Nonius CAD4 diffractometer with graphite monochromated MoKα radiation (λ = 0.71069 A). The structure was solved by the direct method (MULTAN) and the refinement was made with anisotropic temperature factors for all the non-hydrogen atoms and with isotropic thermal parameters for the hydrogens. For details of the data see supplementary section.

The preparation and purification of BNAH[24] and $Ru(bpy)_3Cl_2 \cdot 6H_2O$[25] were carried out according to the literature methods. The carbonyl compounds (**1a-f**) were obtained from Nakarai Chemicals and purified by recrystallization or distillation. Methanol was distilled from magnesium methoxide.

Polarographic measurements were performed for air-free dry solutions containing **1a-f** or BNA^+ ($\sim$ 1 mM) and a supporting electrolyte (0.1 M), sodium perchlorate in methanol or tetraethylammonium perchlorate in acetonitrile, at 20 ± 0.1 °C by using a Yanagimoto P-1100 potentiostat. The reference electrode is an $Ag/AgNO_3$ (0.1 M) in methanol or acetonitrile, and the working electrode was a dropping Hg electrode at a 67-cm pressure operated at a pulse-regulated dropping time of 0.5 s. The $m^{2/3}t^{1/6}$ values were 1.15 $mg^{2/3}s^{1/6}$ in acetonitrile and 1.13 $mg^{2/3}s^{1/6}$ in methanol.

Determination of Quantum Yields. Quantum yields were determined for 4-mL Ar-purged solutions containing **1a-f** (50 mM), BNAH (0.1 M), and $Ru(bpy)_3Cl_2 \cdot 6H_2O$ (3 mM) in quartz cuvettes by using a Reinecke's salt actinometer.[26] The incident light at 520 nm was isolated from an Ushio Xenon lamp (300 W) by using a Hitachi high-intensity monochrometer, and the intensity was determined to be 2.57×10^{17} photons/min. All the procedures were performed in a dark room with a safety lamp. Both the disappearance of **1a-f** and the formation of **2a,b** were analyzed by VPC and plotted against time. Quantum yields were calculated from the slopes of initial linear portion of the plots.

Photosensitized Reaction of 1a. A 100-mL methanolic solution of **1a** (0.96 g, 5.1 mmol), BNAH (2.14 g, 10 mmol), and $Ru(bpy)_3Cl_2 \cdot 6H_2O$ (20 mg, 0.027 mmol) was irradiated at >470 nm for 2h under cooling with water. Details of the irradiation apparatus and the filter solution were described in chapter 1. The irradiated solution was evaporated to 10 mL to give a precipitate, which was filtered and washed with cold methanol (3 mL) to give **5** (0.21 g, 10%) as yellow solids. The filtrate was distilled in vacuo to give **2a** (0.89 g, 97%); bp 105 - 110 °C (1.1 mmHg). To the residue was added dichloromethane (100 mL) and then cold 0.1 M hydrochloric acid (300 mL). After vigorous shaking, the hydrochloric acid layer separated was washed with dichloromethane (100 mL) and then neutralized with cold 0.5 M NaOH to pH 7 under ice cooling. After vacuum evaporation to dryness, the residue was extracted with 300 mL boiling ethanol and then filtered. The filtrate was evaporated to give 1-benzylnicotinamide chloride (**6**) (0.58 g, 23%). A similar treatment of BNAH did not give **6** at all.

Photosensitized Reaction of 1b. Similarly a 140-mL methanolic solution of **1b** (1.25 g, 8.2 mmol), BNAH (3.27 g, 15.3 mmol), and the sensitizer (30 mg, 0.04 mmol) was irradiated for 7 h. The irradiated solution was evaporated to 50 mL to give a precipitate, which was filtered and washed with cold methanol (3 mL) to give **4b** (1.19 g, 60%) as pale yellow solids: mp 223 - 224 °C dec (DMF-water); IR (KBr) ν_{max} 3445 (OH), 3100 (NH), 1685 (C=O and/or C=C), 1659 (C=O), 1570 cm^{-1} (C=C); UV (MeOH) λ_{max} 377 nm (ε 5960); ^1H NMR (CD_3SOCD_3) δ 3.92 (dd, 1H, J = 1.6, 8.0 Hz, H-5), 4.06 (br s, 1H, H-4), 4.46 (s, 2H, CH_2Ph), 6.00 (br d, 1H, J = 8

Hz, H-6), 6.52 (s, 1H, exchanged with D_2O, OH), 7.12 - 7.50 (m, 11H, H-2, 2 x Ph), 10.36 (s, 1H, exchanged with D_2O, NH); ^{13}C NMR (CD_3SOCD_3) δ 41.0, 56.0, 76.4, 96.1, 101.0, 125.1, 126.8, 127.7, 127.4, 127.6, 128.2, 128.7, 131.4, 137.9, 140.2, 141.1, 166.5, 172.7; MS, m/e (relative intensity) 346 (13, M^+), 328 (32, $M-H_2O$), 312 (27, BNA^+), 255 (8, $M-PhCH_2$), 169 (65), 105 (27). 91 (100, $PhCH_2$). Anal. Calcd for $C_{21}H_{18}N_2O_3$: C, 72.82; H, 5.24; N, 8.09. Found: C, 72.56; H, 5.28; N, 8.17. After filtration of **4b**, the filtrate was further evaporated to 10 mL and then cooled to give a precipitate, filtration of which gave 5 (0.31 g, 9%). Vacuum distillation of the filtrate gave **2b** (0.24 g, 18%); bp 75 - 110 C (0.3 mmHg).

Photosensitized Reaction of 1c. A 150-mL methanolic solution of **1c** (1.31 g, 7.5 mmol), BNAH (3.24 g, 15.1 mmol), and the sensitizer (30 mg, 0.04 mmol) was irradiated for 6 h. The photolysate was evaporated and then chromatographed on 100 g of basic alumina (70 - 230 mesh, Merck Art 1076). After elution of BNAH (0.2 g) with 2% methanol in diethy lether (400 mL), further elution with 4 - 50% methanol in diethyl ether (7 x 200 mL) gave mixtures of the diastereomers of **4c** and **4c'** in different ratios. The combined yield was 2.52 g (86%). A small amount of 5 (20 mg) was finally eluted with methanol (200 mL).

The first fraction in which an isomer of **4c** had been enriched was subjected to repeated column chromatography to give the (RS + SR) isomer of **4c** as pale yellow solids: mp 152.5 - 154.0 °C dec (Et_2O-MeOH); IR (KBr) ν_{max} 3430 (OH), 3300, 3175 (NH_2), 1667 (C=C), 1640 (C=O), 1565 cm^{-1} (C=C); UV (MeOH) λ_{max} 335 nm (ε 4680); ^1H NMR (CD_3SOCD_3) δ 3.72 (br

d, 1H, J = 5.6 Hz, H-4), 3.88 (dd, 1H, J = 5.6, 7.6 Hz, H-5), 4.45 (s, 2H, CH_2Ph), 6.13 (d, 1H, J = 7.6 Hz, H-6), 7.04 - 7.76 (m, 13H, H-2, NH_2, 2 x Ph), 9.01 (s, 1H, exchanged with D_2O, OH); ^{13}C NMR (CD_3SOCD_3) δ 43.4, 56.5, 79.7, 100.3, 101.5, 126.8, 127.5, 128.5, 130.2, 137.6, 140.0, 172.8; MS, m/e (relative intensity) 388 (0.2, M^+), 371 (0.2, M - OH), 213 (18, BNA^+), 174 (0.2, $PhCOCF_3$), 169 (2), 123 (5), 105 (7), 91 (100, $PhCH_2$). Anal. Calcd for $C_{21}H_{19}F_3N_2O_2$: C, 64.94; H, 4.93; N, 7.21. Found: C, 64.73; H, 4.82; N, 7.18.

Similarly, repeated column chromatography of another fraction eluted with 7% methanol in diethyl ether gave the (RR + SS) isomer of **4c** as pale yellow solids: mp 176.5 - 177.5 °C dec (Et_2O-MeOH); IR (KBr) ν_{max} 3475 (OH), 3320, 3180 (NH_2), 1675 (C=C), 1635(C=O), 1565 cm^{-1} (C=C); UV (MeOH) λ_{max} 338 nm (ε 5370); ^1H NMR (CD_3SOCD_3) δ 4.08 - 4.28 (3H, m overlaid with s at 4.16, H-4, CH_2Ph), 4.75 - 4.98 (m, 1H, H-5), 6.16 (d, 1H, J = 7.9 Hz, H-6), 6.86 - 7.63 (m, 13 H, H-2, NH_2, 2 x Ph), 8.53 (s, 1H, exchanged with D_2O, OH); ^{13}C NMR (CD_3SOCD_3) δ 43.3, 56.5, 79.7, 100.1, 101.4, 126.8, 127.4, 127.8, 128.5, 130.2, 137.5, 140.0, 172.8; MS, m/e (relative intensity) 388 (0.6, M^+), 371 (1), 213 (56), 174 (0.5), 169 (11), 123 (32), 105 (7), 91 (100). Anal. Calcd for $C_{21}H_{19}F_3N_2O_2$: C, 64.94; H, 4.93; N, 7.21. Found: C, 65.12; H, 5.06; N, 7.26.

Fractions which had been eluted with 30 - 50% methanol in diethyl ether was subjected to preparative HPLC to give (RS + SR)-**4c'** as a yellow oil and (RR + SS)-**4c'** as pale yellow solids in small amounts. Further treatment for purification resulted in consumptions of the compounds.

(RS + SR)-**4c'**: IR ($CHCl_3$ solution) ν_{max} 3480, 3350,

3200, 1645, 1590, 1555 cm^{-1}; ^1H NMR ($CDCl_3$) δ 4.2 - 4.5 (m, 1H, H-6), 4.6 (br s, 1H, exchanged with D_2O, OH), 4.63 (ABq, J = 5 Hz, ν_{AB} = 14, CH_2Ph), 5.67 (br d, J = 9 Hz, H-5), 5.4 - 5.9 (br s, 2H, exchanged with D_2O, NH_2), 5.98 (d, 1H, J = 9 Hz, H-4), 7.0 - 7.7 (m, 11H, H-2, 2 x Ph); MS, m/e (relative intensity) 388 (0.4, M^+), 371 (0.4), 213 (40), 174 (0.4), 169 (7), 123 (16), 105 (16), 91 (100).

(RR + SS)-**4c'**: IR ($CHCl_3$ solution) ν_{max} 3560, 3400, 3100, 1642, 1589, 1548 cm^{-1}; ^1H NMR ($CDCl_3$) δ 3.33 (ABq, 2H, J = 16 Hz, ν_{AB} = 49, CH_2Ph), 4.33 (br, 1H, exchanged with D_2O, OH), 4.63 (d, 1H, J = 6.0 Hz, H-6), 4.7 - 5.2 (m, 1H, H-5), 5.67 (br s, 2H, exchanged with D_2O, NH_2), 6.5 - 7.8 (m, 12H, H-2, H-4, 2 x Ph); MS, m/e (relative intensity) 388 (0.3, M^+), 371 (0.3), 213 (34), 174 (0.3), 169 (7), 123 (11), 105 (11), 91 (100).

Photosensitized Reaction of 1d. After irradiation of a 150-mL methanolic solution of **1d** (0.85 g, 7.9 mmol), BNAH (3.28 g, 15.3 mmol), and the sensitizer (30 mg, 0.04 mmol) for 2h, the irradiated solution was evaporated and then distilled in vacuo to give **2d** (0.1 g, 12%); bp 50 - 70 C (0.1 mmHg). The residue was subjected to column chromatography on basic alumina. Elution with 7% methanol in diethyl ether (400 mL) gave BNAH (0.81 g) and then diastereomeric mixtures of **4d** were eluted with 10% and 20% methanol in diethyl ether (200 mL each); the combined yield of **4d** was 0.82 g (55%). Further elution with 30% methanol in diethyl ether gave **5** (0.13 g, 4%). Repeated column chromatography of the first and second fractions of **4d** resulted in the separation of the diastereoisomers (**4d**-A and **4d**-B) as yellow solids. Further purification of these

compounds could not be made since recrystallization resulted in the deposition of brownish tars.

4d-A: mp 89 - 92 °C dec (CH_2Cl_2); IR (KBr) ν_{max} 3650, 3330, 3000, 1685, 1648, 1600, 1575, 1440, 1405 cm^{-1}; ^1H NMR (CD_3SOCD_3) δ 3.86 (dd, 1H, J = 2.4, 5.6 Hz, H-4), 4.22 (dd, 1H, J = 5.6, 7.8 Hz, H-5), 4.34 (s, 2H, CH_2Ph), 4.58 (dd, 1H, J = 2.4, 5.6 Hz, ArCH(OH)), 5.67 (d, 1H, J = 5.6 Hz, exchanged with D_2O, OH), 6.03 (d, 1H, J = 8.0 Hz, H-6), 6.79 (br s, 2H, exchanged with D_2O, NH_2), 7.04 - 8.60 (m, 10H, H-2, Ph, C_5H_4N); ^{13}C NMR (CD_3SOCD_3) δ 38.1, 56.0, 76.5, 100.7, 101.6, 120.9, 121.4, 126.8, 128.3, 130.6, 135.5, 138.3, 138.9, 147.8, 162.2, 170.2; MS, m/e (relative intensity) 321 (0.5, M^+), 303 (2, M - H_2O), 213 (13, BNA^+), 107 (26, C_5H_4NCHO), 105 (21), 91 (100).

4d-B: mp 161 - 162 °C dec (CH_2Cl_2-MeCN); IR (KBr) ν_{max} 3680, 3330, 3000, 1680, 1665, 1602, 1598, 1574, 1435, 1405 cm^{-1}; UV (MeOH) λ_{max} 338 nm (ε 6599); ^1H NMR (CD_3SOCD_3) δ 3.74 (q, 1H, J = 5.8 Hz, H-4), 4.24 - 4.40 (3H, m overlaid with s at 4.28, H-5, CH_2Ph), 4.49 (dd, 1H, J = 4.4, 5.8 Hz, ArCH(OH), 5.74 (d, 1H, J = 4.4 Hz, exchanged with D_2O, OH), 5.92 (d, 1H, J = 7.6 Hz, H-6), 6.84 (br s, 2H, exchanged with D_2O, NH_2), 6.96 - 8.54 (m, 10H, H-2, Ph, C_5H_4N); ^{13}C NMR (CD_3SOCD_3) δ 38.1, 56.1, 78.1, 101.2, 102.4, 121.9, 122.1, 126.8, 127.2, 128.5, 129.9, 135.6, 138.3, 147.8, 162.0, 170.8; MS, m/e (relative intensity) 321 (0.5, M^+), 303 (2), 213 (11), 107 (22), 105 (23), 91 (100). Anal. Calcd for $C_{19}H_{19}N_3O_2$: C, 71.01; H, 5.96; N, 13.08. Found: C, 70.56; H, 5.88; N, 13.03.

Photosensitized Reaction of 1e. A 150-mL methanolic solution of **1e** (0.90 g, 6.8 mmol), BNAH (3.35 g, 15.6 mmol),

and the sensitizer (30 mg, 0.04 mmol) was irradiated for 5 h, evaporated, and then distilled in vacuo to give **2e** (50 mg, 5%); bp 140 - 150 °C (10 mmHg). The residue was chromatographed on basic alumina as described above to give BNAH (0.82 g), diastereomeric mixtures of **4e** (1.35 g, 63%), and **5** (0.16 g, 6%). Repeated column chromatography of each fraction of **4e** gave a pure sample of the (RR + SS) isomer and a sample of the other isomer contaminated with small amounts of the former and another unknown component. The latter could not be made free from the contamination.

(RR + SS)-**4e**: mp 156.5 - 157.5 °C dec ($CHCl_3$-MeOH); IR (KBr) ν_{max} 3460, 3305, 3175, 2260 (C=N), 1675, 1635, 1550 cm^{-1}; UV (MeOH) λ_{max} 343 nm (ε 7590); ^1H NMR (CD_3SOCD_3) δ 3.72 (dd, 1H, J = 3.2, 5.0 Hz, H-4), 4.20 (s, 2H, CH_2Ph), 4.47 (dd, 1H, J = 3.2, 5.0 Hz, ArCH(OH)), 4.52 (dd, 1H, J = 5.0, 9.0 Hz, H-5), 6.01 (br d, 1H, J = 9 Hz, H-6), 6.38 (br d, 1H, J = 5 Hz, exchanged with D_2O, OH), 6.67 - 7.80 (m, 12H, H-2, NH_2, C_6H_4CN, Ph); ^{13}C NMR (CD_3SOCD_3) δ 40.9, 56.1, 76.8, 100.8, 101.5, 108.9, 119.3, 127.0, 127.2, 127.6, 128.3, 130.6, 131.0, 137.9, 139.3, 149.3, 171.0; MS, m/e (relative intensity) 345 (0.5, M^+), 327 (1), 213 (32), 131 (25, NCC_6H_4CHO), 130 (40, NCC_6H_4CO), 123 (11), 122 (16), 105 (14), 102 (16, NCC_6H_4), 91 (100). Anal. Calcd for $C_{21}H_{19}N_3O_2$: C, 73.02; H, 5.55; N, 12.17. Found: C, 72.87, H, 5.34; N, 12.14.

(RS + SR)-**4e**: mp 158 - 159 °C dec ($CHCl_3$-MeOH); IR (KBr) ν_{max} 3480, 3380, 3200, 2230, 1680, 1640, 1565 cm^{-1}; UV (MeOH) λ_{max} 343 nm (ε 6250); ^1H NMR (CD_3SOCD_3) δ 3.82 (q, 1H, J = 4.8 Hz, H-4), 4.15 (s, 2H, CH_2Ph), 4.52 (dd, 1H, J = 3.0, 4.8 Hz, ArCH(OH)), 4.65 (dd, 1H, J = 4.8, 9.8, H-5), 5.60 (d, 1H, J = 3.0 Hz, exchanged with D_2O, OH), 5.83 (br

d, 1H, J = 9.8 Hz, H-6), 6.57 - 7.80 (m, 12H, H-2, NH_2, C_6H_4, Ph); ^{13}C NMR (CD_3SOCD_3) δ 40.7, 56.0, 75.1, 100.7, 101.8, 109.1, 119.2, 126.7, 127.1, 128.3, 130.1, 130.7, 138.0, 138.5, 149.0, 170.2; MS, m/e (relative intensity) 345 (1, M^+), 327 (1), 213 (33), 131 (26), 130 (40), 123 (11), 122 (16), 105 (14), 102 (16), 91 (100).

Photosensitized Reaction of 1f. A 150-mL methanolic solution of **1f** (0.72 g, 6.8 mmol), BNAH (3.31 g, 15.5 mmol), and the sensitizer (30 mg, 0.04 mmol) was irradiated for 15 h, evaporated, and then chromatographed on basic alumina as described above to give BNAH (0.5 g), diastereomeric mixtures of **4f** (2.0 g, 85%), and **5** (< 20 mg). The diastereoisomers of **4f** were separated by repeated column chromatography. A pure sample of the (RR + SS) isomer was thus obtained whereas the (RS + SR) isomer could not be made free from contamination of small amounts of others.

(RR + SS)-**4f**: mp 171.5 - 172.5 °C dec ($CHCl_3$-MeOH); IR (KBr) ν_{max} 3270, 3115, 1669, 1640, 1554 cm^{-1}; UV (MeOH) λ_{max} 342 nm (ε 4750); ^1H NMR (CD_3SOCD_3) δ 3.70 (dd, 1H, J = 3.2, 5.8 Hz, H-4), 4.23 (s, 2H, CH_2Ph), 4.43 (dd, 1H, J = 2.2, 5.8 Hz, ArCH(OH)), 4.47 (dd, 1H, J = 3.2, 6.0 Hz, H-5), 6.01 (dd, 1H, J = 2.2, 6.0 Hz, H-6), 6.06 (br s, exchanged with D_2O, OH), 6.78 - 7.50 (m, 13H, H-6, NH_2, 2 x Ph); ^{13}C NMR (CD_3SOCD_3) δ 40.9, 56.0, 76.9, 101.6, 126.2, 126.8, 127.1, 128.4, 130.5, 138.1, 139.2, 143.3, 170.9; MS, m/e (relative intensity) 320 (0.5, M^+), 302 (2, M - H_2O), 213 (57), 123 (5), 106 (5, PhCHO), 105 (4), 91 (100). Anal. Calcd for $C_{20}H_{20}N_2O_2$: C,74,97; H, 6.29; N, 8.74. Found: C, 74.70; H, 6.21; N, 8.77.

(RS + SR)-**4f**: mp 162 - 163 °C dec ($CHCl_3$-MeOH); IR

(KBr) ν_{max} 3460, 3340, 3170, 1665, 1635, 1560 cm^{-1}; UV (MeOH) λ_{max} 342 nm (ε 6170); ^1H NMR (CD_3SOCD_3) δ 3.62 (q, 1H, J = 5.6 Hz, H-4), 4.23 (s, 2H, CH_2Ph), 4.38 (dd, 1H, J = 5.6, 7.8 Hz, H-5), 4.45 (dd, 1H, J = 3.8, 5.6 Hz, ArCH(OH)), 5.64 (d, 1H, J = 3.8 Hz, exchanged with D_2O, OH), 5.99 (br d, 1H J = 7.8 Hz, H-6), 6.74 - 7.60 (m, 13H, H-2, NH_2, 2 x Ph); ^{13}C NMR (CD_3SOCD_3) δ 40.4, 56.0, 77.1, 101.6, 102.7, 126.7, 127.1, 127.5, 128.5, 129.7, 138.3, 143.1, 170.7; MS, m/e (relative intensity) 320 (0.5, M^+), 302 (1), 213 (33), 123 (6), 106 (5), 105 (7), 91 (100).

Thermal Reactions. Each 3-mL methanolic solution containing **1a-f** (50 mM) and BNAH (0.2 M) in a Pyrex tube was bubbled with a gentle stream of Ar for 15 min and then heated at 60 ± 0.5 °C in a dark room. All the experimental procedures were performed in the dark in order to avoid exposure of reaction solutions to scattering light. The progress of the reactions was followed by both VPC and HPLC.

2-6 REFERENCES AND NOTES

[1] Steffens, J. J.; Chipman, D. M. J. Am. Chem. Soc. **1971**, 93, 6694.

[2] Ohnishi, Y.; Ohno, A. Chem. Lett. **1976**, 697.

[3] Ohno, A.; Shio, T.; Yamamoto, H.; Oka, S. J. Am. Chem. Soc. **1981**, 103, 2045.

[6] Fukuzumi, S.; Kondo, Y.; Tanaka, T. Chem. Lett. **1983**, 751.

[7] Abels, R. H.; Hutton, R. F.; Westhimer, F. H. J. Am. Chem. Soc. **1957**, 79, 712.

[6] Powell, M. F.; Bruice, T. C. J. Am. Chem. Soc. **1983**, 105, 1014.

[7] Carlson, B. W.; Miller, L. L. J. Am. Chem. Soc. **1985**, 107, 479.

[8] Maltens, F. M.; Verhoeven, J. W.; Gase, R. A.; Pandit, U. K.; Boer, T. J. D. Tetrahedron, **1978**, 34, 443.

[9] (a) Stout, D. M.; Meyers, A. I. Chem. Rev. **1982**, 82, 223. (b) Meyer, H.; Kazda, S.; Belleman, P. "Annual Report of Medicinal Chemistry"; Academie Press: new York, **1983**; Vol. 18.

[10] Mukaiyama, T.; Sato, T.; Hanna, J. Chem. Lett., **1973**, 1041.

[11] Ohnishi, Y.; Kitami, M. Bull. Chem. Soc. Jpn. **1979**, 52, 2674.

[12] Maltens, F. M.; Verhoeven, J. W. Rec. Trav. Chim. Pays-Bas, **1981**, 100, 228.

[13] Evans, D. H. "Encyclopedia of Electrochemistry of the Elements"; Bard, A. J.; Lund, H., Eds.; Marcel Dekker Inc.: New York, 1978; Vol. XII, pp 1 - 259.

[14] Given, P. H.; Peover, M. E. J. Chem. Soc. **1960**, 385.

[15] Michielli, R. F.; Elving, P. J. J. Am. Chem. Soc. **1968**, 90, 1989.

[16] Nadjo, L.; Saveant, J. M. J. Electroanal. Chem. **1971**, 33, 419.

[17] Laviron, E.; Lucy, J. C. Bull. Soc. Chim. Fr. **1966**, 2202.

[18] Unfortunately, the polarography of **1e** in methanol showed only a weak, ambiguous wave at ∿ -1.8 V which is of little electrochemical significance. A major origin of the polarographic behavior can be attributed to the hemiacetal formation, since the IR band of carbonyl streching vibrations at 1720 cm^{-1} disappeared upon addition of methanol to an acetonitrile solution of **1e** and since ^1H NMR signals of the ortho aromatic protons in CD_3CN at lower fields (δ 7.90 - 8.30) moved to higher field upon addition of CD_3OD, finally almost overlapping with those of the other protons at δ 7.26 - 7.87 in CD_3OD.

[19] Blaedel, W. J.; Haas, R. G. Anal. Chem. **1970**, 42, 918.

[20] Jensen, M. A.; Elving, P. J. Biochem. Biophys. Acta **1984**, 764, 310.

[21] (a) The one-electron reduction of BNA^+ with Zn gives the disatereomers of **5** and **7** in a comparable ratio.[15] We have also found that a diastereoisomer of **5** and the both isomers of **7** are quantitatively formed in a 2:2:1 ratio by the fac-$Re(bpy)(CO)_3Br$-photosensitized reduction of BNA^+ by triethylamine which proceeds via photomediated one-electron transfer from the amine to BNA^+.[21b] (b) Pac, C.; Ishitani, O. Abstracts of Papers of Beijing International Conference on Photochemistry; Beijing, China, Oct. 21 - 26, 1985; pp. 315 - 317.

[22] (a) The reported rate constants for the homo coupling

of ArCH(OH)R or NAD· is 6 x 10^6 - 7 x 10^8 $M^{-1}s^{-1}$ in 2-propanol[23b] or 3 x 10^7 $M^{-1}s^{-1}$ in water at pH 9.1[20] each. These rate data indicate that the rate constants of eq 7 should be > 10^9 $M^{-1}s^{-1}$, very large for sterically bulky radicals unless specific interactions operate. (b) Ingold, K. U. "Free Radicals"; Wiley; New york, 1973; Vol. 1, pp. 40 - 56.

[23] Vennesland, B.; Westheimer, F. H. " The Mechanism of Enzyme Action"; McElroy, W. D., Glass, B., Eds., John Hopkins: Baltimore, 1954.

[24] Mauzarall, D.; Westheimer, F. H. J. Am. Chem. Soc. **1955**, 77, 2261.

[25] Broomhead, J. A.; Yaung, C. G. Inorg. Synth. **1983**, 22, 127.

[26] Wagner, E. E.; Adamson, A. W. J. Am. Chem. Soc. **1966**, 88, 394.

2-7 SUPPLEMENTARY SECTION

2-7-1 *Crystallographic Data of 4e*

2-7-2 *Crystallographic Data of 4f*

2-7-1 *Crystallographic Data of 4e*

Crystal Data

Sample:	(R,R and S,S)-N-Benzyl-4-(1-(4-cyanophenyl)-1-hydroxymethyl)-1,4-dihydronicotinamide (4e)
Molecular formula:	$C_{21}H_{18}N_3O_2$
Molecular weight:	345.40
Crystal system:	Triclinic
Space group:	P1 bar
Cell dimensions:	a= 9.310(4) Å
	b= 9.553(2) Å
	c= 11.335(11) Å
	alpha= 74.88(4)°
	beta= 66.17(8)°
	gamma= 73.65(3)°
	V= 872.4(7) $Å^3$
Density:	d_{calcd}= 1.315 g/cm^3
	d_{obs}= 1.310 g/cm^3
	Z= 2
	R= 0.094 (weighted)
	R= 0.086 (unweighted)
No. of reflections observed:	4183
No of unobservedly weak reflections:	1861

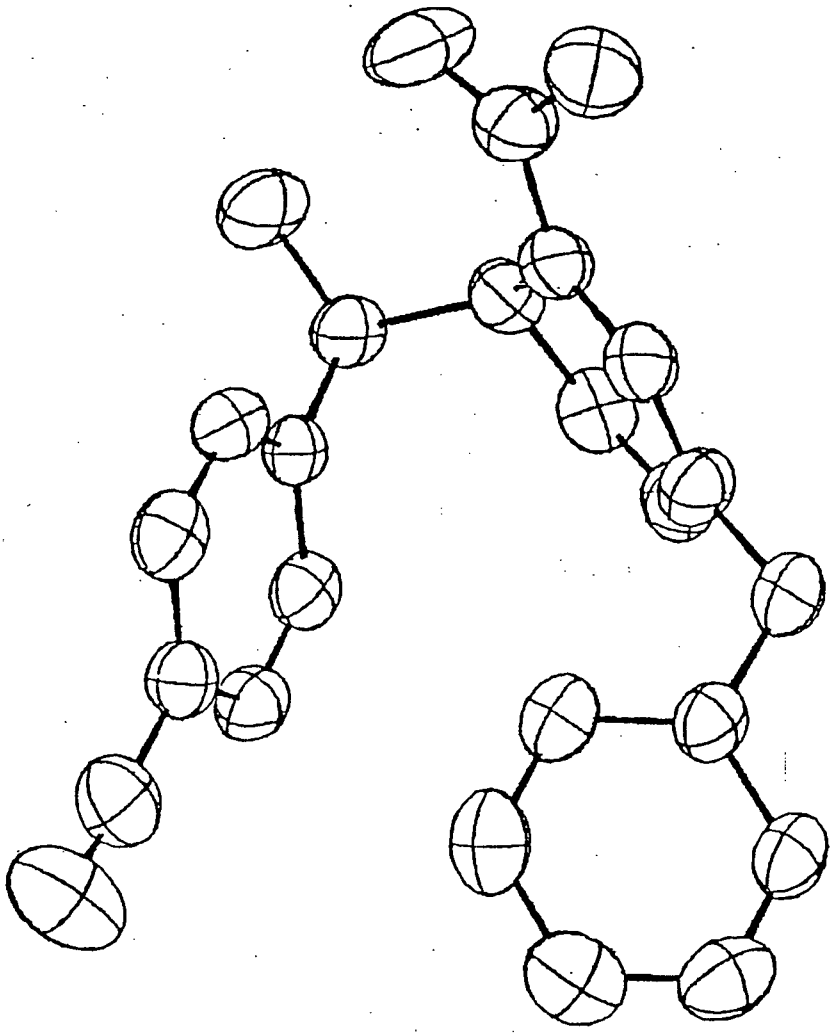

Table of Bond Distances in Angstroms

Atom1	Atom2	Distance	Atom1	Atom2	Distance	Atom1	Atom2	Distance
O1	C13	1.252(7)	C3	C4	1.479(8)	C14	C15	1.517(8)
O2	C14	1.428(7)	C3	C14	1.573(8)	C15	C16	1.399(7)
N1	C1	1.360(7)	C4	C5	1.324(8)	C15	C20	1.356(7)
N1	C5	1.383(7)	C6	C7	1.484(8)	C16	C17	1.373(8)
N1	C6	1.468(7)	C7	C8	1.395(7)	C17	C18	1.369(8)
N2	C13	1.334(7)	C7	C12	1.362(7)	C18	C19	1.402(8)
N3	C21	1.137(8)	C8	C9	1.361(9)	C18	C21	1.435(9)
C1	C2	1.361(7)	C9	C10	1.367(9)	C19	C20	1.372(8)
C2	C3	1.526(7)	C10	C11	1.389(9)			
C2	C13	1.456(8)	C11	C12	1.384(9)			

Numbers in parentheses are estimated standard deviations in the least significant digits.

Table of Bond Distances in Angstroms

Atom1	Atom2	Distance
O1	O2	2.658(6)
O1	N2	2.224(7)
O1	C2	2.352(7)
O1	C3	2.879(7)
O2	C3	2.499(7)
O2	C15	2.404(7)
O2	C20	2.794(7)
N1	C2	2.395(7)
N1	C3	2.880(7)
N1	C4	2.372(7)
N1	C7	2.499(7)
N1	C12	2.936(8)
N2	C1	2.847(8)
N2	C2	2.430(7)
N3	C18	2.572(9)
C1	C3	2.500(7)
C1	C4	2.739(8)
C1	C5	2.352(8)
C1	C6	2.463(8)
C1	C13	2.440(8)
C2	C4	2.454(8)
C2	C5	2.765(8)
C2	C14	2.623(7)
C3	C5	2.467(8)
C3	C13	2.585(8)
C3	C15	2.604(8)
C4	C14	2.512(8)
C5	C6	2.473(9)
C6	C8	2.473(9)
C6	C12	2.512(9)
C7	C9	2.402(8)
C7	C10	2.799(9)
C7	C11	2.389(9)
C8	C10	2.380(9)
C8	C11	2.723(9)
C8	C12	2.360(8)
C9	C11	2.358(9)
C9	C12	2.735(8)
C10	C12	2.413(9)
C14	C16	2.525(8)
C14	C20	2.504(9)
C15	C17	2.403(8)
C15	C18	2.774(8)
C15	C19	2.383(8)
C16	C18	2.382(9)
C16	C19	2.753(8)
C16	C20	2.372(8)
C17	C19	2.389(8)
C17	C20	2.743(7)
C17	C21	2.443(10)
C18	C20	2.395(8)
C19	C21	2.450(10)

Numbers in parentheses are estimated standard deviations in the least significant digits.

Table of Bond Distances in Angstroms

Atom1	Atom2	Distance	Atom1	Atom2	Distance	Atom1	Atom2	Distance
O1	O1	3.523(9)	N3	C6	3.995(10)	C9	C17	3.940(8)
O1	N2	2.950(7)	C1	C4	3.792(8)	C9	C18	3.980(8)
O1	C13	3.695(7)	C1	C5	3.404(8)	C9	C19	3.981(8)
O2	C3	3.373(7)	C2	C5	3.797(8)	C9	C19	3.700(8)
O2	C4	3.777(7)	C2	C6	3.753(9)	C9	C20	3.926(8)
O2	C6	3.349(7)	C3	C6	3.717(8)	C9	C20	3.842(8)
O2	C7	3.753(7)	C4	C6	3.646(9)	C10	C13	3.789(10)
O2	C8	3.431(7)	C5	C17	3.852(8)	C10	C16	3.810(8)
N1	N1	3.687(10)	C5	C21	3.854(9)	C10	C19	3.672(8)
N1	C1	3.732(8)	C7	C17	3.841(8)	C10	C20	3.565(8)
N1	C2	3.871(7)	C7	C19	3.680(8)	C11	C16	3.840(9)
N1	C4	3.751(7)	C8	C8	3.826(12)	C11	C19	3.629(8)
N1	C5	3.609(7)	C8	C9	3.501(8)	C11	C20	3.799(8)
N2	N2	3.858(10)	C8	C14	3.733(8)	C12	C16	3.958(8)
N2	N3	3.369(8)	C8	C15	3.540(7)	C12	C17	3.969(8)
N2	N3	3.847(9)	C8	C16	3.828(8)	C12	C19	3.641(8)
N2	C10	3.646(10)	C8	C16	3.983(7)	C16	C17	3.888(8)
N2	C13	3.831(8)	C8	C19	3.709(8)	C17	C17	3.850(12)
N2	C21	3.811(8)	C8	C20	3.827(7)	C19	C19	3.768(12)
N3	N3	3.507(13)	C9	C9	3.685(13)	C19	C20	3.598(8)
N3	C1	3.737(9)	C9	C15	3.870(8)	C20	C20	3.932(11)
N3	C4	3.990(9)	C9	C16	3.871(8)			
N3	C5	3.875(9)	C9	C16	3.873(8)			

Numbers in parentheses are estimated standard deviations in the least significant digits.

Table of Bond Distances in Angstroms

Atom1	Atom2	Distance
O1	HO21	1.826(0)
O1	H31	2.678(0)
O1	HN21	2.425(0)
O1	HN21	2.019(0)
O2	H31	2.523(0)
O2	H31	2.500(0)
O2	H61	2.763(0)
O2	H81	2.873(0)
O2	H141	1.961(0)
O2	H201	2.513(0)
N1	H11	1.994(0)
N1	H51	2.020(0)
N1	H61	1.978(0)
N1	H62	1.978(0)
N1	H112	2.627(0)
N2	H11	2.537(0)
N2	H101	2.804(0)
N3	H11	2.822(0)
N3	HN22	2.844(0)
C1	H61	2.520(0)
C1	H112	2.866(0)
C1	HN22	2.538(0)
C2	HO21	2.847(0)
C2	H11	1.995(0)
C2	H31	2.003(0)
C2	HN22	2.595(0)
C3	HO21	2.600(0)
C3	H41	2.104(0)
C3	H141	2.015(0)
C4	H31	2.024(0)
C4	H51	1.967(0)
C4	H141	2.510(0)
C5	H41	1.962(0)
C5	H62	2.524(0)
C6	H11	2.603(0)
C6	H51	2.618(0)
C6	H81	2.612(0)
C6	H112	2.689(0)
C7	H61	1.993(0)
C7	H62	1.993(0)
C7	H81	2.037(0)
C7	H112	2.008(0)
C7	H191	2.871(0)
C8	H61	2.817(0)
C8	H62	2.550(0)
C8	H91	2.005(0)
C8	H191	2.820(0)
C9	H81	2.006(0)
C9	H101	2.029(0)
C10	H91	2.011(0)
C10	H111	2.032(0)
C11	H101	2.049(0)
C11	H112	2.028(0)
C12	H111	2.028(0)
C13	HO21	2.579(0)
C13	H11	2.578(0)
C13	H31	2.649(0)
C13	HN21	1.987(0)
C13	HN22	1.987(0)
C14	HO21	1.974(0)
C14	H31	2.028(0)
C14	H41	2.866(0)
C14	H161	2.676(0)
C14	H201	2.647(0)
C15	HO21	2.767(0)
C15	H141	2.010(0)
C15	H161	2.046(0)
C15	H201	1.999(0)
C16	H141	2.552(0)
C16	H171	2.020(0)
C17	H161	2.022(0)
C18	H171	2.016(0)
C18	H191	2.052(0)
C19	H201	2.013(0)
C20	HO21	2.808(0)
C20	H191	2.025(0)
C21	H111	2.722(0)
C21	H171	2.615(0)
C21	H191	2.623(0)

Numbers in parentheses are estimated standard deviations in the least significant digits.

Table of Bond Angles in Degrees

Atom1	Atom2	Atom3	Angle
C1	N1	C5	118.1(5)
C1	N1	C6	121.1(5)
C5	N1	C6	120.3(5)
N1	C1	C2	123.4(5)
C1	C2	C3	119.9(5)
C1	C2	C13	120.0(5)
C3	C2	C13	120.1(5)
C2	C3	C4	109.5(5)
C2	C3	C14	115.6(5)
C4	C3	C14	110.7(5)
C3	C4	C5	123.2(5)
N1	C5	C4	122.4(5)
N1	C6	C7	115.7(5)
C6	C7	C8	118.4(5)
C6	C7	C12	123.8(5)
C8	C7	C12	117.7(6)
C7	C8	C9	121.3(6)
C8	C9	C10	121.5(6)
C9	C10	C11	117.6(6)
C10	C11	C12	121.0(6)
C7	C12	C11	121.0(6)
O1	C13	N2	118.6(6)
O1	C13	C2	120.3(5)
N2	C13	C2	121.0(5)
O2	C14	C3	112.6(5)
O2	C14	C15	109.4(5)
C3	C14	C15	114.9(4)
C14	C15	C16	119.9(5)
C14	C15	C20	121.2(5)
C16	C15	C20	118.8(5)
C15	C16	C17	120.2(5)
C16	C17	C18	120.6(5)
C17	C18	C19	119.2(6)
C17	C18	C21	121.3(6)
C19	C18	C21	119.5(6)
C18	C19	C20	119.4(6)
C15	C20	C19	121.7(5)
N3	C21	C18	177.8(8)

Numbers in parentheses are estimated standard deviations in the least significant digits.

Table of Torsional Angles in Degrees

Atom 1	Atom 2	Atom 3	Atom 4	Angle
H021	02	C14	C3	-46.5
H021	02	C14	C15	82.6
H021	02	C14	H141	-160.7
C5	N1	C1	C2	7.1
C5	N1	C1	H11	-172.9
C6	N1	C1	C2	179.6
C6	N1	C1	H11	-0.4
C1	N1	C5	C4	-8.0
C1	N1	C5	H51	172.0
C6	N1	C5	C4	179.4
C6	N1	C5	H51	-0.6
C1	N1	C6	C7	94.5
C1	N1	C6	H61	-26.4
C1	N1	C6	H62	-144.6
C5	N1	C6	C7	-93.2
C5	N1	C6	H61	145.9
C5	N1	C6	H62	27.7
HN21	N2	C13	01	3.7
HN21	N2	C13	C2	-180.0
HN22	N2	C13	01	-176.3
HN22	N2	C13	C2	0.0
N1	C1	C2	C3	7.3
N1	C1	C2	C13	-172.9
H11	C1	C2	C3	-172.7
H11	C1	C2	C13	7.1
C1	C2	C3	C4	-18.9
C1	C2	C3	C14	107.0
C1	C2	C3	H31	-138.4
C13	C2	C3	C4	161.4
C13	C2	C3	C14	-72.7
C13	C2	C3	H31	41.9
C1	C2	C13	01	-166.0
C1	C2	C13	N2	17.7
C3	C2	C13	01	13.7
C3	C2	C13	N2	-162.5
C2	C3	C4	C5	18.7
C2	C3	C4	H41	-161.3
C14	C3	C4	C5	-109.9
C14	C3	C4	H41	70.1
H31	C3	C4	C5	134.9
H31	C3	C4	H41	-45.1
C2	C3	C14	02	72.3
C2	C3	C14	C15	-53.8
C2	C3	C14	H141	-169.8
C4	C3	C14	02	-162.4
C4	C3	C14	C15	71.4
C4	C3	C14	H141	-44.5
H31	C3	C14	02	-43.0
H31	C3	C14	C15	-169.2
H31	C3	C14	H141	74.9
C3	C4	C5	N1	-6.3
C3	C4	C5	H51	173.7
H41	C4	C5	N1	173.7
H41	C4	C5	H51	-6.3
N1	C6	C7	C8	157.9
N1	C6	C7	C12	-25.7
H61	C6	C7	C8	-81.2
H61	C6	C7	C12	95.2
H62	C6	C7	C8	37.0
H62	C6	C7	C12	-146.6
C6	C7	C8	C9	175.4
C6	C7	C8	H81	-4.6
C12	C7	C8	C9	-1.3
C12	C7	C8	H81	178.7
C6	C7	C12	C11	-175.2
C6	C7	C12	H112	4.8
C8	C7	C12	C11	1.2
C8	C7	C12	H112	-178.8
C7	C8	C9	C10	0.6
C7	C8	C9	H91	-179.4
H81	C8	C9	C10	-179.4
H81	C8	C9	H91	0.6
C8	C9	C10	C11	0.1
C8	C9	C10	H101	-179.9
H91	C9	C10	C11	-179.9
H91	C9	C10	H101	0.1
C9	C10	C11	C12	-0.1
C9	C10	C11	H111	179.9
H101	C10	C11	C12	179.9
H101	C10	C11	H111	-0.1
C10	C11	C12	C7	-0.6
C10	C11	C12	H112	179.4
H111	C11	C12	C7	179.4
H111	C11	C12	H112	-0.6
02	C14	C15	C16	144.0
02	C14	C15	C20	-33.4
C3	C14	C15	C16	-88.2
C3	C14	C15	C20	94.4
H141	C14	C15	C16	25.6
H141	C14	C15	C20	-151.7
C14	C15	C16	C17	-177.4
C14	C15	C16	H161	2.6
C20	C15	C16	C17	0.1
C20	C15	C16	H161	-179.9
C14	C15	C20	C19	176.5
C14	C15	C20	H201	-3.5
C16	C15	C20	C19	-0.9
C16	C15	C20	H201	179.1
C15	C16	C17	C18	1.3
C15	C16	C17	H171	-178.7
H161	C16	C17	C18	-178.7
H161	C16	C17	H171	1.3
C16	C17	C18	C19	-1.8
C16	C17	C18	C21	-179.8
H171	C17	C18	C19	178.2
H171	C17	C18	C21	0.2
C17	C18	C19	C20	0.9
C17	C18	C19	H191	-179.1
C21	C18	C19	C20	179.0
C21	C18	C19	H191	-1.0
C17	C18	C21	N3	152.8
C19	C18	C21	N3	-25.2
C18	C19	C20	C15	0.4
C18	C19	C20	H201	-179.6
H191	C19	C20	C15	-179.6
H191	C19	C20	H201	0.4

2-7-2 *crystallographic Data of 4f*

Crystal Data

Sample:	(R,R and S,S)-N-Benzyl-4-(1-hydroxy-1-phenylmethyl)-1,4-dihydronicotinamide (4f)
Molecular formula:	$C_{20}H_{20}N_2O_2$
Molecular weight:	320.4
Crystal system:	Triclinic
Space group:	P1 bar
Cell dimensions:	a= 10.416(2) Å
	b= 10.557(9) Å
	c= 16.543(6) Å
	alpha= 76.72(5)°
	beta= 71.56(2)°
	gamma= 89.82(3)°
	V= 1675(2) $Å^3$
Density:	d_{calcd}= 1.271 g/cm^3
	d_{obs}= 1.245 g/cm^3
	Z= 4
	R= 0.217 (weighted)
	R= 0.215 (unweighted)
No. of reflections observed:	8086
No of unobservedly weak reflections:	3454

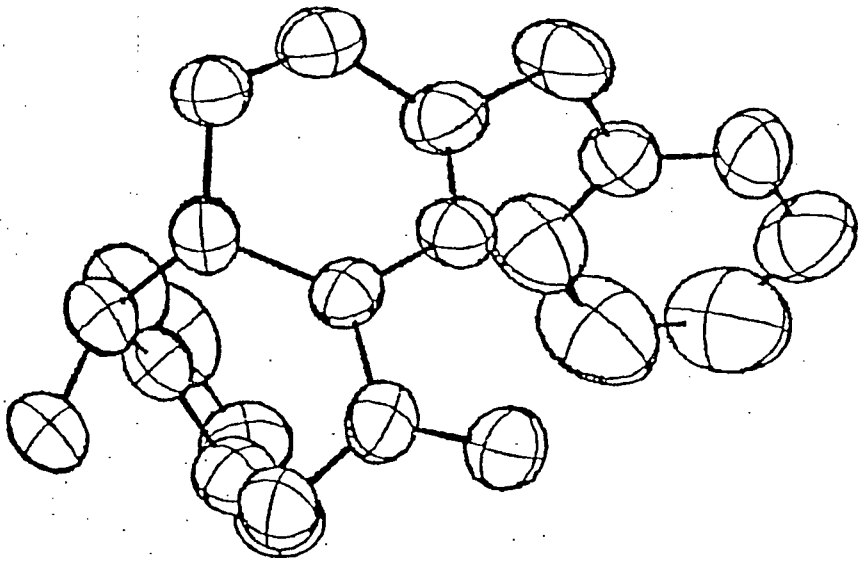

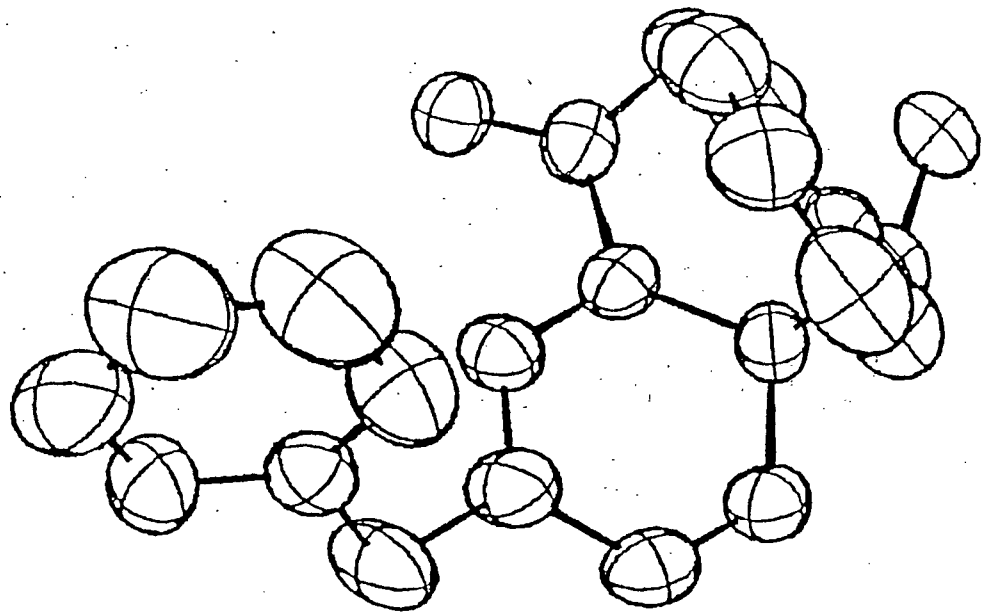

Table of Bond Distances in Angstroms

Atom1	Atom2	Distance	Atom1	Atom2	Distance	Atom1	Atom2	Distance
O1	C13	1.238(6)	C6	C7	1.499(7)	C23	C26	1.575(7)
O2	C6	1.425(6)	C7	C8	1.387(8)	C24	C25	1.328(8)
O3	C33	1.246(6)	C7	C12	1.383(8)	C26	C27	1.503(7)
O4	C26	1.417(6)	C8	C9	1.437(9)	C27	C28	1.374(8)
N1	C1	1.355(7)	C9	C10	1.388(10)	C27	C32	1.392(8)
N1	C5	1.408(7)	C10	C11	1.373(10)	C28	C29	1.429(9)
N1	C14	1.467(7)	C11	C12	1.411(8)	C29	C30	1.396(10)
N2	C13	1.342(7)	C14	C15	1.523(8)	C30	C31	1.365(10)
N3	C21	1.391(7)	C15	C16	1.389(8)	C31	C32	1.419(8)
N3	C25	1.369(7)	C15	C20	1.396(8)	C34	C35	1.520(8)
N3	C34	1.470(7)	C16	C17	1.423(11)	C35	C36	1.382(8)
N4	C33	1.332(7)	C17	C18	1.402(13)	C35	C40	1.420(8)
C1	C2	1.358(7)	C18	C19	1.379(14)	C36	C37	1.433(11)
C2	C3	1.500(7)	C19	C20	1.379(10)	C37	C38	1.417(13)
C2	C13	1.496(7)	C21	C22	1.353(7)	C38	C39	1.383(13)
C3	C4	1.515(7)	C22	C23	1.524(7)	C39	C40	1.375(10)
C3	C6	1.593(7)	C22	C33	1.495(7)			
C4	C5	1.330(7)	C23	C24	1.510(7)			

Numbers in parentheses are estimated standard deviations in the least significant digits.

Table of Bond Distances in Angstroms

Atom1	Atom2	Distance	Atom1	Atom2	Distance	Atom1	Atom2	Distance
O1	N2	2.250(6)	C2	C4	2.448(7)	C21	C33	2.392(8)
O1	C1	2.698(7)	C2	C5	2.768(7)	C21	C34	2.476(8)
O1	C2	2.375(6)	C2	C6	2.659(7)	C22	C24	2.456(7)
O2	N2	2.779(6)	C3	C5	2.512(8)	C22	C25	2.754(7)
O2	C3	2.475(6)	C3	C7	2.606(7)	C22	C26	2.667(7)
O2	C7	2.384(6)	C3	C13	2.630(7)	C23	C25	2.499(8)
O2	C12	2.873(7)	C4	C6	2.475(7)	C23	C27	2.598(7)
O3	N4	2.255(6)	C5	C14	2.483(9)	C23	C33	2.648(7)
O3	C21	2.689(7)	C6	C8	2.470(8)	C24	C26	2.473(7)
O3	C22	2.372(6)	C6	C12	2.524(8)	C25	C34	2.479(9)
O4	N4	2.785(6)	C7	C9	2.430(9)	C26	C28	2.476(8)
O4	C23	2.463(6)	C7	C10	2.823(9)	C26	C32	2.528(8)
O4	C27	2.380(7)	C7	C11	2.420(8)	C27	C29	2.428(9)
O4	C32	2.868(7)	C8	C10	2.462(10)	C27	C30	2.821(9)
N1	C2	2.380(7)	C8	C11	2.784(10)	C27	C31	2.433(9)
N1	C3	2.908(7)	C8	C12	2.399(9)	C28	C30	2.450(10)
N1	C4	2.386(7)	C9	C11	2.371(11)	C28	C31	2.778(10)
N1	C15	2.457(7)	C9	C12	2.771(10)	C28	C32	2.391(9)
N1	C16	2.853(9)	C10	C12	2.430(9)	C29	C31	2.378(11)
N2	C2	2.437(7)	C14	C16	2.533(9)	C29	C32	2.777(10)
N2	C3	2.967(7)	C14	C20	2.492(9)	C30	C32	2.426(9)
N3	C22	2.396(7)	C15	C17	2.401(10)	C34	C36	2.531(10)
N3	C23	2.919(7)	C15	C18	2.745(11)	C34	C40	2.506(9)
N3	C24	2.375(7)	C15	C19	2.414(9)	C35	C37	2.415(10)
N3	C35	2.478(7)	C16	C18	2.437(12)	C35	C38	2.773(10)
N3	C36	2.879(9)	C16	C19	2.839(11)	C35	C39	2.420(10)
N4	C22	2.429(7)	C16	C20	2.435(9)	C36	C38	2.456(12)
N4	C23	2.970(7)	C17	C19	2.437(14)	C36	C39	2.832(11)
C1	C3	2.512(7)	C17	C20	2.781(11)	C36	C40	2.447(9)
C1	C4	2.748(7)	C18	C20	2.365(13)	C37	C39	2.441(14)
C1	C5	2.370(8)	C21	C23	2.531(7)	C37	C40	2.805(11)
C1	C13	2.397(8)	C21	C24	2.764(7)	C38	C40	2.388(12)
C1	C14	2.459(8)	C21	C25	2.369(8)			

Numbers in parentheses are estimated standard deviations in the least significant digits.

Table of Bond Distances in Angstroms

Atom1	Atom2	Distance	Atom1	Atom2	Distance	Atom1	Atom2	Distance
O1	O1	3.666(8)	N2	N2	3.702(9)	C9	C18	3.723(12)
O1	O4	2.683(5)	N2	N3	3.827(7)	C9	C19	3.963(12)
O1	N2	2.917(6)	N2	C13	3.702(7)	C10	C18	3.865(13)
O1	N4	3.945(6)	N2	C21	3.496(7)	C10	C19	3.983(12)
O1	C13	3.720(7)	N2	C34	3.781(9)	C11	C28	3.839(9)
O1	C23	3.691(6)	N4	C1	3.480(7)	C14	C33	3.754(8)
O1	C26	3.454(6)	N4	C14	3.764(9)	C17	C17	3.85(2)
O2	O3	2.680(5)	C2	C4	3.745(7)	C20	C31	3.804(10)
O2	C20	3.611(8)	C3	C3	3.947(10)	C22	C24	3.732(7)
O2	C22	3.934(6)	C3	C4	3.656(7)	C23	C23	3.951(10)
O2	C24	3.416(7)	C3	C5	3.973(8)	C23	C24	3.651(7)
O2	C33	3.353(6)	C4	C4	3.968(11)	C23	C25	3.994(8)
O3	N1	3.567(6)	C5	C35	3.892(8)	C24	C24	3.951(11)
O3	N2	3.943(6)	C5	C39	3.708(10)	C26	C40	3.963(8)
O3	C3	3.696(6)	C5	C40	3.628(8)	C27	C39	3.916(11)
O3	C5	3.755(7)	C6	C20	3.984(8)	C27	C40	3.937(8)
O3	C6	3.458(6)	C7	C19	3.930(11)	C28	C39	3.922(11)
O3	C14	3.268(8)	C7	C20	3.965(8)	C29	C38	3.724(12)
O4	C2	3.947(6)	C8	C19	3.942(11)	C29	C39	3.962(11)
O4	C4	3.398(7)	C8	C31	3.814(10)	C30	C38	3.882(13)
O4	C13	3.351(6)	C8	C32	3.965(9)	C30	C39	3.982(12)
O4	C40	3.591(8)	C8	C39	3.910(11)	C37	C37	3.84(2)
N1	N4	3.825(7)	C9	C9	3.995(14)			

Numbers in parentheses are estimated standard deviations in the least significant digits.

Atom1	Atom2	Atom3	Angle	Atom1	Atom2	Atom3	Angle	Atom1	Atom2	Atom3	Angle
C1	N1	C5	118.2(5)	C10	C11	C12	121.6(7)	O4	C26	C27	109.1(4)
C1	N1	C14	121.2(5)	C7	C12	C11	120.0(6)	C23	C26	C27	115.1(4)
C5	N1	C14	119.5(5)	O1	C13	N2	121.4(5)	C26	C27	C28	118.7(5)
C21	N3	C25	118.3(5)	O1	C13	C2	120.3(5)	C26	C27	C32	121.7(5)
C21	N3	C34	119.8(5)	N2	C13	C2	118.2(5)	C28	C27	C32	119.6(6)
C25	N3	C34	121.6(5)	N1	C14	C15	110.6(5)	C27	C28	C29	120.0(6)
N1	C1	C2	122.7(5)	C14	C15	C16	120.8(6)	C28	C29	C30	120.3(7)
C1	C2	C3	123.0(5)	C14	C15	C20	117.2(6)	C29	C30	C31	119.0(7)
C1	C2	C13	114.2(5)	C16	C15	C20	121.9(6)	C30	C31	C32	121.3(7)
C3	C2	C13	122.7(4)	C15	C16	C17	117.2(7)	C27	C32	C31	119.9(6)
C2	C3	C4	108.6(4)	C16	C17	C18	119.2(8)	O3	C33	N4	122.0(5)
C2	C3	C6	118.5(4)	C17	C18	C19	122.5(9)	O3	C33	C22	119.6(5)
C4	C3	C6	105.6(4)	C18	C19	C20	118.1(8)	N4	C33	C22	118.4(5)
C3	C4	C5	123.9(5)	C15	C20	C19	120.9(7)	N3	C34	C35	111.9(5)
N1	C5	C4	121.3(5)	N3	C21	C22	121.7(5)	C34	C35	C36	121.4(6)
O2	C6	C3	110.1(4)	C21	C22	C23	123.2(5)	C34	C35	C40	116.9(6)
O2	C6	C7	109.2(4)	C21	C22	C33	114.2(5)	C36	C35	C40	121.7(6)
C3	C6	C7	114.8(4)	C23	C22	C33	122.6(4)	C35	C36	C37	118.2(7)
C6	C7	C8	117.6(5)	C22	C23	C24	108.1(4)	C36	C37	C38	119.0(8)
C6	C7	C12	122.2(5)	C22	C23	C26	118.8(4)	C37	C38	C39	121.3(8)
C8	C7	C12	120.1(6)	C24	C23	C26	106.5(4)	C38	C39	C40	119.9(8)
C7	C8	C9	118.7(6)	C23	C24	C25	123.3(5)	C35	C40	C39	119.9(7)
C8	C9	C10	121.2(7)	N3	C25	C24	123.5(5)				
C9	C10	C11	118.3(7)	O4	C26	C23	110.6(4)				

Numbers in parentheses are estimated standard deviations in the least significant digits.

Table of Torsional Angles in Degrees

Atom 1	Atom 2	Atom 3	Atom 4	Angle
C5	N1	C1	C2	-13.1
C14	N1	C1	C2	178.4
C1	N1	C5	C4	10.4
C14	N1	C5	C4	179.1
C1	N1	C14	C15	-63.9
C5	N1	C14	C15	127.8
C25	N3	C21	C22	7.4
C34	N3	C21	C22	-178.6
C21	N3	C25	C24	-4.9
C34	N3	C25	C24	-178.8
C21	N3	C34	C35	61.1
C25	N3	C34	C35	-125.1
N1	C1	C2	C3	1.9
N1	C1	C2	C13	179.0
C1	C2	C3	C4	10.4
C1	C2	C3	C6	-110.0
C13	C2	C3	C4	-166.4
C13	C2	C3	C6	73.2
C1	C2	C13	O1	-14.0
C1	C2	C13	N2	165.3
C3	C2	C13	O1	163.0
C3	C2	C13	N2	-17.6
C2	C3	C4	C5	-13.0
C6	C3	C4	C5	115.0
C2	C3	C6	O2	-78.7
C2	C3	C6	C7	45.0
C4	C3	C6	O2	159.4
C4	C3	C6	C7	-76.8
C3	C4	C5	N1	3.5
O2	C6	C7	C8	-133.6
O2	C6	C7	C12	44.4
C3	C6	C7	C8	102.1
C3	C6	C7	C12	-79.8
C6	C7	C8	C9	177.3
C12	C7	C8	C9	-0.8
C6	C7	C12	C11	-177.2
C8	C7	C12	C11	0.7
C7	C8	C9	C10	0.7
C8	C9	C10	C11	-0.5
C9	C10	C11	C12	0.4
C10	C11	C12	C7	-0.6
N1	C14	C15	C16	-33.7
N1	C14	C15	C20	149.5
C14	C15	C16	C17	179.0
C20	C15	C16	C17	-4.4
C14	C15	C20	C19	179.7
C16	C15	C20	C19	2.9
C15	C16	C17	C18	5.6
C16	C17	C18	C19	-5.6
C17	C18	C19	C20	3.9
C18	C19	C20	C15	-2.5
N3	C21	C22	C23	2.6
N3	C21	C22	C33	-177.1
C21	C22	C23	C24	-12.9
C21	C22	C23	C26	108.5
C33	C22	C23	C24	166.8
C33	C22	C23	C26	-71.9
C21	C22	C33	O3	15.9
C21	C22	C33	N4	-164.6
C23	C22	C33	O3	-163.8
C23	C22	C33	N4	15.7
C22	C23	C24	C25	15.5
C26	C23	C24	C25	-113.2
C22	C23	C26	O4	78.3
C22	C23	C26	C27	-46.0
C24	C23	C26	O4	-159.6
C24	C23	C26	C27	76.1
C23	C24	C25	N3	-7.7
O4	C26	C27	C28	133.5
O4	C26	C27	C32	-44.8
C23	C26	C27	C28	-101.4
C23	C26	C27	C32	80.3
C26	C27	C28	C29	-178.4
C32	C27	C28	C29	-0.1
C26	C27	C32	C31	178.1
C28	C27	C32	C31	-0.1
C27	C28	C29	C30	0.4
C28	C29	C30	C31	-0.5
C29	C30	C31	C32	0.3
C30	C31	C32	C27	0.0
N3	C34	C35	C36	31.6
N3	C34	C35	C40	-148.6
C34	C35	C36	C37	-179.8
C40	C35	C36	C37	0.4
C34	C35	C40	C39	-179.1
C36	C35	C40	C39	0.7
C35	C36	C37	C38	-1.5
C36	C37	C38	C39	1.5
C37	C38	C39	C40	-0.4
C38	C39	C40	C35	-0.7

Chapter 3

EFFECTS OF MAGNESIUM (II) ION ON THE $Ru(bpy)_3^{2+}$-PHOTOMEDIATED REDUCTION OF OLEFINS BY 1-BENZYL-1,4-DIHYDRONICOTINAMIDE: METAL-ION CATALYSIS OF ELECTRON TRANSFER PROCESSES INVOLVING AN NADH MODEL.

3-1 INTRODUCTION

It is known that Mg(II) and Zn(II) ions can catalyze net hydride transfer from the NADH models to unsaturated substrates such as carbonyl and olefinic compounds;[1-4] this constitutes a metal-ion catalysis of biological interest related to the essential role of Zn(II) ion in enzymatic redox reactions involving the pyridine nucleotide coenzymes.[5] However, it still remains controversial whether the metal ions activate the NADH models,[2, 6, 7] the substrates,[1, 4, 8] or both.[9, 10] In particular, crucial questions arise as to the mechanistic origin of the catalysis, since the mechanisms of the net hydride transfer continue to be debated, involving the one-step transfer of a hydride ion,[4, 11, 12] the sequential transfer of an electron and a hydrogen atom,[4] or the sequential electron-proton-electron transfer.[10]

In chapters 1 and 2, the author described that the mechanism of the redox-photosensitized reactions of BNAH with olefinic and carbonyl compounds involves $Ru(bpy)_3^{2+}$-photomediated electron transfer from BNAH to substrates followed by electron-transfer and/or radical-coupling reactions between radical intermediates as is shown in Scheme 1. Therefore, the effect of Mg(II) ion on the redox-photo-

sensitized reduction may provide a clue to the catalytic behavior of the metal ion in electron-transfer reactions of NADH models. We have thus investigated, in some detail, the effect of Mg(II) ion on the $Ru(bpy)_3^{2+}$-photosensitized reduction of dimethyl fumarate and several selected olefins by BNAH.

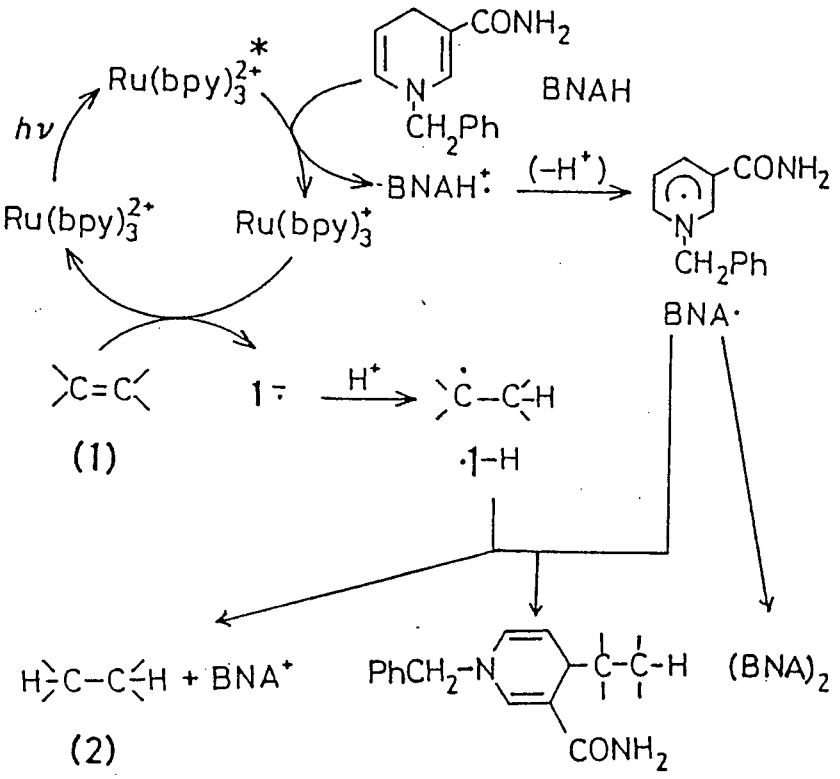

Scheme 1

3-2 RESULTS

Net Effect of Mg(II) Ion on Photosensitized Reactions. The photosensitized reactions were carried out by visible-light (> 470 nm) irradiation of methanolic and pyridine-methanol (10:1 v/v) solutions. In the present investigation, $Mg(ClO_4)_2$ was used as the source of Mg(II) ion at 0.05 or 0.1 M in 10:1 pyridine-methanol and at 0.025 M in methanol. Higher concentrations of $Mg(ClO_4)_2$ in methanol were avoided because of the precipitation of a red-orange solid upon admixture of the reactants. Scheme 2 shows the products isolated, details of which have been already described chapter 1. In the present investigation, both the disappearance of **1a-g** and the formation of **2a-g** were followed by VPC, while the other products were not analyzed.

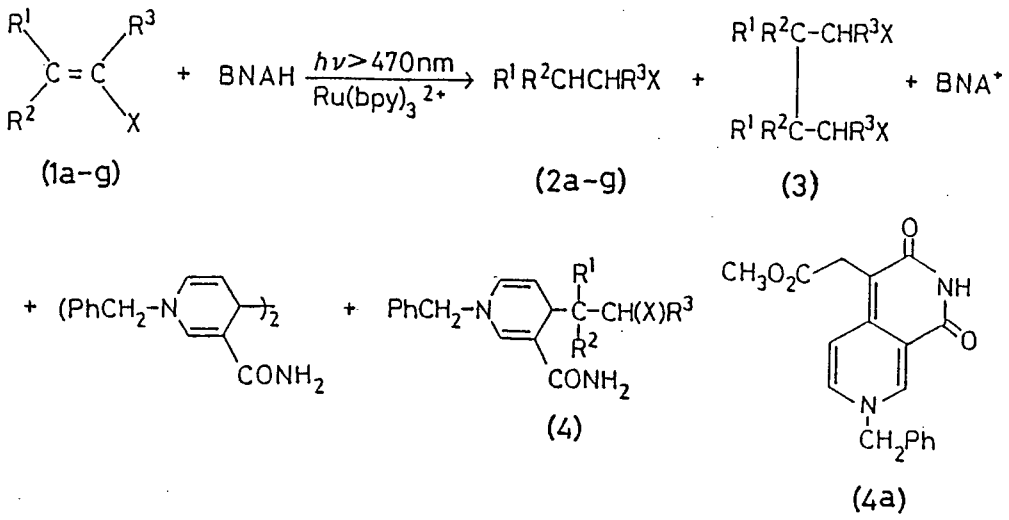

Scheme 2

It was confirmed that no reaction occurs in the dark. Moreover, **3** and **4** gave neither **1** nor **2** under the photoreaction conditions with $Mg(ClO_4)_2$.

Table I summarizes conversions of **1a-g** and chemical yields of **2a-g** in the presence or absence of $Mg(ClO_4)_2$ and Table 2 lists relative quantum yields for the disappearance of **1** (Φ_{-1} and Φ_{-1}^{M}) and the formation of **2** (Φ_2 and Φ_2^{M}) together with half-wave reduction potentials of **1** ($E_{1/2}$), and other electrochemical data (vide infra). These results clearly demonstrate the catalytic effects of $Mg(ClO_4)_2$, which are specific for Mg(II) ion since neither NH_4ClO_4 nor $LiClO_4$ exerts much effect on the photosensitized reduction of **1c** as is shown in Figure 1.

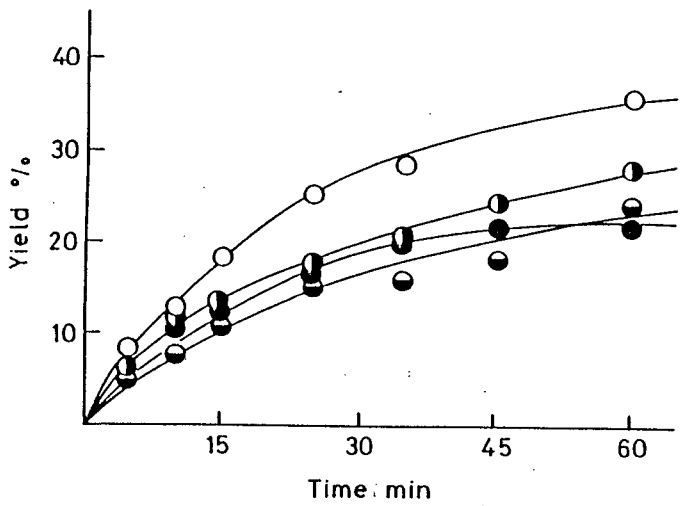

Figure 1. Effects of added salts on the formation of **2c** by the $Ru(bpy)_3^{2+}$-photosensitized reduction of **1c** by BNAH in MeOH; no added salt (●), $LiClO_4$ (50 mM) (◑), NH_4ClO_4 (50 mM) (◒), $Mg(ClO_4)_2$ (25 mM) (○); [$Ru(bpy)_3^{2+}$] 0.3 mM. [BNAH] 25 mM, [**1a**] 12.5 mM; irradiation at > 470 nm.

Table I. $Ru(bpy)_3^{2+}$-Photosensitised Reduction of 1 by BNAH and Effects of Mg(II) Ion[a]

Olefin					Irrad.		Convn. of 1/%[c]		Yield of 2/%[c,d]	
	R^1	R^2	R^3	X	Time/m	Solvent[b]	Without Mg^{2+}	With Mg^{2+}	Without Mg^{2+}	With Mg^{2+}
1a	CO_2Me	H	H	CO_2Me	20	A	67	72	40	80
						B	58	93	70	80
1b	p-C_6H_4CN	H	H	CO_2Me	20	A	49	49	63	83
						B	74	96	100	100
1c	p-$C_6H_4CO_2Me$	H	H	CO_2Me	20	A	17	22	70	90
						B	58	86	72	90
1d	Ph	Ph	H	CO_2Me	100	A	22	42	59	88
						B	15	31	25	57
1e	H	Ph	Ph	CN	60	B	22	67	30	47
1f	Ph	Ph	H	CN	60	B	38	60	32	55
1g	Ph	H	Ph	COMe	20	B	24	87	0	7

[a] For 3-cm^3 solutions irradiated at >470 nm. [b] A = methanolic solutions containing $Ru(bpy)_3^{2+}$ (0.3 mM), BNAH (25 mM), 1 (12.5 mM), and $Mg(ClO_4)_2$ (25 mM); B = 10:1 pyridine-methanol solutions containing $Ru(bpy)_3^{2+}$ (1.0 mM), BNAH (100 mM), 1 (50 mM), and $Mg(ClO_4)_2$ (50 mM). [c] Conversion and yields at level-off points determined by G.C. [d] Based on 1 unrecovered.

Table II. Relative Quantum Yields in the Presence and Absence of Mg(II) ion[a,b]

Olefin	$-E_{1/2}^{c}$/V	$-E_{1/2}^{pred}$/V	ΔE^{e}/V	Solvent	Φ_{-1}^{M}/Φ_{-1}	Φ_{2}^{M}/Φ_{2}	Φ_{2}/Φ_{-1}	$(\Phi_{2}/\Phi_{-1})^{M}$
1a	1.72	1.49	0.23	A	1.1	2.0	0.41	0.80
				B	1.6	1.6	0.85	0.86
1b	1.80	1.63	0.17	A	1.0	1.3	0.72	0.92
				B	1.3	1.3	1.0	1.0
1c	1.88	1.65	0.23	A	1.1	1.4	0.7	0.85
				B	1.7	1.7	1.0	1.0
1e	1.95	1.82	0.13	B	2.1	3.6	0.37	0.63

[a] Relative quantum yields determined at the concentrations of the reactants described in the footnote of Table I. [b] The quantum-yield abbreviations with and without superior M denote those with and without Mg(II)ion. [c] Polalographic reduction potentials vs. $Ag/AgNO_3$ in MeCN. [d] Half-wave potentials of prewaves observed with $Mg(ClO_4)_2$ one-half equialent to the olefins. [e] $E_{1/2}^{pre} - E_{1/2}$.

It was found that the quantum yields for the photoreduction of **1a** are almost independent of concentration of **1a** (Figure 2).

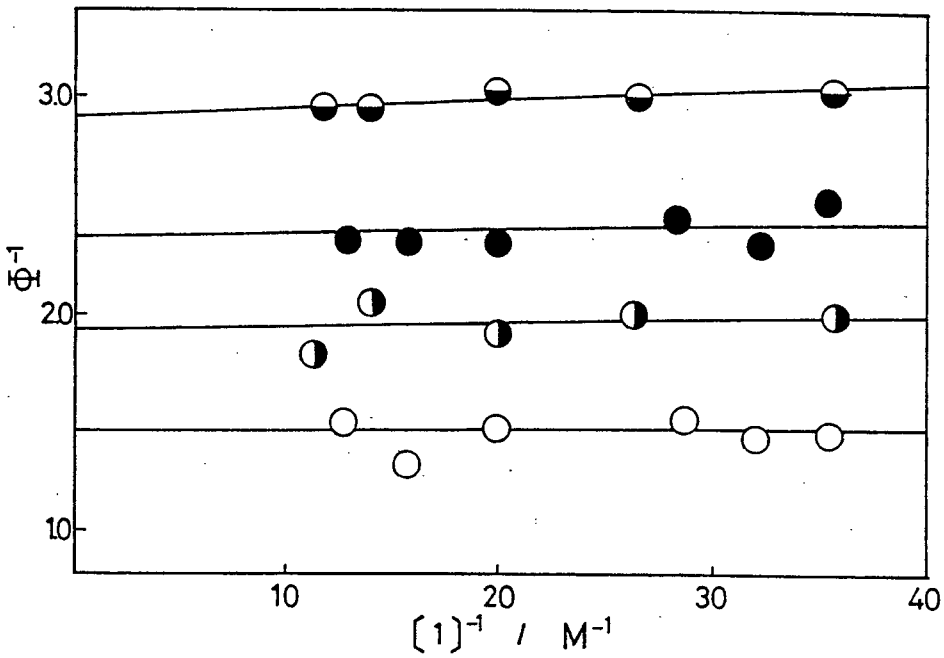

Figure 2. Double-reciprocal plots of quantum yield vs. concentration of **1a** for the disappearance of **1a** with (○) and without (●) Mg^{2+} and for the formation of **2a** with (◑) and without (◒) Mg^{2+}; $[Ru(bpy)_3{}^{2+}]$ 1.0 mM, [BNAH] 0.1 M. $[Mg^{2+}]$ 0.1 M in 10:1 pyridine-methanol; irradiation at 520 nm.

Interactions of Mg(II) Ion with BNAH and Olefins. It is known that NADH models form complexes with Mg(II) and Zn(II) ions.[2, 13, 14] Although Mg(II) ion caused only a little

shift of the absorption maximum of BNAH at < 10^{-4} M in either methanol or 10:1 pyridine-methanol, the end absorption of BNAH at a relatively high concentration (1 x 10^{-3} M) significantly increases with concentration of $Mg(ClO_4)_2$. The spectral change was analyzed according to the Ketelaar's equation[15] (Eq. 2), where d and d_0 represent

$$\text{BNAH} + Mg^{2+} \underset{\longleftarrow}{\overset{K}{\longrightarrow}} \text{BNAH---}Mg^{2} \equiv C \qquad (1)$$

$$\frac{[\text{BNAH}]}{d - d_0} = \frac{1}{\varepsilon_c - \varepsilon_b}\left(1 + \frac{1}{K[Mg^{2+}]}\right) \qquad (2)$$

optical densities at 410 nm in the presence and absence of $Mg(ClO_4)_2$, respectively; ε_b and ε_c denote the molar absorption coefficients at 410 nm for free BNAH and the BNAH-Mg^{2+} complex, respectively. Figure 3 shows double-reciprocal plots of $(d - d_0)$ vs. $[Mg^{2+}]$, the intercepts and slopes of which give the equilibrium constants, K. The observed values listed in Table III are smaller by two or three order of magnitude than those reported for pairs of the same or similar NADH models and Mg(II) or Zn(II) ions,[2, 5, 13, 14] the metal ion is stabilized by the coordination of methanol.

On the other hand, no complex formation between Mg(II) ion and the olefins was indicated by spectroscopic measurements; admixture of $Mg(ClO_4)_2$ in an equimolar caused no essential change in IR spectra of KBr disks, $CHCl_3$ solutions, and Nujol mulls, UV spectra of methanolic solutions, and ^1H and ^{13}C NMR spectra of CD_3CN solutions.

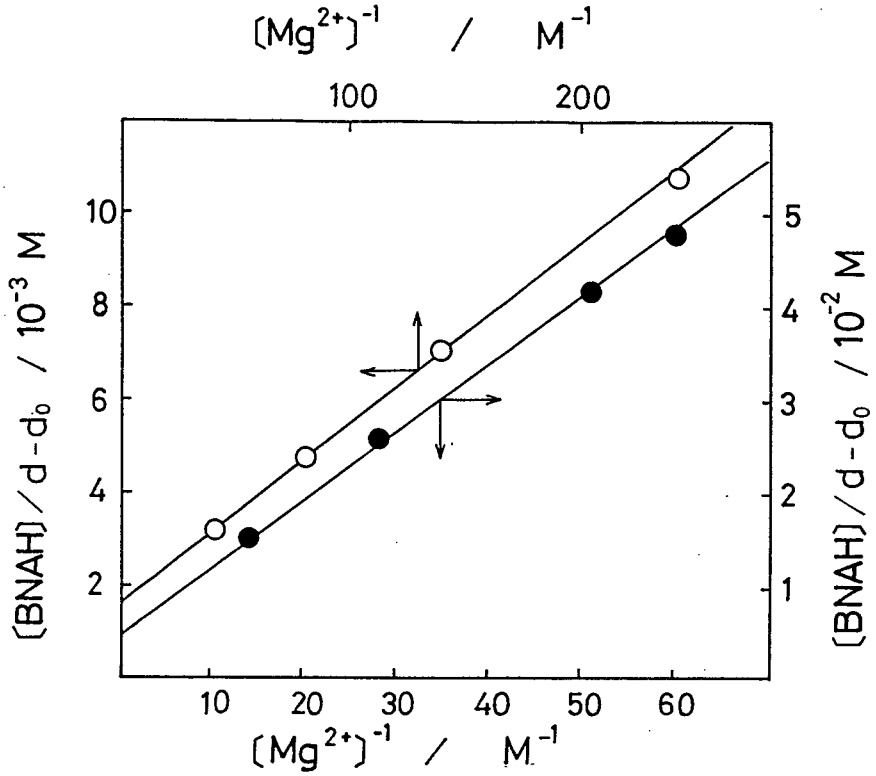

Figure 3. Ketelaar's plots for the complex formation of BNAH with Mg^{2+} in MeOH (●) and in 10:1 pyridine-methanol (○); [BNAH] 1.0 mM.

Table III. Equilibrium Constants and Luminescence-Quenching Rate Constants

Solvent[a]	K /mM^{-1}	τ[b] /ns	k_q^{app} /M^{-1}s^{-1}	k_q^{B} /M^{-1}s^{-1}	k_q^{C} /M^{-1}s^{-1}
A	7	730(800)	1.4×10^8	1.5×10^8	9×10^7
B	42	850(960)	1.1×10^8	3.7×10^8	ca.5×10^6

[a] A = methanol and B = 10:1 pyridine-methanol. [b] The observed luminescence lifetimes of $Ru(bpy)_3^{2+}$ at 20 °C in the presence of $Mg(ClO_4)_2$ at 25 mM in methanol and at 0.1 mM in pyridine-methanol. In parentheses are the lifetimes without Mg^{2+}.

In contrast, Mg(II) ion remarkably affected polarographic behaviors of the olefins such that pre-waves appear at more positive potentials than $E_{1/2}$ and increase in currents with an increase in concentration of Mg(II) ion (Figure 4). Table 2 includes the half-wave potentials of the pre-waves ($E_{1/2}^{pre}$), which were taken with $Mg(ClO_4)_2$ in an amount of one-half equiv. to each olefin, where the pre-waves clearly appeared without significant effects of adsorption on the electrode. Since Mg(II) ion does not form complexes with the olefins as discussed above, the appearance of the pre-waves is not static but dynamic in nature, probably arising from the stabilization of the anion radical of the olefins by ion pairing or complex formation with Mg(II) ion on electrode.[16]

$$1 + e^- \rightleftharpoons 1^{\cdot-} \overset{Mg^{2+}}{\rightleftharpoons} Mg^{2+} \cdots 1^{\cdot-}$$

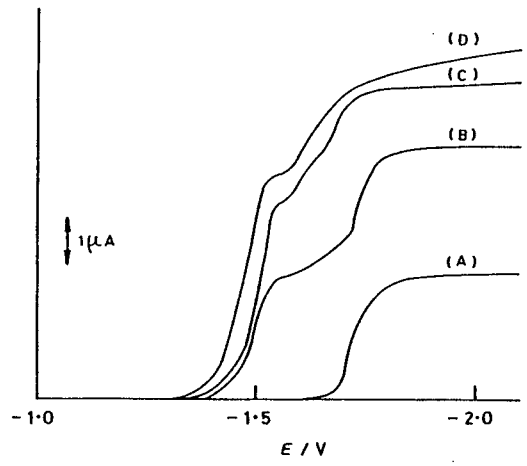

Figure 4. Polarograms of **1a** without Mg^{2+} (A) and with $Mg(ClO_4)_2$ at 0.45 (B), 1.0 (C), and 2.0 mM (D) in dearated MeCN; [**1a**] 1.0 mM, [Et_4NClO_4] 0.1 mM; scan rate 5 mVs^{-1}.

3-3 DISCUSSION

The luminescence of $Ru(bpy)_3^{2+}$ was quenched by BNAH either without or with Mg(II) ion following linear Stern-Volmer relationships. The Stern-Volmer constants when Mg(II) ion is present are smaller than those in its absence. Since the luminescence lifetimes are little affected by Mg(II) ion, the apparent quenching rate constants (k_q^{app}) are the quantities to be examined for the metal-ion effects. If the luminescence quenching occur with both free BNAH and BNAH-Mg^{2+} complex with rate constants of k_q^B and k_q^C respectively, equation 3 gives an approximate kinetic representation of k_q^{app} in cases where $c_B << c_M$; c_B and c_M denote the total concentrations of BNAH and $Mg(ClO_4)_2$ respectively.

$$\frac{\Phi_L}{\Phi_L^0} = 1 + k_q^{app}\tau c_B \simeq 1 + \left[k_q^B - (k_q^B - k_q^C)\left(\frac{K \cdot c_M}{1 + K \cdot c_M}\right)\right]\tau c_B \qquad (3)$$

Table III lists the calculated values of k_q^C together with k_q^B and K. Since $k_q^B > k_q^C$ in each case, the complex formation evidently suppresses the electron-donating capabilities of BNAH, an observation in line with Mg^{2+}-induced positive shifts of the electrochemical oxidation wave of BNAH.[17]

It should be noted however that complex formation has little effect on the photoreduction, since $k_q^B(c_B - [C]) >> k_q^C[C]$ under the photoreaction conditions. In other words, only free BNAH participates in the initiation process of the photosensitized reactions even in the presence of Mg(II) ion, i.e., electron transfer from free BNAH to luminescent

excited-state $Ru(bpy)_3^{2+}$ (^{3}MLCT) (Eq. 5). This means that the observed effects of Mg(II) ion are not static but dynamic in nature. Calculations show that net quenching of ^{3}MLCT by BNAH with or without Mg(II) ion under the photoreaction conditions is complete in pyridine-methanol and similar in efficiency (72% and 75%, respectively) in methanol.

The quantum yields for the disappearance of 1 are diagnostic for possible effects of Mg(II) ion on the processes involved in the first one-electron reduction of 1, (Eqs. 4-7); the probabilities of equations 5a and 8

$$Ru(bpy)_3^{2+} \xrightarrow{h\nu} {}^3MLCT \qquad (4)$$

$$^3MLCT + BNAH \xrightarrow{k_q^B} \{Ru(bpy)_3^{+} \; BNAH^{+\cdot}\} \xrightarrow{p_1(p_1^M)} Ru(bpy)_3^{+} + BNAH^{+\cdot} \qquad (5a)$$

$$\{Ru(bpy)_3^{+} \; BNAH^{+\cdot}\} \xrightarrow{1-p_1(p_1^M)} Ru(bpy)_3^{2+} + BNAH \qquad (5b)$$

$$Ru(bpy)_3^{+} + 1 \xrightarrow{k_6(k_6^M)} Ru(bpy)_3^{2+} + 1^{-\cdot} \qquad (6)$$

$$Ru(bpy)_3^{+} + X \xrightarrow{k_7(k_7^M)} Ru(bpy)_3^{2+} + X_{red} \qquad (7)$$

$$1^{-\cdot} + H^{+}(Solvent) \xrightarrow{p_2(p_2^M)} {}^{\cdot}1\text{-}H \qquad (8)$$

$$1^{-\cdot} + Y \xrightarrow{1-p_2(p_2^M)} 1 + Y_{red} \qquad (9)$$

(X and Y ; impurities)

occurring are represented by P_1 and P_2 without Mg^{2+} or by P_1^M and P_2^M with the metal ion, respectively. The regeneration of 1 from ·1-H can be neglected since the photoreduction of **1a** and dimethyl maleate in MeOD results in no deuterium incorporation in the recovered olefins as well as in no stereomutation described in chapter 1. In the case of **1a**, moreover, both the quantum yields for the disappearance of **1a** and for the formation of **2a** are independent of the concentration of **1a** in either the presence or absence of Mg(II) ion, thus demonstrating that $k_6[\mathbf{1a}]/k_7$ is unaffected by Mg(II) ion. Therefore, equation 10 represents the metal-ion effects on the first one-electron reduction of **1a** and may also hold in cases of the other olefins.

$$\frac{\Phi_{-1}^M}{\Phi_{-1}} = \left(\frac{P_1^M}{P_1}\right)\left(\frac{P_2^M}{P_2}\right) \qquad (10)$$

Since $\Phi_{-1}^M > \Phi_{-1}$ in pyridine-metanol, Mg(II) ion may enhance the separation of the ion pair, $[Ru(bpy)_3^+ \; BNAH^{+\cdot}]$, by microenvironmental electrostatic effects and/or may stabilize $1^{-\cdot}$ by ion pairing or complex formation to prevent the loss of an electron from $1^{-\cdot}$ as is shown in equation 11. Although P_1 (P_1^M) and P_2 (P_2^M) cannot be factored out

$$1^{-\cdot} + Mg^{2+} \rightleftharpoons Mg^{2+}\text{---}1^{-\cdot} \xrightarrow[(-Mg^{2+})]{H^+} \cdot 1\text{-H} \qquad (11)$$

from Φ_{-1} (Φ_{-1}^M) by usual steady-state kinetics, the appearance of the pre-wave in the electrochemical reduction of **1** in the presence of Mg(II) ion suggests that equation 11 is an important pathway for the metal-ion effects in 10:1 pyridine-methanol. On the other hand, Mg(II) ion had

little effect on the disappearance of **1** in methanol this being particularly so for **1a**, **1b**, and **1c**. In this solvent, $1^{-\bullet}$ may be much more efficiently protonated than the loss of an electron and/or the Mg(II) ion exclusively exists as $Mg(MeOH)_6^{2+}$ that may be inactive in the stabilization of $1^{-\bullet}$.

The formation of **2** after the one-electron reduction involves the deprotonation of $BNAH^{+\bullet}$ (Eq. 12a), and the one-electron reduction of $^{\bullet}$**1**-H by $BNA^{\bullet}$ (Eq. 13a) as key mechanistic pathways. The net efficiency for the formation of **2** from $^{\bullet}$**1**-H can be represented by Φ_2/Φ_{-1} without Mg(II) ion or by $(\Phi_2/\Phi_{-1})^M$ with the metal ion, which approximately equals $P_3 \cdot P_4$ or $P_3^M \cdot P_4^M$ each; P_3 (P_3^M) and P_4 (P_4^M) denote the efficiencies of equations 12a and 13a, respectively, in the absence (presence) of Mg(II) ion.

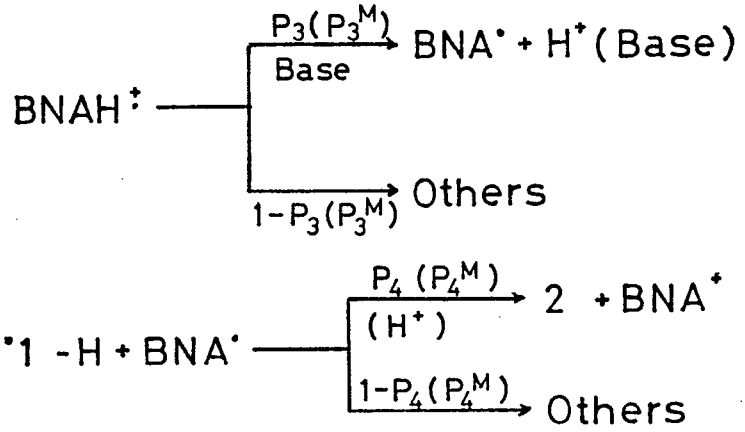

Since the rapid abstraction of a proton from $BNAH^{+\bullet}$ by pyridine has been well established,[18] it is reasonable to assume that $P_3 \simeq P_3^M \simeq 1$ in 10:1 pyridine-methanol and hence that $\Phi_2/\Phi_{-1} \simeq P_4$ and $(\Phi_2/\Phi_{-1})^M \simeq P_4^M$ in this solvent. In other words, the quantum-yield ratios in 10:1 pyridine-methanol or, less accurately, the yields of **2** in Table I

provide a convenient clue to the effects of Mg(II) ion on equation 13a. However, it should be noted that such presumptions are varid only in cases where $\Phi_2/\Phi_{-1} < 1$. For **1a**, **1b**, and **1c**, no metal-ion effect was observed since $\Phi_2/\Phi_{-1} \simeq 1$.

In the case of **1e**, $(\Phi_2/\Phi_{-1})^M$ is significantly greater than Φ_2/Φ_{-1}, and the yield of **2d** with Mg(II) ion is twice as high as that without the metal ion. In sharp contrast to the complete lack of the photoreduction to **2g** without the metal ion, the photosensitized reduction of **1g** to **2g** did occur in the presence of Mg(II) ion in low yield. These observations clearly demonstrate that Mg(II) ion catalyzes the electron transfer from BNA$^{\cdot}$ to $^{\cdot}$**1**-H. The mechanism of the catalysis is, perhaps, similar to that discussed in the metal-ion effect on the first one-electron reduction of **1** as follows.

$$\text{BNA}^{\cdot} + {}^{\cdot}\text{1-H} \rightleftharpoons \text{BNA}^{+} + {}^{-}\text{1-H} \xrightarrow{Mg^{2+}} Mg^{2+}\cdots{}^{-}\text{1-H}$$

It was found that $(\Phi_2/\Phi_{-1})^M > \Phi_2/\Phi_{-1}$ in the photoreduction of **1a**, **1b**, and **1c** in MeOH. In this solvent, however, possible effects on equation 12a should be taken into account, since $P_3 < 1$ because of the low basic nature of MeOH.[18] The deprotonation of BNAH$^{+\cdot}$ would be enhanced by the additional positive charge upon encounter with Mg(II) ion.

3-4 EXPERIMENTAL SECTION

Methanol was distilled from magnesium methoxide. Pyridine was refluxed over anhydrous KOH and then distilled before use. BNAH[19] and $Ru(bpy)_3Cl_2 \cdot 6H_2O$[20] were prepared according to the literature methods. Dimethyl fumarate (**1a**) was reagent grade (Tokyo Kasei). The other olefins were prepared according to the methods described in chapter 1. $Mg(ClO_4)_2$, $LiClO_4$, and NH_4ClO_4 were thoroughly dried by heating at 120 °C in vacuo for > 20 h.

Analytical VPC was carried out on a Shimadzu GC-3BF machine with flame ionization detectors usings 2 m x 4 mm column packed with 2% OV-17 on Shimalite W. ^1H NMR spectra were recorded on a JEOL JNM-PS-100 spectrometer, ^{13}C NMR spectra on a JEOL JNM-FX-100 spectrometer, IR spectra on a Hitachi 260-10 spectrometer, UV and visible absorption spectra on a Hitachi 220-A spectrometer, and emission spectra on a Hitachi MPF-4 spectrofluorometer.

Polarographic measurements were carried out for N_2-saturated dry acetonitrile solutions at 20 ± 0.1 °C using a dropping mercury electrode, an $Ag/AgNO_3$ (0.1 M) reference electrode, Et_4NClO_4 (0.1 M) as the supporting electrolyte, and a Yanagimoto P-1000 potentiostat.

Photoreactions and Quantum Yields. All volumetric flasks, pipettes, and reaction vessels were dried in vacuo in a desiccator. The concentrations of the sensitizer, BNAH, the olefins, and the salts are indicated in the footnotes of Tables I and II and Figures 1 and 2. The equipment for irradiation and the filter solution was the same as that described in chapter 1. Aliquots (3 cm^3) of solutions were

introduced into Pyrex tubes (8 mm i.d.), deaerated by bubbling with a gentle stream of Ar, and then irradiated with a Matsushita tungsten-halogen lamp (300 W) at > 470 nm under cooling with water using a "merry-go-round" turntable. Both the disappearance of **1** and the formation of **2** were followed by VPC and plotted against time (see Figure 1). The conversions of **1** and the yields of **2** in Table I were those at level off points of the plots. The relative quantum yields in Table II were obtained from the slopes of initial linear portion of the plots. The quantum yields in Figure 2 were determined at 520 nm by using a Reinecke's salt actinometer,[21] a Hitachi MPF-2A monochromator, and a xenon lamp. All the procedures were performed in a dark room with a safety lamp.

3-5 REFERENCES

[1] Creighton, D. J.; Sigman, D. S. J. Am. Chem. Soc. **1971**, 93, 1525.

[2] Ohno, A.; Yamamoto, T.; Okamoto, S.; Oka, S.; Ohnishi, Y. Bull. Chem. Soc. Jpn. **1977**, 50, 2385.

[3] Ohnishi, M; Kagami, T.; Numakunai, T.;Ohno, A. Chem. Lett. **1976**, 915.

[4] Gase, R. A.; Pandit, U. K. J. Am. Chem. Soc. **1979**, 101, 7059.

[5] Pattinson, S. E.; Dunn, M. F. Biochemistry, **1976**, 15, 3691 and 3696.

[6] (a) Ohno, A.; Kimura, T.; Yamamoto, H.; Kim, S. G.; Oka, S.; Ohnishi, H. Bull. Chem. Soc. Jpn. **1977**, 50, 1535. (b) Ohno, A.; Yasui, S.; Yamamoto, H.; Oka, S.; Ohnishi, Y. ibid., **1978**, 51, 294.

[7] Hughes, M.; Prince, R. H. J. Inorg. Nucl. Chem. **1978**, 40, 703.

[8] Gase, R. A.; Boxhoorn, G.; Pandit, U. K. Tetrahedron Lett. **1976**, 2889.

[9] (a) Hughes, M.; Prince, R. H. Chem. Ind. (London), **1975**, 648. (b) Kitani, A.; Sasaki, K. J. Electroanal. Chem. **1978**, 94, 201.

[10] Ohno, A,; Nakai, J.; Nakamura, T.; Goto, T.; Oka, S. Bull. Chem. Soc. Jpn. **1981**, 54, 3482 and references cited there in.

[11] (a) Norcoss, B. E.; Klinedinst, D. E.; Westheimer, F. J. J. Am. Chem. Soc. **1962**, 84, 797. (b) Wallenfels, K.; Ertel, W.; Friedlich, K. Liebigs Ann. Chem. **1973**, 1663. (c) MacInnes, I.; Nonhebel, D. C.; Orszulik, S. T.; Suckling, C. J. J. Chem. Soc., Perkin Trans. 1, **1983**, 2777.

[12] Powell, M. F.; Bruce, T. C. J. Am. Chem. Soc. **1983**, 105, 1014.

[13] Fukuzumi, S.; Kondo, Y.; Tanaka, T. Chem. Lett. **1983**, 485.

[14] Ohno, A.; Yasui, S.; Gase, R. A.; Oka, S.; Pandit, U. K. Bioorg. Chem. **1980**, 9, 199.

[15] Ketelaar, J. A. A.; Stope, C. V.; Gersmann, H. R. Recl. Trav. Chim. **1952**, 70, 499.

[16] Kitani, A.; Sasaki, S. Nippon Kagaku Kaishi, **1978**, 817.

[17] Kitani, A.; Hashimoto, N.; Sasaki, K. Nippon Kagaku Kaishi, **1978**, 1103.

[18] (a) Blasel, W. J.; Haas, R. G. Anal. Chem. **1970**, 42, 918. (b) Martens, F. M.; Verhoeven, J. W. J. Photochem. **1983**, 22, 99.

[19] Mauzerall, D.; Westheimer, F. M. J. Am. Chem. Soc. **1955**, 77, 2261.

[20] Fujita, I.; Kobayashi, H. Ber. Bunsenges. Phys. Chem. **1972**, 70, 115.

[21] Wegner, E. E.; Adamson, A. W. J. Am. Chem. Soc. **1966** 88, 394.

Chapter 4

PHOTOCHEMISTRY OF 4-ALKYLATED NADH MODELS, 1-BENZYL-4-(1-HYDROXYALKYL)-1,4-DIHYDRONICOTINAMIDES

4-1 INTRODUCTION

As has been shown in chapter 1 and 2, the photosensitized reactions of BNAH with either olefins or aromatic carbonyl compounds by $Ru(bpy)_3^{2+}$ yield 1:1 adducts, new classes of 4-alkylated 1,4-dihydronicotinamides. These findings prompted the author to investigate chemical behaviors of these adducts, since chemistry of 4-substituted 1,4-dihydronicotinamides has been of synthetic and biological significance.[1-4] It was found that the adducts with carbonyl compounds (**1a-c**) reveal interesting behaviors in either the direct photolysis or the photosensitization by $Ru(bpy)_3^{2+}$.

4-2 RESULTS AND DISCUSSION

Direct Photolysis. Irradiation of a methanolic solution of **1a-c** (50 mM) at >330 nm mainly gave a carbonyl compound (**2a-c**) and the three isomeric dimers of 1-benzyl-3-carbamoyldihydro-4-pyridinyl radical, i.e. the 4,4'-bonded dimer (**3**), 4,6'-bonded dimer (**4**), and the diastereoisomer of **4** (**5**), as shown in Scheme 1. The dimers were isolated and identified by direct comparison with authentic samples,[5] while the other isomers could not be detected. In the case of **1a**, 1,2-diphenyl-1,2-ethanediol was formed in a 12% yield by VPC. Although the diol formation from 1b,c can be

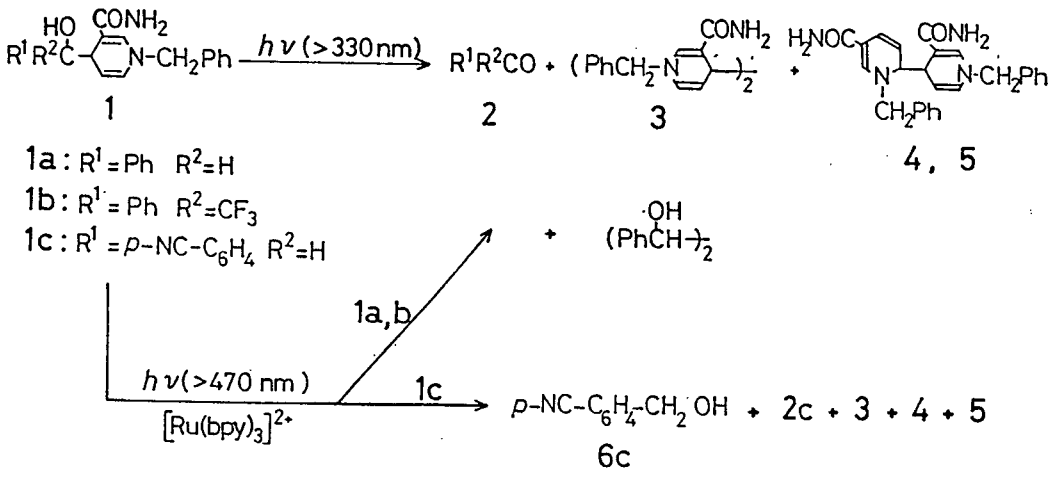

Scheme 1

presumed to occur, VPC and HPLC methods could not be used for the analysis.[6] In any case, moreover, we could not detect the alcohols, $R^1R^2CH(OH)$, nor the positional isomers of **1a-c** by extensive VPC and HPLC analyses. Table 1 summarizes yields of 2-5.

Table I. Direct Photolysis of 1a-c[a]

	1		Time	Convn.	Yield/%[b]			
	R^1	R^2	h	%	2	3	4	5
a	Ph	H[c]	4	47	49	37	26	17
b	Ph	CF_3	12	25	52	80	7	4
c	p-NCC_6H_4	H	10	35	57	43	26	20

a) For 3-cm^3 methanolic solutions containing **1a-c** (0.05 M) irradiated at >330 nm. b) Based on **1a-c** consumed. c) 1,2-Diphenyl-1,2-ethandiol was formed in a 12% yield.

These observations strongly suggest that the photoexcitation of **1a-c** results in a selective homolytic fission to generate a pair of $R^1R^2\dot{C}(OH)$ and the dihydropyridinyl radical (BNA·). The radical pair might diffuse apart out of a solvent cage in competition with the radical coupling regenerating **1a-c**. The free BNA· exclusively dimerizes to give **3**, **4**, and **5** in a kinetic controlled ratio. The predominant formation of **3** in the photolysis of **1b** appears to arise from a consequence of a secondary photoreaction, since irradiation of either **4** or **5** leads to the selective isomerization to **3** though the reverse photoisomerization does not occur as described in chapter 5. On the other hand, the $R^1R^2\dot{C}(OH)$ are perhaps oxidized to 2a-c by impurities and/or by unreclaimed reactions in competition with the dimerization. the author attempted to detect other possible products arising from the $R^1R^2C(OH)$ fragment, since yields of **2a-c** are lower than the combined yields of **3-5** in each case. However, other definite products than those mentioned here could not be detected. A possible mechanism is shown in Eqs. 1-6.

$$R^1R^2C(OH)\text{-BNA} \underset{}{\overset{h\nu}{\rightleftharpoons}} \overline{R^1R^2\dot{C}(OH) \quad BNA\cdot} \qquad (1)$$

$$\overline{R^1R^2\dot{C}(OH) \quad BNA\cdot} \longrightarrow R^1R^2\dot{C}(OH) + BNA\cdot \qquad (2)$$

$$R^1R^2\dot{C}(OH) \xrightarrow[-H\cdot]{} R^1R^2C{=}O \qquad (3)$$

$$2R^1R^2\dot{C}(OH) \longrightarrow R^1R^2C(OH)C(OH)R^1R^2 \qquad (4)$$

$$R^1R^2\dot{C}(OH) \longrightarrow \text{Others} \qquad (5)$$

$$2BNA\cdot \longrightarrow 3 + 4 + 5 \qquad (6)$$

It is of interest to note that the radical pair can be regarded as a mechanistic equivalent to a key intermediate that is involved in an ECE mechanism[7] proposed for the reduction of carbonyl compounds by BNAH in the dark as shown in Eqs. 7 and 8. According to this mechanism, BNA· could donate an electron to $PhC^{\cdot}(OH)CF_3$ and p-$NCC_6H_4\dot{C}H(OH)$ since the reductions of trifluoroacetophenone and p-cyanobenzaldehyde by BNAH do occur in the dark to give the corresponding alcohols. However, the photolysis of either **1b** or **1c** did not afford the coresponding alcohols, thus indicating that BNA· is incapable of undergoing one-electron reduction of $R^1R^2\dot{C}(OH)$.[8]

Furthermore, the lack of the BNAH formation in the photolysis of **1a-c** suggests that transfer of a hydrogen-atom equivalent from $R^1R^2\dot{C}(OH)$ to BNA·, the reverse pathway of Eq. 7, is very unlikely to occur.

$$R^1R^2C{=}O + BNAH \rightleftarrows \overline{R^1R^2CO^{-}\cdot \; BNAH^{+}\cdot} \rightleftarrows \overline{R^1R^2\dot{C}(OH) \quad BNA\cdot} \qquad (7)$$

$$\overline{R^1R^2\dot{C}(OH) \; BNA\cdot} \rightleftarrows \overline{R^1R^2\bar{C}(OH) \; BNA^{+}} \xrightarrow{H^{+}} R^1R^2CH(OH) + BNA^{+} \qquad (8)$$

Photosensitization by $Ru(bpy)_3^{2+}$. The photosensitized reactions of **1a-c** were carried out by the irradiation at >470 nm in order to achieve the selective photoexcitation of $Ru(bpy)_3^{2+}$. In the cases of **1a,b**, the results are similar to those of the direct photolysis with some differences in product ratios. The major products are again **2a,b** and the BNA· dimers without the formation of BNAH and $R^1R^2CH(OH)$, and 1,2-diphenyl-1,2-ethanediol was also formed in a 13% yield in the case of **1a**.[6] Prominently, the photosensitized reaction of **1c** yielded p-cyanobenzyl alcohol (**6c**)

in a 50% yield along with **2c** and the BNA· dimers, showing a sharp contrast to the lack of the alcohol formation in the direct photolysis. In this case, moreover, it is notable that the combined yield of **3**-**5** is significantly lower than that of **2c** and **6c** though BNAH is not formed, an observation contrary to those of the other cases. The results are summarized in Table II and in Scheme 1.

Table II. $Ru(bpy)_3^{2+}$-Photosensitized Reactions[a]

	1		Time	Convn.	Yield/%[b]				
	R^1	R^2	h	%	**2**	**3**	**4**	**5**	**6**
a	Ph	H[c]	8	67	67	56	30	10	0
b	Ph	CF_3	16	10	30	50	20	12	trace
c	p-NCC_6H_4	H	10	20	40	10	22	29	50

[a] For 3-cm^3 methanolic solutions containing **1a-c** (0.05 M) and $Ru(bpy)_3Cl_2 \cdot 6H_2O$ (1 mM) irradiated at >470 nm. [b] Based on **1a-c** consumed. [c] 1,2-Diphenyl-1,2-ethanediol and hydrogen were detected in 13% and 2% yields respectively.

The luminescence of $Ru(bpy)_3^{2+}$ was quenched by 1a-c at rate constants, which are significantly smaller than the quenching rate constant of BNAH and which decrease with increasing inductive effects of R^1 and/or R^2 as shown in Table III. It is therefore reasonable to assume that electron transfer from **1a-c** to $Ru(bpy)_3^{2+}$ in the metal-to-ligand charge-transfer excited state occurs to initiate the photosensitized reactions (Eq. 9). Electron-withdrawing inductive effects of the aromatic rings and the trifluoromethyl group should weaken the electron donating power of

the dihydronicotinamide moiety of **1a-c** compared with BNAH.

$$\mathbf{1a\text{-}c} + \mathbf{Ru(bpy)_3^{2+}} \underset{}{\overset{h\nu}{\rightleftharpoons}} \mathbf{1a\text{-}c^{+\cdot}} + \mathbf{Ru(bpy)_3^{+}} \quad (9)$$

The follow-up reaction of **1a-c**$^{+\cdot}$ has two choices; one is the bond cleavage to yield **2a-c**, H^+, and BNA$^\cdot$ (Eq. 10) and the other involves the formation of $R^1R^2\dot{C}(OH)$ and BNA (Eq. 11). Although there is no unequivocal evidence supporitng either or both of the two pathways, comparisons of reduction potentials between **2a-c** and BNA^+ in methanol might imply that Eq. 10 is thermodynamically more favorable than Eq. 11. The polarographic reduction waves of **2a** and **2c** in methanol appear at -1.86 V and -1.52 V vs. Ag/Ag^+, respectively, which are more negative than the reduction wave of BNA^+ (-1.445 V).[9] Reduction waves of aromatic carbonyl compounds in the presence of a proton donor usually occur as the consequences arising from the formation of $R^1R^2\dot{C}(OH)$ by sequential electron-proton transfer to R^1R^2CO.[10] Therefore electron transfer from $R^1R^2C(OH)$ to BNA^+ should be exothermic to yield **2a-c** and BNA$^\cdot$ (Eq. 12).

$$\mathbf{1a\text{-}c^{+\cdot}} \longrightarrow \mathbf{R^1R^2CO} + \mathbf{H^+} + \mathbf{BNA^\cdot} \quad (10)$$

$$\mathbf{1a\text{-}c^{+\cdot}} \longrightarrow \mathbf{R^1R^2\dot{C}(OH)} + \mathbf{BNA^+} \quad (11)$$

$$\mathbf{R^1R^2\dot{C}(OH)} + \mathbf{BNA^+} \xrightarrow[(\Delta G < 0)]{} \mathbf{R^1R^2CO} + \mathbf{H^+} + \mathbf{BNA^\cdot} \quad (12)$$

However, the formation of 1,2-diphenyl-1,2-ethanediol implies the intervention of $Ph\dot{C}H(OH)$. This can be easily interpreted by assuming the occurrence of electron transfer from $Ru(bpy)_3^+$ to **2a** (Eq. 13), which has already been discussed in chapter 2. This might be a major origin for

lower yields of **2a,b** compared with the BNA· dimers, provided that **2a,b**$^{-}$· and $R^1R^2\dot{C}(OH)$ afford unreclaimed products even in part.

$$Ru(bpy)_3^{+} + \textbf{2a-c} \longrightarrow Ru(bpy)_3^{2+} + \textbf{2a-c}^{-}\cdot \quad (13)$$

$$\textbf{2a-c}^{-}\cdot + H^{+} \longrightarrow R^1R^2\dot{C}(OH) \quad (14)$$

$$2R^1R^2\dot{C}(OH) \longrightarrow R^1R^2CH(OH)CH(OH)R^1R^2 \quad (15a)$$

$$\textbf{2a-c}^{-}\cdot \text{ and } R^1R^2\dot{C}(OH) \longrightarrow \text{Others} \quad (15b)$$

The formation of **6c** is of particular interest with regard to the electron-transfer mechanism. In order to obtain further mechanistic insights, the author carried out the $Ru(bpy)_3^{2+}$-photosensitized reactions of **1a-c** in the presence of BNAH or N,N-dimethyl-p-toluidine (DMT) in an equimolar amount, a concen-

Table III. Rate Constants for Quenching of $Ru(bpy)_3^{2+}$ Luminescence[a]

Quencher	$kq\tau/M^{-1}$	$kq^b/M^{-1}s^{-1}$
1a	57	7.1×10^7
1b	17	2.1×10^7
1c	15	1.9×10^7
BNAH	120	1.5×10^8
DMT[c]	840	1.1×10^9
3	1700	2.1×10^9

[a] Obtained from linear Stern-Volmer plots of the luminescence quenching for deaerated methanolic solutions. [b] Calculated from the $kq\tau$ values using τ = 800 ns at 20°C in methanol.[2] [c] N,N-Dimethyl-p-toluidine.

tration at which excited $Ru(bpy)_3^{2+}$ is exclusively quenched by BNAH or DMT (Table III) via electron transfer (Eq. 16). Interestingly, the photosensitized reaction of **1c** in the presence of either BNAH or DMT selectively gave **6c** at a rate 3.7 or 2 times each more efficient than that in its absence, while **2c** was not formed at all. Furthermore, we could not detect BNAH in the photoreaction with DMT but **3**, **4**, and **5** though yields were not determined. In contrast, the photosensitized reactions of **1a,b** in the presence of BNAH or DMT did not give the corresponding alcohols at all.

$$Ru(bpy)_3^{2+} + D \xrightarrow{h\nu} Ru(bpy)_3^{+} + D^{+\cdot} \quad (16)$$
(D = BNAH or DMT)

$$Ru(bpy)_3^{+} + 1c \longrightarrow Ru(bpy)_3^{2+} + 1c^{-\cdot} \quad (17)$$

$$Ru(bpy)_3^{+} + 1a,b \not\longrightarrow Ru(bpy)_3^{2+} + 1a,b^{-\cdot} \quad (18)$$

$$1c^{-\cdot} + H^{+} \longrightarrow p\text{-}NC\text{-}C_6H_4\text{-}CH_2OH + BNA^{\cdot} \quad (19)$$

$$1c^{-\cdot} + H^{+} \not\longrightarrow p\text{-}CN\text{-}C_6H_4\text{-}\dot{C}H(OH) + BNAH \quad (20)$$

On the basis of these observations, the formation of 6c can be interpreted in terms of Eqs. 16, 17, and 19. A key pathway is the electron transfer from $Ru(bpy)_3^{+}$ to **1c**, in which the cyanophenyl group should be essential because of the electron-accepting nature. Since **3** is a much more efficient quencher of excited $Ru(bpy)_3^{2+}$ than either **1c** or BNAH (Table III), it is expected that the BNA· dimers formed can also act as D in Eq. 16, being thus consumed during the photosensitized reaction of **1c**. This would be a reason for the lower yield of the BNA· dimers compared with the combined yield of **2c** and **6c** as shown in Table I. On the other hand, $Ru(bpy)_3^{+}$ appears to be incapable of donating an

electron to **1a,b** since the phenyl group has no extra electron-withdrawing substituent. The anion radical ($1c^{-\cdot}$) thus formed undergoes a bond cleavage to give **6c** and BNA$^{\cdot}$ in the presence of a proton donor. On the other hand, little participation of Eq. 20 can be expected, since both **2c** and BNAH were not formed in the photoreaction in the presence of DMT.

4-3 CONCLUSION

The present investigation exemplifies chemical behaviors of photoexcited **1a-c**, the cation radicals, and the anion radical of 1c as shown in Scheme 2. In the direct photolysis, the photoexcitation should be localized on the BNA moiety since it absorbs the incident light at >330 nm. This leads to the homolysis between the $R^1R^2C(OH)$ and BNA moieties, while intramolecular electron transfer from the excited BNA chromophore to the R^1 group does perhaps not occur. Likewise, the positive charge of $\mathbf{1a\text{-}c}^{+\cdot}$ should be localized on the BNA chromophore, being apparently the driving force for the bond cleavage between $R^1R^2C(OH)$ and BNA. This is reminescent of the very acidic nature of $BNAH^{+\cdot}$.[11] On the other hand, the negative charge of $\mathbf{1c}^{-\cdot}$ should be localized on the p-cyanophenyl group, thus leading to the formation of p-cyanobenzyl alcohol. In any case, BNA$^{\cdot}$ is commonly formed.

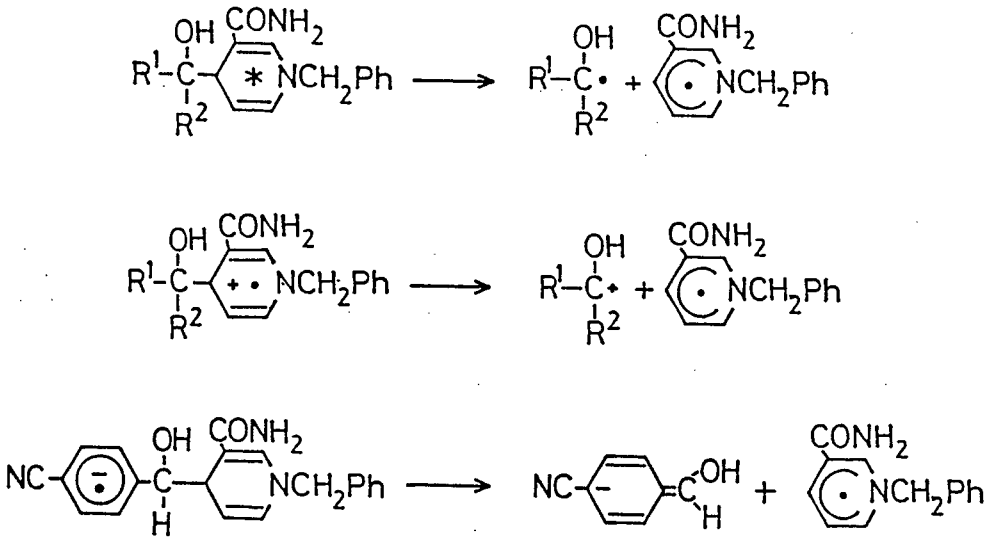

Scheme 2

4-4 EXPERIMENTAL SECTION

Materials. The preparation and purification of BNAH[12] and $Ru(bpy)_3Cl_2 \cdot 6H_2O$[13] were carried out according to the literature methods. The 4-alkylated dihydronicotinamides, **1a-c**, were obtained as 1:1 mixtures of the diastereoisomers by the $Ru(bpy)_3^{2+}$-photosensitized reactions of BNAH with benzaldehyde, 1,1,1-trifluoroacetophenone, and p-cyanobenzaldehyde as described in chapter 2. The diastereoisomers were separated by either repeated column chromatography on basic alumina or HPLC. However, we confirmed that the photochemical behaviors of the isolated diastereoisomers are essentially identical with those of 1:1

mixtures. Therefore, we used 1:1-diastereoisomeric mixtures of **1a-c** in the present investigation. The other materials were obtained from Nakarai Chemicals and used after distillation and/or recrystarization.

Analytical Methods. The formation of **2**, **6c**, and 1,2,-diphenyl-1,2-ethanediol was followed by VPC, whereas both the disappearance of **1a-c** and the formation of 3-5 were analyzed by HPLC. VPC was carried out on a Shimadzu GC-7A dual column instrument with flame-ionization detectors, and HPLC analysis were done on a Chemicosorb 7-ODS-H column using a Toyosoda CCPD dual pump coupled with a Yanaco M-315 spectromonitor working at 355 nm. A Hitachi 850 spectrofluorometer was used for luminescence-quenching experiments; deaerated solutions of the ruthenium complex (0.25 mM) were photoexcited at 550 nm and intensities of the luminescence were monitored at 610 nm. Polarographic mesurements were carried out for N_2-saturated water-free methanolic solutions containing **2a-c** (1 mM) and $NaClO_4$ (0.1 M) as the supporting electrolyte using an $Ag/AgNO_3$ reference electrode, a dropping mercury working electrode, and a Yanagimoto P-1100 potentiostat.

Direct Photolysis. A 3 mL-methanolic solution containing **1a-c** (50 mM) was bubbled with a gentle stream of Ar for 15 min and then irradiated with a high-pressure mercury lamp using a uranil glass filter (>330 nm) under cooling with water. The progress of the photoreactions was followed by VPC and HPLC.

Photosensitized reactions by $Ru(bpy)_3^{2+}$. A 3 mL-

methanolic solution containing **1a-c** (50 mM) and $Ru(bpy)_3^{2+}$ (1 mM) was bubbled with Ar for 15 min and then irradiated with a tungsten-halogen lamp using a solution filter of potasium chromate (20 g mL^{-1}) sodium nitrate (200 g mL^{-1}) and sodium hydroxide (6.7 g mL^{-1}) (> 470 nm) under cooling with water. The progress of the reactions was followed by VPC and HPLC.

4-5 REFERENCES AND NOTES

[1] For a review, see: Staut, D. M.; Meyers, A. I. Chem. Rev. **1982**, 82, 223.

[2] Ohno, A.; Nakai, J.; Nakamura, K.; Goto, T.; Oka, S. Bull. Chem. Soc. Jpn. **1981**, 54, 3482.

[3] Mashraqui, S. H.; Kellogg, D. M. J. Am. Chem. Soc. **1983**, 105, 7792.

[4] Meyers, A. I.; Oppenlaender, T. J. Am. Chem. Soc. **1986**, 108, 1989.

[5] Ohnishi, Y.; Kitami, M. Bull. Chem. Soc. Jpn. **1979**, 52, 2674.

[6] The diols, $[p\text{-}NC\text{-}C_6H_4CH(OH)]_2$ and $[PhC(OH)CF_3]_2$, which had been independently prepared, revealed no peak on VPC, whereas HPLC peaks of the diols were inseparably overlapped with many other peaks.

[7] Steffens, J. J.; Chipman, D. M. J. Am. Chem. Soc. **1971**, 93, 6694.

[8] In chapter 2, the autor described that the $Ru(bpy)_3^{2+}$-photosensitized reactions of BNAH with **2b** and **2c** give the corresponding alcohols (**6c** and **6d**) as minor products. Although these observations would indicate the occurence of

electron transfer from BNA$^{\cdot}$ to R_1R_2COH, close analysis of the reactions demonstrate that **6c** is not a primary product but a secondary one, perhaps from the $Ru(bpy)_3^{2+}$-photosensitized reduction of 1c by BNAH as described in the present paper; see Eqs. (16), (17), and (19).

[9] In polarography, **2b** shows no significant reduction wave in methanol because of the formation of the hemiacetal described in chapter 2.

[10] Evans, D. H. "Encyclopedia of Electrochemistry of the Elements", Vol. XII; Ed. Bard, A. J.; Lund, H.; Marcel Dekker Inc.: New York, 1978; pp 1-259.

[11] Maltens, F. M.; Verhoven, J. W. Rec. Trav. Chim. Pays-Bas, **1981**, 100, 228.

[12] Mauzarall, D.; Westheimer, F. M. J. Am. Chem. Soc. **1955**, 77, 2261.

[13] Broomhead, J. A.; Yaung, C. G. Inorg. Synth. **1983**, 22, 127.

Chapter 5

PHOTOSENSITIZED AND DIRECT PHOTOLYTIC ISOMERIZATIONS OF THE TETRAHYDRO DIMERS OF 1-BENZYLNICOTINAMIDE

5-1 INTRODUCTION

The pyridine nucleotide coenzymes ($NAD(P)^+/NAD(P)H$) reveal unique redox capabilities of undergoing specific transfer of a hydride equivalent (or two electrons) with a variety of substrates.[1] However, one-electron redox reactions can also very often occur with the coenzymes in the absence of oxido-reduction enzymes and particularly with their models in homogeneous solution, giving the tetrahydrodipyridines (NAD_2)[2-4] which are considered to be dead-end products incapable of undergoing two-electron redox reactions. Therefore, little has been investigated on chemical properties of NAD_2.

Nevertheless, it is certainly of chemical significance to explore chemistry of NAD_2 because of the unique azacyclohexadienyl structures and because of potential electron-donating nature. From this point of view, we have investigated chemical behaviors of NAD_2 using 1,1'-dibenzyl-3,3'-dicarbamoyltetrahydrodipyridines (BNA_2) which are selectively formed either by one-electron reduction of 1-benzylnicotinamide (BNA^+), a typical NAD^+ model, or by one-electron oxidation of BNAH. This capter deals with photochemical isomerizations of the 4,4'-dipyridine (**1**) and the 4,6' isomer (**2**) (Scheme 1).

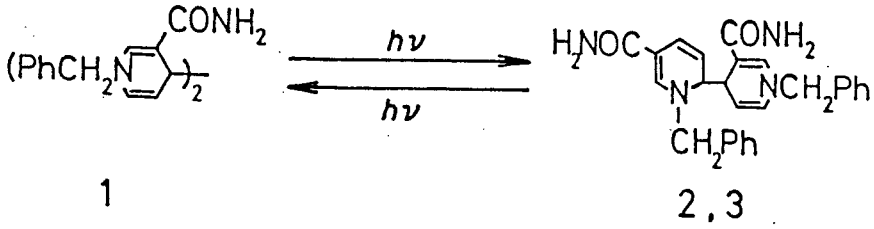

1 2,3

Scheme 1

5-2 RESULTS AND DISCUSSION

The zinc reduction of 1-benzylnicotinamide gave a mixture of the corresponding tetrahydrodipyridines,[2] from which one of the 4,4'-bonded diastereomers (1) and one of the 4,6'-bonded diastereomers (2) were obtained in purities enough for the present photochemical investigation, while the other isomer of 2 (3) could be isolated only in a small amount. On the other hand, what appears to be the other isomer of 1[2] was able to be detected by HPLC but not isolated because of its minor formation and difficulties of the isolation. Therefore, the author used 1 and 2 as the starting materials and N,N-dimethylformamide (DMF) as the solvent.

Irradiation of a deaerated solution of 1 (2.5 mM) and fac-Re(bpy)$(CO)_3$Br (0.8 mM) at 436 nm resulted in the isomerization of 1 to 2 and 3, thus giving a 2:2:1 mixture of 1, 2, and 3 at a photostationary state (Fig. 1). The photosensitized isomerization of 2 to 1 and 3 again occurrd to reach an identical photostationary state. Similarly,

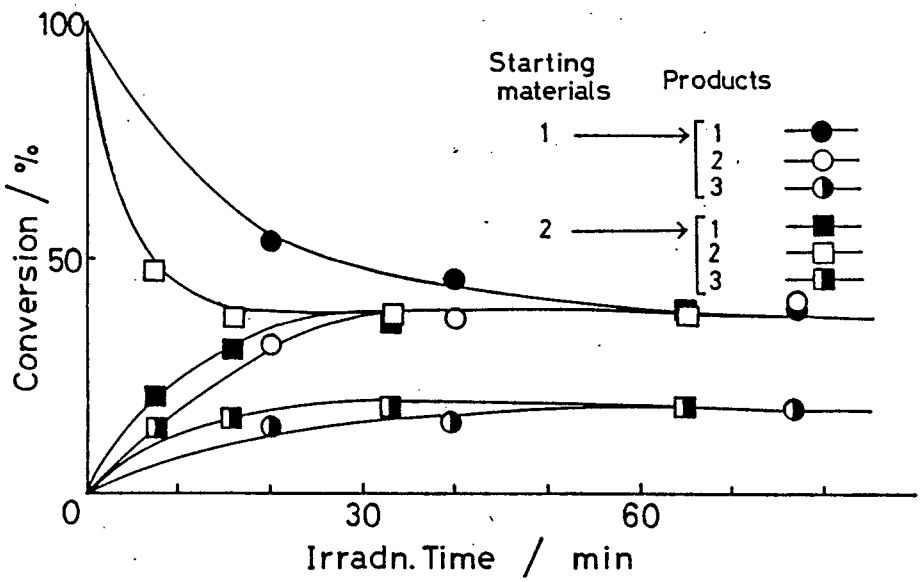

Figure 1. Time-Conversion plots for the fac-$Re(bpy)(CO)_3Br$-photosensitized isomerization of **1** and **2** at 436 nm; [**1**] or [**2**] = 2.5 mM and [fac-$Re(bpy)(CO)_3Br$] = 0.8 mM.

$Ru(bpy)_3^{2+}$ was effectively used as the photosensitizer for the isomerizations while the irradiation was carried at >470 nm. In all the runs, HPLC analyses showed the formation of a few common products in small amounts at retention times identical with those of the minor products in the zinc reduction of BNA^+.[2] Table I summarizes the photostationary-state ratios of **1**, **2**, and **3**.

The efficient photosensitized isomerization of **1** to **2** and **3** is of synthetic and mechanistic interest, since either thermal[2] or direct photoexcitation can effect the one-way isomerization from **2** to **1** for the most part. Upon heating a DMF solution of **2** at 60 °C or 100 °C, a reaction proceeded

Table I. Photosensitized Isomerization of 1 and 2 by fac-Re(bpy)$(CO)_3$Br and $Ru(bpy)_3^{2+}$ [a]

Starting Materials	Sensitizers [b]	Irradn. Time/min	Yields [c]/% 1	2	3	$kq\tau$ [d] M^{-1}	kq [e] $M^{-1}s^{-1}$
1	fac-Re(bpy)$(CO)_3$Br	35	40	40	19	182	3.7×10^9
	$Ru(bpy)_3^{2+}$	90	25	28	12	1340	1.4×10^9
2	fac-Re(bpy)$(CO)_3$Br	35	36	39	18	571	1.2×10^{10}
	$Ru(bpy)_3^{2+}$	25	32	29	14	680	7.3×10^8

[a] For deaerated DMF solutions containing 1 or 2 (2.5mM) and the sensitizers (0.8mM). [b] Irradiated at 436 nm for the fac-Re(bpy)$(CO)_3$Br runs and at >470 nm for the $Ru(bpy)_3^{2+}$ runs. [c] Based on the 1 or 2 used. [d] Slopes of linear Stern-Volmer plots for quenching of the sensitizer-luminescence by 1 or 2 in deaerated DMF solutions at 20 C. [e] Calculated from the $kq\tau$ values in DMF using the observed luminescence lifetimes of fac-Re(bpy)$(CO)_3$Br (49 ns) and $Ru(bpy)_3^{2+}$ (928 ns).

to give 1 only in poor yields along with substantial amounts of untractable materials, while little isomerization of 1 to either 2 or 3 ocurred at 60 °C and even at 100 °C being accompanied by substantial consumption of 1, as shown in TableII. This means that the isomerization of 1 and 2 is only a negligible or minor pathway in the ground-state reactions. On the other hand, direct photoexcitation of 2 in DMF at 436 nm resulted in the isomerization to 1 along with very minor formation of 3 (Fig. 2), while 1 was found to be quite stable under the irradiation at 436 nm.

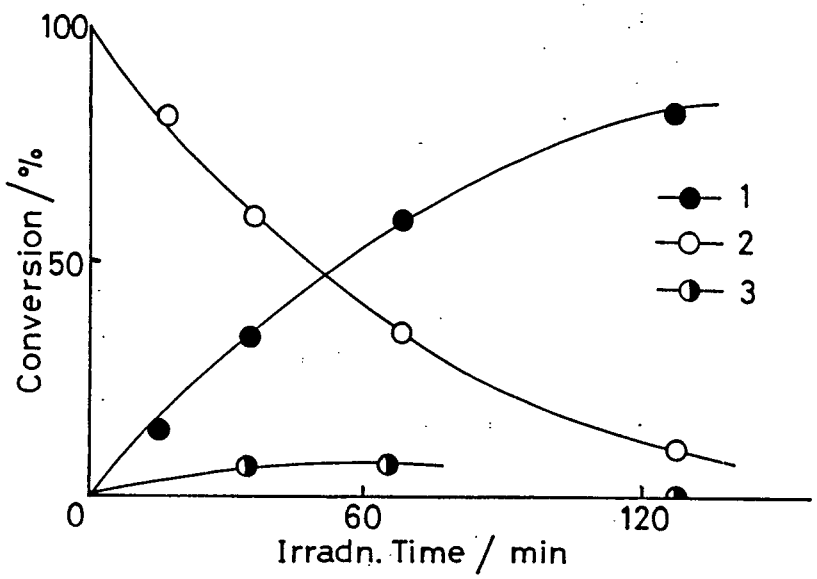

Figure 2. Time-Conversion plots for the direct photolytic isomerization of 1 at 436 nm; [1] = 2.5 mM.

In the excited state(s), 2 might cross to a reactive state or might give reactive intermediates while physical and chemical decays to the original ground state should predominantly occur with 1.

Table II. Isomerizations of 1 and 2 by Direct Photolysis and Thermal Activation[a]

Starting Materials	Reaction[b] Conditions	Reaction Time/min	Yields[c]/% 1	2	3
1	Photolysis	100	95	trace	0
2	Photolysis	130	73	11	trace
1	60 °C	960	94	trace	trace
1	100 °C	300	56	trace	trace
2	60 °C	960	2	78	1
2	100 °C	300	14	2	1

[a] For deaerated DMF solutions containing 1 or 2 (2.5 mM). [b] "Photolysis" means the reactions by direct photoexcitation at 436 nm, whereas the temperatures indicate the reaction temperatures for the thermal reactions in the dark. [c] Based on the 1 or 2 used.

For mechanistic elucidation, it shoud be noted that either chemical or electrochemical one-electron reduction of BNA^+ affords a mixture of 1, 2, and 3 in comparable amounts along with the other minor isomers in ratios depending on reaction conditions.[2] We also observed that a 2:2:1 mixture of 1, 2, and 3 is quantitatively formed by the photosensitized one-electron reduction of BNA^+ with triethylamine described in chapter 6. It is therefore conceivable that the formation of mixtures of 1, 2, and 3 should arise as the consequences of kinetic-controlled dimerization of the 1-benzylazacyclohexadienyl radicals ($BNA^{\cdot}$), since $BNA^{\cdot}$ is certainly a common intermediate in the chemical, electrochemical, and photochemical one-electron reductions of BNA^+.

These arguments strongly suggest that the photosensitized isomerizations of 1 and 2 involve BNA$^{\cdot}$ as a key intermediate. In this regard, it should be noted that the luminescence of fac-Re(bpy)$(CO)_3$Br or $Ru(bpy)_3^{2+}$ is efficiently quenched by 1 and 2 at the rate constants listed in Table I. In chapter 1, the author demonstrated that the luminescence of $Ru(bpy)_3^{2+}$ is quenched by BNAH at 2.0×10^8 M^{-1} s^{-1} in DMF by way of electron transfer from the quencher to the ruthenium(II) complex. Therefore, it is resonable to assume that electron transfer from 1 and 2 to the luminescent excited-state sensitizers occurs to initiate the isomerizations, since 1 and 2 have the dihydronicotinamide chromophores. The dimeric structures of 1 and 2 imply that these compounds should be stronger electron donors compared with BNAH, a presumption being in accord with the greater quenching rate constants for 1 and 2. Furthermore, the observation that the luminescence quenching is more efficient for fac-Re(bpy)$(CO)_3$Br than for $Ru(bpy)_3^{2+}$ can be reasonably understood according to the electron-transfer mechanism, since the excited-state reduction potential of fac-Re(bpy)$(CO)_3$Br is more positive by ca. 0.24 eV than that of $Ru(bpy)_3^{2+}$.[5,6] An alternative mechanism involving triplet-energy transfer from the sensitizers to 1 and 2 is unlikely to operate in the photosensitized isomerizations, since such organic triplet photosensitizers as coronene and chrysene were found to be totally ineffective.

According to the above discussion, the author proposes a possible mechanism for the photosensitized isomerizations in Eqs. 1-5. The key mechanistic sequence is the fragmentation of $BNA_2^{+\cdot}$ ($1^{+\cdot}$ and $2^{+\cdot}$) to BNA$^{\cdot}$ and BNA^+ (Eq. 3) followed by back electron transfer from $S^{-\cdot}$ (fac-

$Re(bpy)(CO)_3Br^{-\cdot}$ or $Ru(bpy)_3^{+}$) to BNA^+ to generate $BNA^\cdot$ (Eq. 4). It can be predicted that electron transfer from $S^{-\cdot}$ to BNA^+ (Eq. 4) rapidly occurs since the reduction potentials of fac-$Re(bpy)(CO)_3Br$ (-1.35 V vs. SCE in acetonitrile)[7] and $Ru(bpy)_3^{2+}$ (-1.36 V)[8] are substantially more negative than that of BNA^+ (ca. -1.0 V).[9] The final products are thus formed by free-radical coupling of $BNA^\cdot$ (Eq. 5). Since material balances are excellent in the photosensitized isomerizations, the fragmentation of $BNA_2^{+\cdot}$ (Eq. 3) appears to be efficient, thus predominating over Eq. 2.

$$S + BNA_2 \xrightarrow{h\nu} S^{-\cdot} + BNA_2^{+\cdot} \quad (1)$$

$$BNA_2^{+\cdot} \longrightarrow \text{Others} \quad (2)$$

$$BNA_2^{+\cdot} \longrightarrow BNA^+ + BNA^\cdot \quad (3)$$

$$S^{-\cdot} + BNA^+ \longrightarrow S + BNA^\cdot \quad (4)$$

$$2BNA^\cdot \longrightarrow 1 + 2 + 3 \quad (5)$$

(S = fac-$Re(bpy)(CO)_3Br$ or $Ru(bpy)_3^{2+}$; BNA_2 = 1-3)

On the other hand, the participation of $BNA^\cdot$ appears to be negligible or minor in the isomerizations of ground-state and excited-state BNA_2, since only the one-way isomerization from 2 to 1 can occur. Furthermore, the free-radical mechanism disagrees with the negligible formation of 3 from 2 upon either thermal activation or direct photoexcitation, since the isomerization of 2 to 3 should comparably occur, at least at an early stage of the reactions, by this mechanism. Presumably, the photoisomerization of 2 might mainly proceed via 1,3-sigmatropic migration of the 1,4-dihydropyridinyl moiety from the 6' position to the 4'

position of the 1,6-dihydropyridine ring, which is an orbital-symmetry-allowed process in the excited state (Scheme 2).[10] The reverse sigmatropic migration (i.e. 1 to 2) would be thermodynamically unfavorable. According to

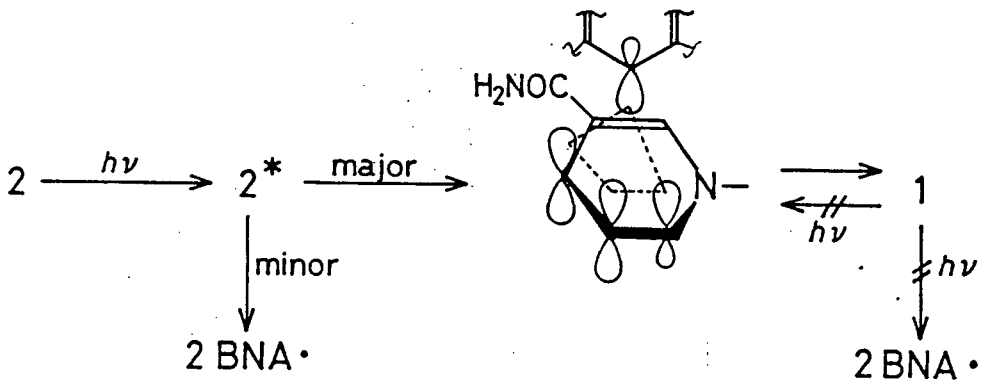

Scheme 2

this mechanism, it can be reasonably understood that the thermal isomerization of 2 occurs only in poor yields, since a suprafacial 1,3-sigmatropic rearrangement is forbidden in the ground state.

5-3 EXPERIMENTAL SECTION

Materials. The sensitizers, fac-$Re(bpy)(CO)_3Br$[11] and $Ru(bpy)_3Cl_2 \cdot 6H_2O$,[12] were prepared and purified according to the literature methods. The preparation and isolation of 1, 2, and 3 was carried out according to the Ohnishi's method[2] utilizing the reduction of 1-benzylnicotinamide chloride with activated zinc powder in the presence of copper(II) sulfate. The isolated tetrahydrodipyridines,

particularly 2 and 3, were carefully recrystallized from deaerated DMF-H_2O solution below room temperature in order to avoid the contamination of untractable materials due to thermal decomposition and oxidation. The ^1H-NMR spectra of the isolated samples were essentially identical with the published data.[2]

Analytical Methods. Both the disappearance and the formation of **1**, **2**, and **3** were followed by HPLC, which was carried out on a Chemicosorb 7-ODS-H column with a Yanaco M-315 spectromonitor working at 355 nm. The mobile phase was a 6:4 (v/v) mixture of methanol and an NaOH-KH_2PO_4 buffer solution (pH 7) at a flow rate of 0.8 mL min^{-1}. A Hitachi 850 spectrofluorometer was used for luminescence-quenching experiments; the ruthenium complex (0.25 mM) in DMF was excited at 550 nm and intensities of the luminescence were monitored at 610 nm, whereas the luminescence of the rhenium complex (0.75 mM) excited at 420 nm was monitored at 600 nm.

Photoreactions. Deaerated DMF solutions of **1** or **2** (2.5 mM) in the presence or absence of the sensitizers (0.8 mM) were irradiated under cooling with water (20 ± 2 °C), and the progress of the reactions was followed by HPLC. It was confirmed that no reaction of **1** and **2** occurred in the dark under the conditions. The $Ru(bpy)_3^{2+}$-photosensitized reactions were run by the irradiation with a tungsten-halogen lump (300 W) using a 1-cm pathlength filter solution of K_2CrO_4 (20 g mL^{-1}), $NaNO_3$ (200 g mL^{-1}), and NaOH (6.7 g mL^{-1}) which cuts off the light shorter than 470 nm as described in chapter 1. In both the fac-$Re(bpy)(CO)_3Br$-photosensitized runs and the direct photolyses, an Eikosha high-

pressure mercury arc (300 W) was used; the 436-nm resonance line was isolated by the passage through a 1-cm pathlength solution of $CuSO_4$ in 28% ammonium hydroxide.[13] In the fac-$Re(bpy)(CO)_3Br$-photosensitized reactions, contributions of reactions due to direct light absorption of the reactants are negligible, since the optical density of the sensitizer at 436 nm is 7-8 times greater than that of each reactant and since the photosensitized reactions are much more efficient than the direct photolyses.

Thermal Reactions. Deaerated DMF solutions of **1** or **2** (2.5 mM) were heated at 60 ± 0.5 °C or at 100 ± 0.5 °C in a dark room. The progress of the reactions was followed by HPLC. All the procedures were done with care in order to avoid exposure of the reactant solutions to scattering light.

5-4 REFERENCES

[1] Bruice, T. C. "Progress in Bioorganic Chemistry" Vol. IV, Kaiser, F. T.; Kendy, F. J., Eds.; Wiley: New york, 1976;

[2] Ohnishi, Y; Kitami, M. Bull. Chem. Soc. Jpn. **1979**, 52, 2674. [3] Schmakel, C. O.; Sonthanan, K. S. V. Elving, P. J. J. Am. Chem. Soc. **1975**, 97, 3083. Kano, K.; Matsuo, T. Bull. Chem. Soc. Jpn. **1976**, 49, 3269. Nezu, H.; Kaneko, N.; Wakabayashi, S. Denki Kagaku, **1979**, 47, 559. Jensen, M. A.; Elving, P. J. Biochem. Biophys. Acta, **1984**, 764, 310.
[4] McNamara, F. T.; Nieft, J. W.; Ambrose, J. F.; Huyser, E. S. J. Org. Chem. **1977**, 42, 988.

[5] Luong, J. C.; Nadjo, L.; Wrighton, M. S. J. Am. Chem. Soc. **1978**, 100, 5790.

[6] Ballardini, R.; Varani, G.; Indelli, M. T.; Scandola, F.; Balzani, V. J. Am. Chem. Soc. **1978**, 100, 7219.

[7] Sullivan, B. P.; Bolinger, C. M.; Conrad, D.; Vining, W. J.; Meyer, T. J. J. Chem. Soc., Chem. Commun. **1985**, 1414.

[8] Bock, C. R.; Connor, J. A.; Gutierrez, A. R.; Meyer, T. J.; Whitten, D. G.; Sulliron, B. P.; Nagle, J. K. J. Am. Chem. Soc. **1979**, 101, 4815.

[9] Blaedel, W. J.; Haas, R. G. Anal. Chem. **1965**, 42, 918.

[10] Woodward R. B.; Hoffman, R. J. Am. Chem. Soc. **1965**, 87, 2511.

[11] Wrighton, M. S.; Morse, D. L. J. Am. Chem. Soc. **1974**, 96, 998.

[12] Broomhead, J. A.; Yang, C. G. Inorg. Synth. **1983**, 22, 127.

[13] Turro, N. J.; Engel, R. J. Am. Chem. Soc. **1969**, 91, 7113.

Chapter 6

PHOTOCHEMISTRY OF fac-Re(bpy)(CO)$_3$Br WITH TRIETHYLAMINE: PHOTOSENSITIZED REDUCTION OF 1-BENZYLNICOTINAMIDE AND PHOTOCHEMICAL ALKYLATION OF THE 2,2'-BIPYRIDINE LIGAND

6-1 INTRODUCTION

Since Lehn and co-workers reported that the visible-light irradiation of fac-Re(bpy)(CO)$_3$X (X = Br, Cl) in an aliphatic amine/dimethylformamide (DMF) solvent results in the chemoselective reduction of carbon dioxide to carbon monoide without the hydrogen evolution.[1] The rhenium complexes are photobleached during the photocatalytic reactions.[1,2] It was syggested that a rhenium hydride complex would be formed as a key intermediates after photochemical one-electron transfer from the amine to the rhenium complex,[1-3], though mechanistic details of the two-electron reduction process are still remained unknown.

If this is the case, NAD^+ and its model compounds can be reduced NADH and the corresponding dihydropyridines, respectively, upon photocatalysis by fac-Re(bpy)(CO_3X in amine-DMF solvent.[4,6,7] If the formtion of a hydride complex from fac-Re(bpy)(CO)$_3X^-$ is very slow or does not occur, the one-electron reduction of NAD^+ and the models should exclusively occur to give the half-reduced dimers (Scheme 1).[4-6]

This chapter describes that fac-Re(bpy)(CO)$_3$Br acts as a good one-electron photomediator from triethylamine (TEA) to 1-benzylnicotinamide (BNA^+), whereas photoalkylation of

2,2'-bipyridine ligand of the rhenium complex occurred by TEA in the absence of BNA^+.

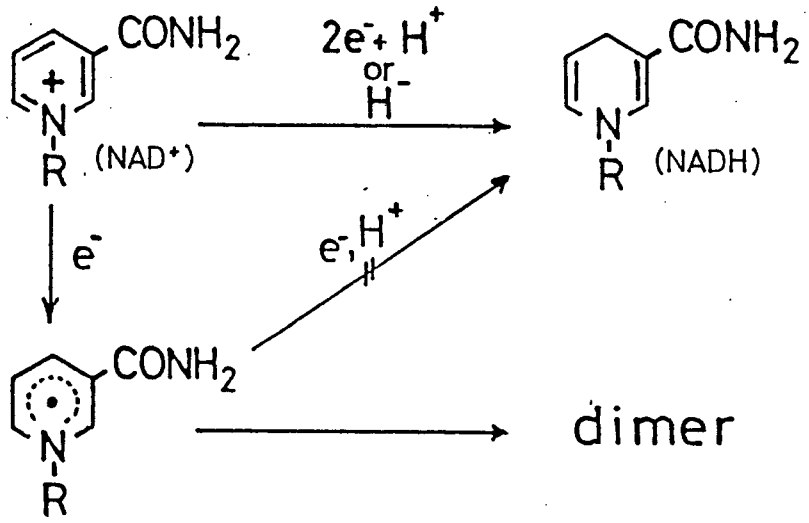

Scheme 1

6-2 RESULTS AND DISCUSSION

Reduction of BNA^+ Irradiation of a DMF solution of fac-Re(bpy)$(CO)_3$Br, BNA^+, and TEA at 436 nm gave the diastereomers of 1,1'4,6'-tetrahydro-4,6'-dimers (1, 2) and one of the diastereomeric 1,1',4,4'-tetrahydro-4,4'-tetrahydro-4,4'-dimers (3) in quantitative yield (Eq. 1 and Fig. 1), while BNAH was not detected at all. The quantum yield of this reaction was 0.13 at 436 nm.

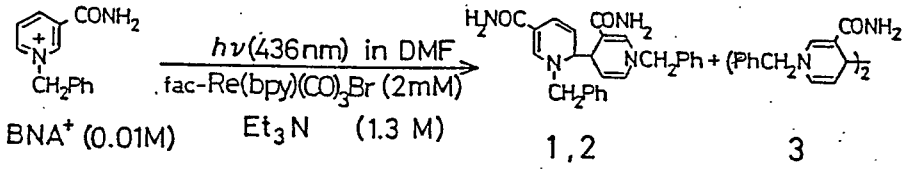

(1)

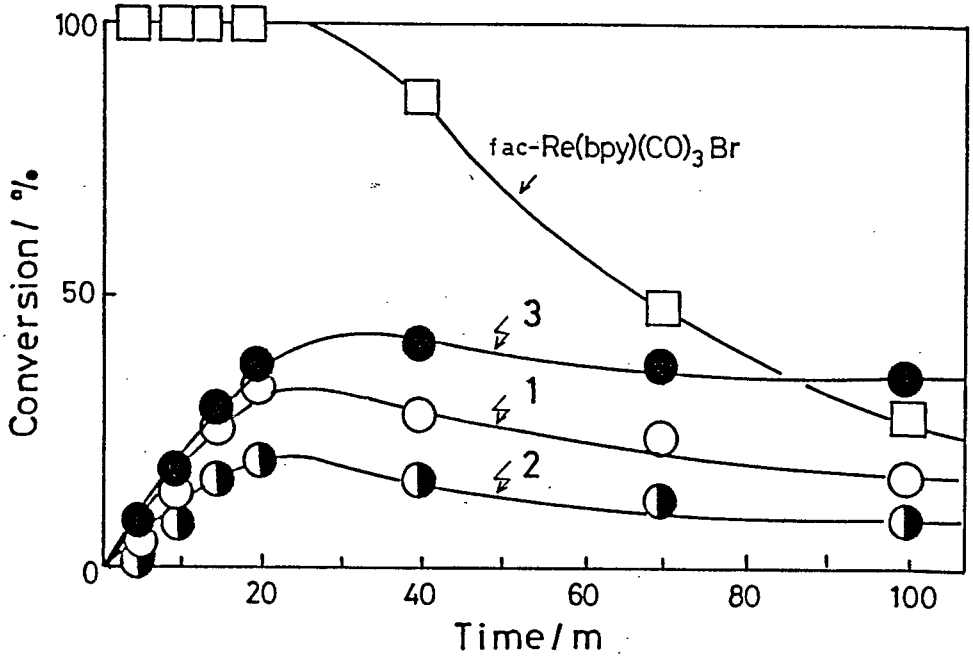

Figure 1. Time-Conversion plots for the formation of 1 (○), 2 (◑), and 3 (●) and the disappearance of fac-Re(bpy)$(CO)_3$Br (□) by irradiation of 3-mL DMF solutions of fac-Re(bpy)$(CO)_3$Br (1 mM), BNA^+ (10 mM), and TEA (1.4 M) at 436 nm.

It is therefore indicated that BNA^+ efficiently receives an electron from fac-Re(bpy)$(CO)_3Br^-$ generated by photoelectron

transfer between the rhenium complex and TEA, while the formaton of a hydride complex from fac-Re(bpy)$(CO)_3Br^-$ does not occur or should be much slower than electron transfer from fac-Re(bpy)$(CO_3Br^-$ to BNA^+.

The electron-transfer sequence for the one-electron reduction of BNA^+ (Scheme 2) is supported by the following

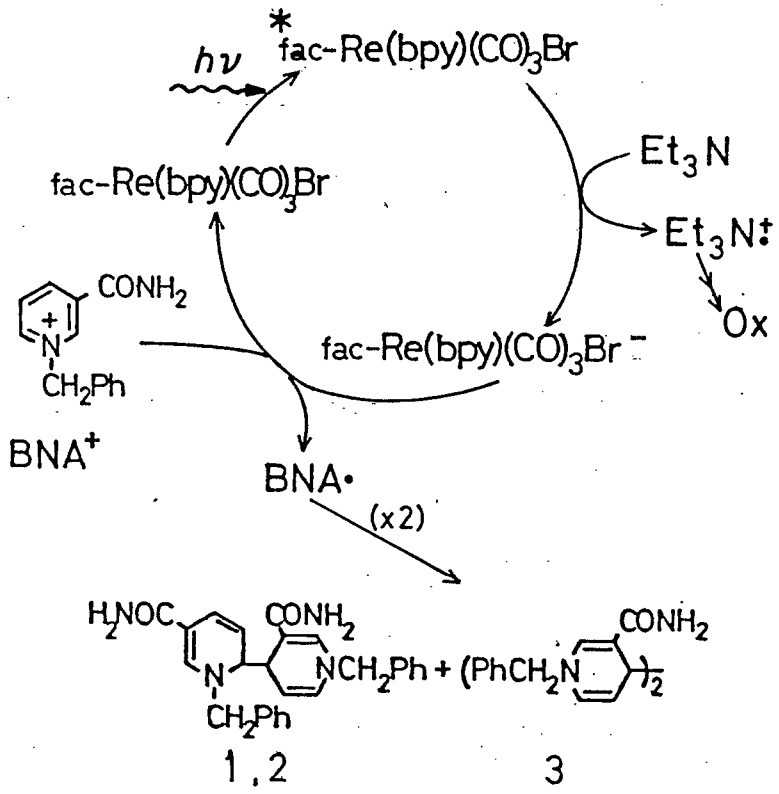

Scheme 2

observations. Firstly, the luminescence of fac-Re(bpy)$(CO)_3Br$ was quenched by TEA but not by BNA^+ as shown in Table I; This process is calcurated to be exergoniv by ∿ 0.2 eV.[8] Secondly, the calculated free-energy change associated with electron transfer from fac-Re(bpy)$(CO)_3Br^-$

to BNA^+ is ∿ - 0.3 eV, a value significantly exergonic for the rapid occurrence of this electron-transfer pathway. As a result, BNA· is generated to undergo the exclusive dimerization giving the dimers in a kinetic-controlled ratio.[8]

Table I. Rate Constants for Quenching of fac-Re(bpy)$(CO)_3$Br Luminescence[a]

Quencher	$k_q\tau$[b]/M^{-1}	k_q/M^{-1} s^{-1}
TEA[c]	4	8.2×10^7
$BNAClO_4$	0.2	4.1×10^6
$(n\text{-}Bu)_4NBr$	59	1.2×10^9
$(n\text{-}Bu)_4NClO_4$	∿ 0	$<< 10^6$

[a] Determined by Stern-Volmer plots of the luminescence quenching for deaerated solutions by 375-nm excitation. [b] Observed lifetime of the fac-Re(bpy)$(CO)_3$Br luminescence, τ = 49 ns. [c] Triethylamine.

Alkylation of the bpy Ligand Although the rhenium complex is stable eithr the presence or absence of **both** TEA and BNA^+, a photobleaching of the complex occurred upon irradiation of a DMF solution in the presence TEA but in the absence of BNA^+ (Fig. 1). A major product (**4**) was isolated by column chromatography on basic alumina and purified by HPLC (Eq. 2 and Fig. 2).

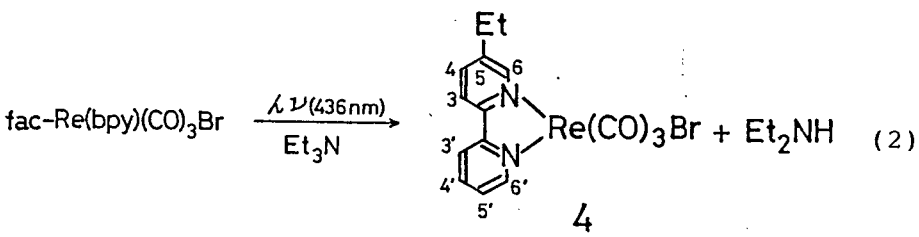

(2)

4

This product was identified as tricarbonylbromo(5-ethyl-2,2'-bipyridine)rhenium (I) by the spectroscopic properties (see Experimental Section). The quantum yield for the

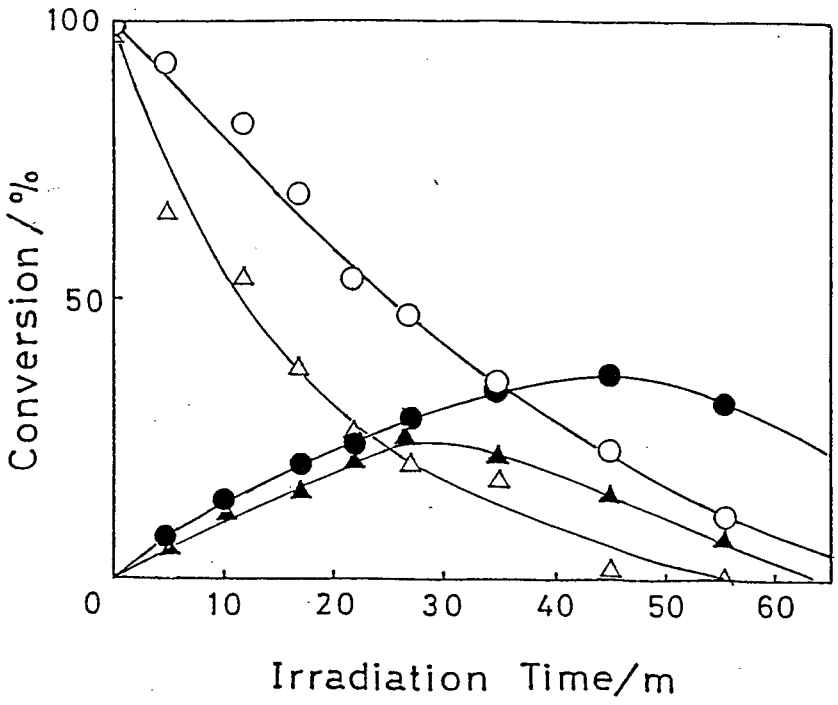

Figure 2. Time-Conversion plots for the formation of **4** (●, ▲) and the disappearance of fac-Re(bpy)$(CO)_3$Br (○, △) in the presence (●, ○) or the absence (▲, △) of Br^- by irradiation of 3-mL DMF solutions of fac-Re(bpy)$(CO)_3$Br (2 mM) and TEA (1.5 M) at 436 nm.

disappearance of the startin complex and for the formation of **4** were 0.07 and 0.03 respectively. Addition of Br^- (0.2 M) caused consumption of fac-Re(bpy)$(CO)_3$Br to retard and the yield of **4** to improve (Fig. 2).

Scheme 3 shows a possible mechanism for the photochemical ethylation of the bpy ligand, which has a precedent proposed by Ohashi and his coworkers for the photoelectron-transfer induced ethylation of p-dicyanobenzene by TEA.[12] The mechanistic sequence involves (1) the electron transfer

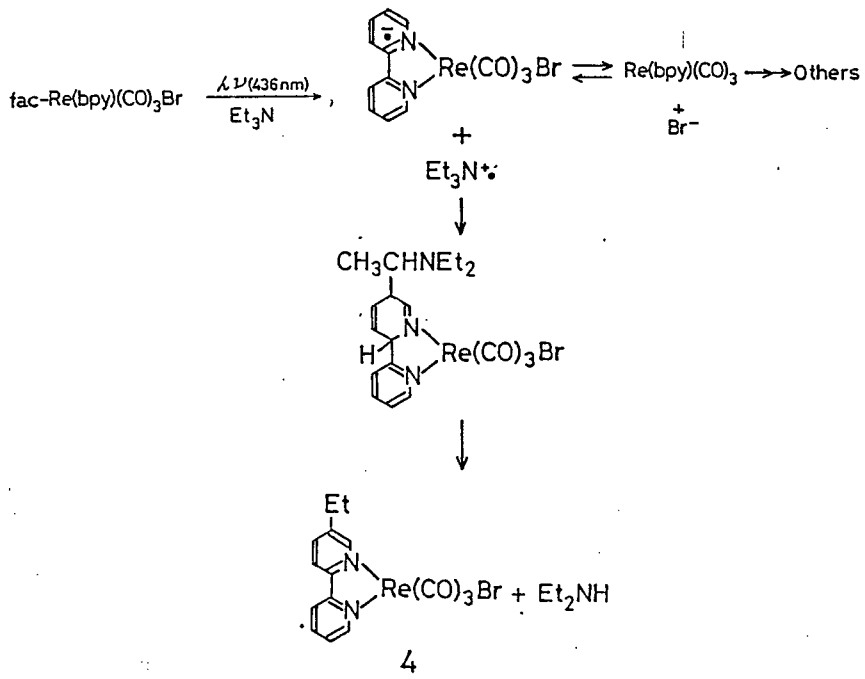

4

Scheme 3

from TEA to the luminescent excited state of fac-$Re(bpy)(CO)_3Br$ to generate $TEA^{+\cdot}$ and fac-$Re(bpy)(CO)_3Br^-$, (2) the abstraction of a protone from the α position to the N atom of $TEA^{+\cdot}$ to generate Et_2NCHCH_3, (3) a radical coupling of the aminoalkyl radical at 5-position of the bpy ligand of fac-$Re(bpy)(CO)_3Br^-$ to result in the α-amino-ethylation of the bpy ligand, and (4) the elimination of diethylamine from the intermediatory product to give **4** as the final product. The alkylation of the bpy ligand might be the consequence arising from the localization of an odd electron on the bpy ligand in fac-$Re(bpy)(CO)_3Br^-$.[13] According to this mechanism, the effects of Br^- can be

easily understood since the Br^- added can suppres the detachement of Br^- from fac-Re(bpy)$(CO)_3Br^-$, a competitive pathway leading to other reactions.[18]

Although it was reported that methyl radical is oxidatively coupled with 1,10-phenanthroline coordinating iron (III) ion,[14] the photochemical alkylation of the bpy ligand via reduction of the metal complex seems to bethe first example.

6-3 EXPERIMENTAL SECTION

Materials. The preparation and purification of BNACl[15] and fac-Re(bpy)$(CO)_3Br$[1,16] were carried out according to the literature methods. Addition of a slight excess of sodium perchlorate to an aqueous solution of BNACl yielded $BNAClO_4$ as a white crystalline precipitate, which was filtered, washed with cold water, and recrystallized from methanol. N,N-Dimethylformamide was distilled from molecular sieves 4A 1/16 (Nakarai) and triethylamine was distilled from potasium hydroxide.

Analytical Methods. The formation of **1**, **2**, **3**, and **4** and the disappearance of fac-Re(bpy)$(CO)_3Br$ was followed by HPLC. HPLC was carried out on a Chemicosorb 7-ODS-H column using a Toyosoda CCPD dual pump coupled with a Yanaco M-315 spectromonitor working at 355 nm for the analyses of **1**-**3** and 400 nm for teh rhenium complexes. A Hitachi 850 spectrofluorometer was used for luminescence-quenching experiments: a deaerated solution containing fac-Re(bpy)$(CO)_3Br$ was photoexcited at 375 nm and intensities of the luminescence

were monitored at 600 nm. Lifetime were determined with a Horiba NAES-1100 time-resolved spectrometer. A polarographic measurement was carried out for N_2-saturated DMF solution containing fac-Re(bpy)$(CO)_3$Br (1 mM) and Et_4NClO_4 (0.1 M) as the supporting electrolyte using an $Ag/AgNO_3$ reference electrode, a dropping mercury working electrode, and a Yanagimoto P-1100 potentiostat. ^1H NMR and ^{13}C NMR spectra were recorded on a JEOL JNM-GX 270FT NMR (270 MHz), IR spectram on a Hitachi 220-10 spectrometer, and UV and visible asorption spectram on a Hitachi RMU-6E.

Photosensitized Reduction of BNA$^+$. A 3-mL DMF solution of fac-Re(bpy)$(CO)_3$Br (1 mM), $BNAClO_4$ (10 mM), and TEA (1.4 M) was irradiated at 436 nm. The 436-nm light was obtained froma high-pressure mercury lamo by the passage through a saturated sodium nitrite solution (2-cm pathlength) and cupper(II) sulfate solution (40 g mL^{-1}) in 25% ammonium hydroxide (1-cm pathlength) hydroxide (436 nm). The progress of the reactions was followed by HPLC. The quantum yield was determined for a degassed DMF solution containing fac-Re(bpy)$(CO)_3$Br (2 mM), $BNAClO_4$ (0.01 M) and TEA (1.4 M) by trioxalateferrate(III) actinometry.[17] was isolated The intensity of the insident light at 436 nmwas determined to be 2.99×10^{16} photons s^{-1}. The total yields of 1-3 were plotted against time. The quantum yield was calculated from the slope of initial linear portion of the plot.

Photoreaction of fac-Re(bpy)$(CO)_3$Br with TEA. A 100-mL DMF solution containing fac-Re(bpy)$(CO)_3$Br (2 mM) and TEA (1.5 M) was irradiated at 436 nm under cooling with

water. The progress of the photoreaction was followed by HPLC. The quantum yields were determined for thoroughly degassed solution containing fac-Re(bpy)$(CO)_3$Br (2 mM) and TEA (1.5 M)

Isolation of 4. The irradiation was carried out for 100-mL solutions as described above until 50% fac-Re(bpy)$(CO)_3$Br had been consumed. After removal of the solvent in vacuo, the photolysate was chromatographed on 50 g of basic alumina (70 - 230 mesh, Merck Art 1076) by using dichioromethane as the eluent. The first fraction eluted was subjected to preparative HPLC to give **4** as yellow solids: IR (tetrahydrofurane) ν_{max} 2030, 1920, 1900 cm^{-1}; (CH_2Cl_2) λ_{max} 385 nm; ^{1}H NMR ($CDCl_3$) δ 1.37 (t, J = 7.63 Hz, 3H, CH_3), 2.83 (q, J = 7.63 Hz, 2H, CH_2), 7.51 (ddd, J = 1.2, 5.5, 7.9 Hz, 1H, H-5'), 7.89 (dd, J = 1.8, 8.6 Hz, 1H, H-4), 8.04 (dt, J = 1.8, 7.9 Hz, 1H, H-4'), 8.11(d, J = 8.5 Hz, 1H, H-3), 8.15 (d, J = 7.9 Hz, 1H, H-3'), 8.89 (d, J = 1.8 Hz, 1H, H-6), 9.06 (dd, J = ∿ 0.5, 5.5 Hz, 1H, H-6'); ^{13}C NMR ($CDCl_3$) δ 14.155, 25.954, 122.685, 122.792, 126.673, 138.190, 138.764, 144.011, 152.832, 153.209, 153.263, 155.886, 189.016, 196.886.

6-4 REFERENCES AND NOTS

[1] Hawecker, J.; Lehn, J. M.; Ziessel, R. J. Chem. Soc., Chem. Commun. **1983**, 536.

[2] Kutal, C.; Weber, M. A.; Ferraudi, G.; Geiger, D. Organometallics, **1985**, 4, 2161.

[3] Sullivan, B. P.; Bolinger, C. M.; Canrad, D.; Vining,

W. J.; Meyer, T. J. J. Chem. Soc., Chem. Commun. **1985**, 1414. O'Toole, T. R.; Marrgen, L. D.; Westmoreland, T. D.; Vining, W. J.; Murray, R. W.; Meyer, T. J. Ibid. **1985**, 1416.

[4] Kiwi, J. J. Photochem. **1981**, 16, 193.

[5] Wienkamp, R.; Steckhan, E. Angew. Chem., Int. Ed. Engl. **1983**, 22, 497.

[6] Kano, K.; Matsuo, T. Bull. Chem. Soc. Jpn. **1976**, 49, 3269.

[7] Einsner, U.; than, J. J. Chem. Rev. **1972**, 72, 1.

[8] Redox-potentials vs. $Ag/AgNo_3$ are as followes: *fac-$Re(bpy)(CO)_3Br/fac\text{-}Re(bpy)(CO)_3Br^-$ ∿ 0.75 V,[9] $TEA/TEA^{+\cdot}$ ∿ 0.52 V,[10] $fac\text{-}Re(bpy)(CO)_3Br/fac\text{-}Re(bpy)(CO)_3Br^-$ ∿ -1.75 V which was measured in this work. $BNA^+/BNA^\cdot$ ∿ -1.3 V.[11]

[9] Luong, J. C.; Nadjo, L.; Wrighton, M. S. J. Am. Chem. Soc. **1978**, 100, 5790.

[10] Evans, D. H. "Encyclopedia of Electrochemistry of the Elements"; Bard, A. J.; Lund, H., Eds.; Marcel Dekker Inc.: New York, 1978; Vol. XV, p 8.

[11] Blaedel, W. J.; Haas, R. G. Anal. Chem. **1970**, 42, 918.

[12] Ohashi, M; Miyake, K.; Tsujimoto, K. Bull. Chem. Soc. Jpn. **1980**, 53, 1683.

[13] Sullivan, B. P.; Meyer, T. J. J. Chem. Soc., Chem. Commun **1984**, 23, 2104.

[14] Rollick, K. L.; Kochi, J. K. J. Org. Chem. **1982**, 47, 435.

[15] Mauzarall, D.; Westheimer, F. H. J. Am. Chem. Soc. **1955**, 77, 2261.

[16] Wrighton, M.; Morse, D. L. J. Am. Chem. Soc. **1974**, 96, 998.

[17] Hatchard, C. G.; Parker, C. A. Proc. Roy. Soc. (London), **1956**, A235, 518.

[18] Although $(n\text{-}Bu)_4NBr$ was a good quencher of the luminescence of fac-$Re(bpy)(CO)_3Br$, no disappearance of fac-$Re(bpy)(CO)_3Br$ was detected by irradiation of DMF solution of fac-$Re(bpy)(CO)_3Br$ (1 mM) and $(n\text{-}Bu)_4NBr$ (0.2 M) in the absence of TEA.

Chapter 7

$Ru(bpy)_3^{2+}$-PHOTOINDUCED REDOX REACTION OF AN NAD+ MODEL IN THE PRESENCE OF TRIETHYLAMINE

7-1 INTRODUCTION

Tris(2,2'-bipyridine)ruthenium(II), $Ru(bpy)_3^{2+}$, has been widely used as a typical photosensitizer in studies aiming solar energy conversion,[1] and the photosensitizer generally involves electron transfer in the luminescent excited state (^{3}MLCT).[2] The capabilities of $Ru(bpy)_3^{2+}$ in photoredox reactions have been utilized to explore electron-transfer chemistry of the NAD^+/NADH couple and model systems.[3,4] sa shown in Chapters 1-3.

On the other hand, ligand substitution is now recognized to be a general event in the photochemistry of $Ru(bpy)_3^{2+}$ and related complexes.[5] Nevertheless, little is known on catalytic reactions involving photochemical ligand substitution of such complexes.[6] In this chapter, the author will shown that $Ru(bpy)_3^{2+}$ is susceptible to photochemical ligand substitution by triethylamine (TEA) which gives a new complex capable of catalysing a novel type of reaction of BNA^+.

7-2 RESULTS AND DISCUSSION

Irradiation of a methanolic solution of $Ru(bpy)_3^{2+}$, BNA^+, and TEA at > 470 nm gave BNAH and the isomeric half reduced dimers (**1**, **2**, and **3**) as shown in Figure 1. Interestingly, $Ru(bpy)_3^{2+}$ was photobleached during the photo-

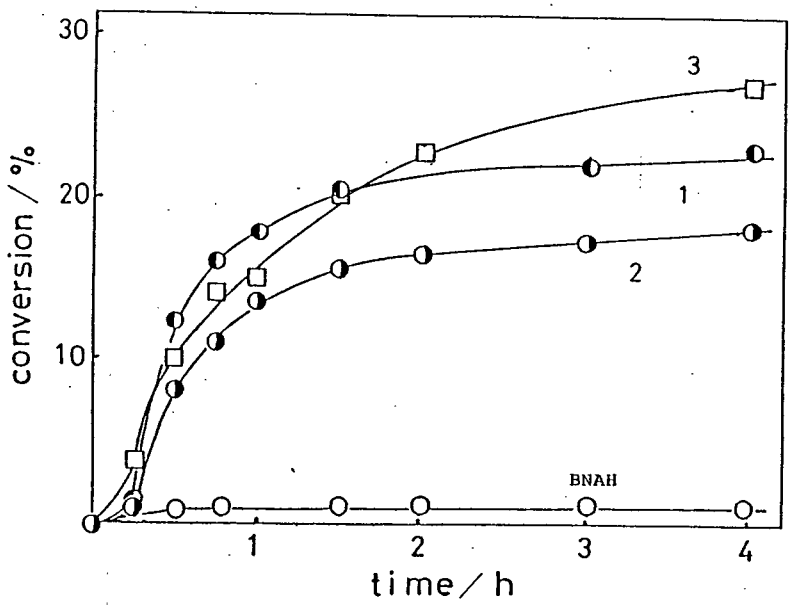

Figure 1. Time-conversion plots for the formation of BNAH and 1-3 by irradiation of a methanolic solution of $Ru(bpy)_3^{2+}$ (1 mM), BNA^+ (10 mM), and TEA (0.5 M) at > 470 nm using a tungsten-halogen lamp.

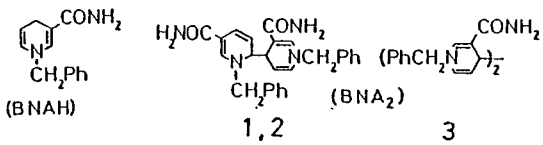

reaction. It was confilmed that the photobleaching is induced by TEA, but not at all by BNA^+, to give an air-stable initial product (P480) showing the absorption maximum at 480 nm and then an air-stable dead-end product (P520) showing the absorption maximum at 520 nm (Fig. 2). Therefore, a mechanism involving ligand substitution by TEA seems to be responsible for the photoreaction.

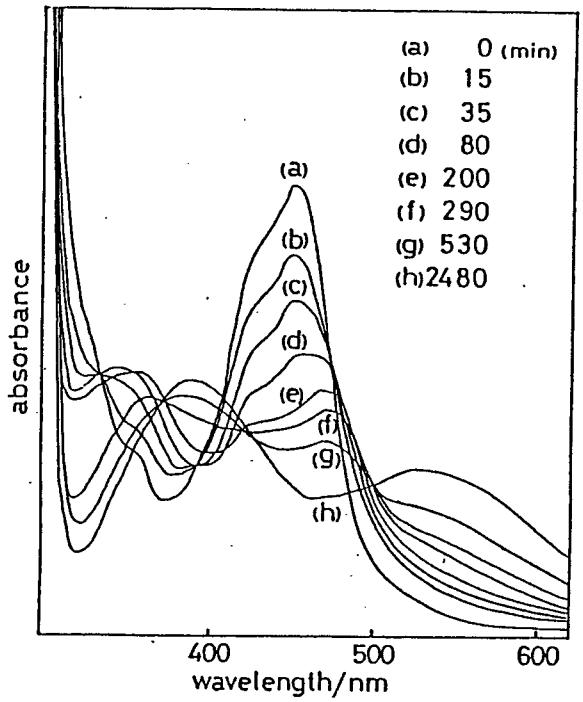

Figure 2. Absorption spectra of methanolic solution of $Ru(bpy)_3^{2+}$ (0.5 mM) taken at different times following irradiation at > 470 nm in the presence of TEA (0.5 M).

Although all atempts for the isolation of P480 and P520 failed because of extreme unstabilities in the absence of excess TEA, P520 can be assigned to $Ru(bpy)_2(TEA)_2^{2+}$ since the absorption spectrum (h) of P520 in Figure 2 is almost identical with that of solution obtained by either a thermal reaction of $Ru(bpy)_2Cl_2$ or a photoreaction of $Ru(bpy)_2(pyridine)_2^{2+}$ [7] with excess TEA in methanol. Since P520 is the photoproduct from P480, the latter should be $Ru(bpy)_2(py\text{-}py)(TEA)^{2+}$; py-py denotes the bpy acting as a

monodentate ligand. A support of this assignment is that $Ru(bpy)_3^{2+}$ was recovered in 70 - 80% yield upon removing TEA from a photobleached solution containing mostly P480. Furthermore, $Ru(bpy)_2[2\text{-}(2\text{-diethylaminoethyl})pyridine]^{2+}$ which was prepared as an electronic model of P480 reveals the absorption maximum at 485 nm. The spectral changes in Figre 2 can therefore be attributed to be the consequences of sequential ligand substitution by TEA (Eq. 1). Indeed, no photobleaching of $Ru(bpy)_3^{2+}$ was induced at all by tribenzylamine, a much bulkier amine than TEA.

$$Ru(bpy)_3^{2+} + TEA \xrightarrow{h\nu} \underset{P480}{Ru(bpy)_2(py\text{-}py)(TEA)^{2+}} \xrightarrow[+\ TEA\ -\ bpy]{h\nu} \underset{P520}{Ru(bpy)_2(TEA)_2^{2+}} \qquad (1)$$

It was found that a dark reaction of BNA^+ is catalysed by P480, but not at all by P520, in a photobleached methanolic solution, giving 1-benzyl-4-methoxy-1,4-dihydronicotinamide (BNAOMe) and BNAH (Fig. 3). The assignment of BNAOMe is based on their spectroscopic properties, which are comparable with those of 4-substituted 1-benzyl-1,4-dihydronicotinamide derivatives described in Chapters 1 and 2; the 1,4-dihydronicotinamide structure is strongly indicated by the multiplet at δ 3.8 characteristic of H-4 and by the ^{13}C signal at δ 81.5 (see Experimental Section). It should be noted that

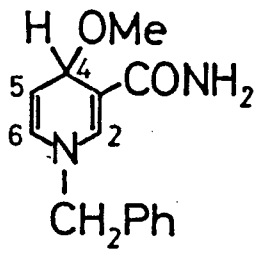

BNAOMe

BNAOMe was not formed either in the absence of P480 even after 40 h nor a direct reaction of BNA^+ with methoxide anion.

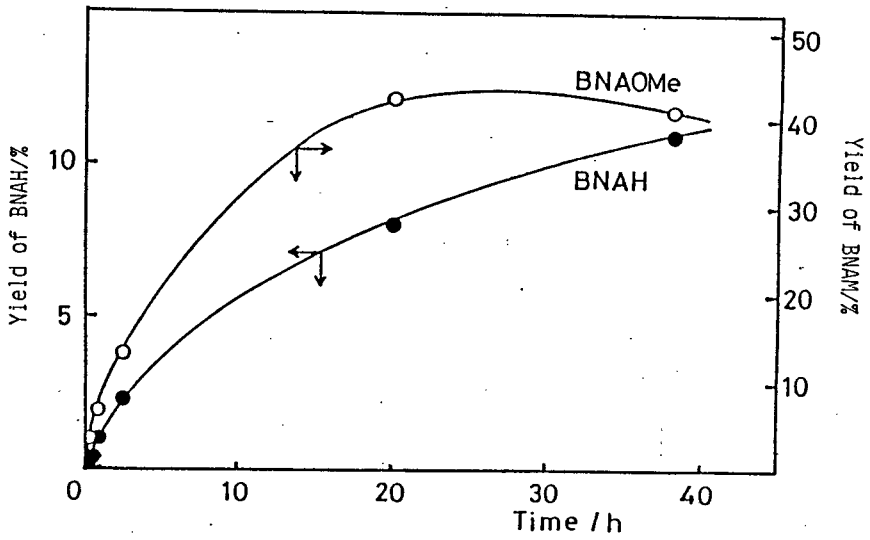

Figure 3. Time-conversion plots for the formation of BNAOMe (○) and BNAH (●) by a P480-catalyzed reaction of BNA^+ (10 mM) in a photobleached methanolic solution obtained from $Ru(bpy)_3^{2+}$ (1 mM) and TEA (0.5 M).

Reaction of 1-alkylpyridinium compounds with nucleophiles are of synthetic and biological significance,[8] giving adducts of dihydropyridine structures in many cases. However, reactions of 1-alkylnicotinamides, typical models of NAD^+, with alkoxide anions and alcohols reveal complex features to give no definite adducts but the corresponding dihydronicotinamides in low yields.[9-12] The mechanism of the P480 catalysis which is still unknown is not simple,

since the oxidation of TEA concurrently occurred to give diethylamine in comparable amounts. On the other hand, The BNAH formation should be the consequence of a secondary reaction, since an attempted reaction of BNA^+ with BNAOMe quantitatively gave BNAH, an interesting observation in relation with mechanisms of the reductions of NAD^+ models by alcohols or alkoxide anions.[10-12]

The formation of **1-3**
in the photoreaction certainly involves $Ru(bpy)_3^{2+}$-photo-mediated electron transfer from TEA and/or BNAOMe to BNA^+.[13] Consequently, the net photoreaction of the $Ru(bpy)_3^{2+}$-BNA^+-TEA system in methanol can be described by the sequential pathways of Eqs. 1 - 5.

$$BNA^+ + MeOH \xrightarrow[dark]{P480,\ TEA} BNAOMe + H^+ \qquad (2)$$

$$BNA^+ + BNAOMe \xrightarrow[dark]{} BNAH + Others \qquad (3)$$

$$Ru(bpy)_3^{2+} + D \xrightarrow{h\nu} Ru(bpy)_3^{+} + D^{+\cdot} (\longrightarrow Others) \qquad (4)$$

(D = BNAOME, TEA)

$$Ru(bpy)_3^{+} + BNA^+ \longrightarrow Ru(bpy)_3^{2+} + 1/2\ BNA_2 \quad (1 + 2 + 3) \qquad (5)$$

7-3 EXPERIMENTAL SECTION

Material. The preparation and purification of BNACl[14], and $Ru(bpy)_3Cl_2 \cdot 6H_2O$[15], $Ru(bpy)_2Cl_2 \cdot 2H_2O$[16], and 2-

(2-diethylaminoethyl)pyridine[17] were carried out according to the literature methods. Methanol was distilled from magnesium methoxide. Triethylamine was refluxed over anhydrous potassium hydroxide and then distilled before use.

Synthesis of $Ru(bpy)_2$[2-(2-diethylaminoethyl)-pyridine]PF_6. A 50-mL aqueous ethanol solution (1:1) containing cis-$Ru(bpy)_2Cl_2 \cdot 2H_2O$ (0.93 g, 2.1 mmol) and 2-(2-diethylaminoethyl)pyridine (0.60 g, 3.4 mmol) was refluxed for 5 h, condensed to 20 - 30 mL in vacuo, and then stored in a refregerator for 12 h. After filtration of precipitate, a 10-mL saturated aqueous solution of anmonium tetrafluorophosphate was added to the filtrate and then the solution was cooled on an ice bath for several hours. Dark red solids were precipitated, and filtered, and washed with water and then with diethylether to give the complex. ^1H NMR (CD_3COCD_3) δ 1.43 (t, J = 7.0 Hz, 9H, CH_3), 3.47 (q, J = 7.0 Hz, 6H, CH_2), 3.1 - 3.9 (m, 4H, CH_2CH_2), 6.63 - 9.30 (m, 20H).

Photoreaction of BNA^+. A 3-mL methanol solution containing BNACl (10 mM), $Ru(bpy)_3Cl_2 \cdot 6H_2O$ (1 mM), and TEA (0.5 M) was irradiated with a tungsten-halogen lamp using the solution filter (> 470 nm), described in chapter 1, under cooling with water . The progress of the reactions was followed by HPLC.

Photobleaching of $Ru(bpy)_3^{2+}$. A 3-mL methanolic solution containing $Ru(bpy)_3Cl_2 \cdot 6H_2O$ (0.5 mM) and TEA (0.5 M) was irradiated at > 470 nm under cooling with water. The progress of the reactions was followed by UV-visible

absorption spectra.

P480-Catalyzed Reaction of BNA^+ with Methanol. A 100- mL methanolic solution containing $Ru(bpy)_3Cl_2 \cdot 6H_2O$ (1 mM) nd TEA (0.5 M) was irradiated as described above. The complete formation of P480 required the irradiation for 10 - 15 h. To the P480 solution BNACl (1 mM) was added and then the mixture was stirred at room temperature for 30 - 60 min. The progress of the reactions was followed by HPLC. The solution was poured into 500-mL water and extracted with three 300-mL portions of dichloromethane. After evaporation, the residure was subjected to HPLC to give BNAOMe as a yellow oil: IR (film) ν_{max} 3300, 1680, 1640, 1070 cm^{-1}; UV (methanol) λ_{max} 364 nm; ^1H NMR ($CDCl_3$) δ 3.3 (s, 3H, OCH_3), 3.8 (m, 1H, H-4), 4.3 (s, 2H, NCH_2), 4.3 - 4.6 (br s, 2H, exchanged with D_2O, NH_2), 4.6 (dd, H-5), 5.8 (m, H-6), 7.1 - 7.5 (m, H-2 and C_6H_5); ^{13}C NMR ($CDCl_3$) δ 54.2, 57.6, 81.5, 100.1, 106.8, 127.3, 128.0, 128.9, 129.7, 137.2, 139.3, 167.2.

7-4 REFERENCES AND NOTES

[1] See, e. g., (a) "Photochemical Conversion and Storage of Solar Energy"; Connoly, J. S., Ed.; Academic Press: New York, 1981. (b) "Energy Resources through Photochemistry and Catalysis"; Grätzel, M., Ed.; Academic Press: New York, 1983.

[2] (a) Meyer, T. J. Acc. Chem. Res. **1978**, 11, 94. (b) Sutin, N. J. Photochem. **1979**, 10, 19. (c) Whitten, D. G. Acc. Chem. Res. **1980**, 13, 83. (d) Watts, R. J. J. Chem.

Educ. **1983**, 60, 834.

[3] Kiwi, J. J. Photochem. **1981**, 16, 193.

[4] Wienkanp, R.; Steckhan, E. Angew. Chem., Int. Ed. Engl. **1983**, 22, 497.

[5] (a) Gleria, M.; Minto, F.; Giannotti, C.; Bortolus, P. J. J. Chem. Soc., Chem. Commun. **1978**, 285. (b) Durham, B.; Walsh, J. L.; Carter, C. L.; Meyer, T. J. Inorg. Chem. **1980**, 19, 860. (c) Caspar, J. V.; Meyer, T. J. J. Am. Chem. Soc. **1983**, 105, 5583.

[6] (a) Choudhury, D.; Cole-Hamilton, D. J. J. Chem. Soc., Dalton Trans. **1982**, 1885. (b) Hawecker, J.; Lehn, J.-M.; Zeissel, R. J. Chem. Soc., Chem. Commun. **1985**, 56.

[7] Casper, J. V.; Meyer, T. J. Inorg. Chem. **1983**, 22, 2444.

[8] For reviews see; (a) Eismer, U.; Kuthan, J. Chem. Rev. **1972**, 72, 1. (b) Stout, D. A.; Meyers, A. I. Chem. Rev. **1982**, 82, 223.

[9] Anderson, Jr., A. G.; Berkelhammer, G. J. Org. Chem. **1958**, 23, 1109.

[10] Shirra, A.; Suckling, C. J. J. Chem. Soc., Perkin II **1977**, 759.

[11] Ohnishi, Y.; Kitami, M. Tetrahedron Lett. **1978**, 42, 4035.

[12] Ohno, A.; Ushida, S.; Oka, S. Bull. Chem. Soc. Jpn. **1983**, 56, 1822.

[13] BNAOMe efficientry quenched the luminescence of $Ru(bpy)_3^{2+}$. On the other hand, the author could not detect the luminescence quenching of $Ru(bpy)_3^{2+}$ by TEA even at 1.0 M nor by 0.1 M BNACl im methanol. However, irradiation to a solution containing $Ru(bpy)_3^{2+}$ and TEA gave $Ru(bpy)_3^{+}$, which was detected by a Union MCPD-200.

[14] Mauzarall, D.; Westheimer, F. M. J. Am. Chem. Soc. **1955**, 77, 2261.

[15] Broomhead, J. A.; Yaung, C. G. Inorg. Synth. **1983**, 22, 127.

[16] Sullivan, B. P.; Salmon, D. J.; Meyer, T. J. Inorg. Chem. **1978**, 17, 3334.

[17] Reich, H. E.; Levine, R. J. Am. Chem. Soc. **1974**, 96, 998.

SUMMARY

The results obtained from the present investigation are summarized as follows;

Chapter 1: It was found that reactions of 1-benzyl-1,4-dihydronicotinamide (BNAH) with dimethyl fumarate, dimethyl maleate, aryl-substituted enones, and derivatives of methyl cinnamate and cinnamonitrile were photosensitized by $Ru(bpy)_3^{2+}$. The reduction of carbon-carbon double bonds commonly requires the substitution of either an electron-withdrowing group or two phenyl groups at the α-carbon atom of the olefins. With enones which possess one aryl substituent with no extra electron-withdrowing group at the β position, the photosensitized reactions resulted in no two-electron reductions but gave 1:1 adducts along with half-reduced dimers of olefins and a half-oxidized dimer of BNAH. The observed results can be easily interpreted by assuming the intervention of BNA$^{\cdot}$ and half-reduced species of the olefins as key intermediates that are formed by mediated electron-proton transfer from BNAH to the olefins in which $Ru(bpy)_3^{2+}$ acts as a one-electron shuttle upon photoexcitation in the initial electron transfer. Whether BNA$^{\cdot}$ undergoes electron transfer to or a radical coupling reaction with half-reduced radicals of the olefins depend on steric and electronic properties of the half-reduced species of the olefins which should be affected by the substituents at the radical center. Mechanistic implications for thermal reactions of NADH models with olefins in the dark were briefly discussed on the basis of these observations.

Chapter 2: Photosensitized reactions of aromatic carbonyl compounds with BNAH by $Ru(bpy)_3^{2+}$ were investigated. The reduction to the corresponding alcohols

occurred with di(2-pyridyl) ketone in a quantitative yield and with methyl benzoylformate in a 18% yield. Noteworthy is the efficient formation of 1:1 adducts, a new class of 4-alkyl-1,4-dihydronicotinamides, in 55 - 85% isolated yields; in the case of methyl benzoylformate a single isomer of a condensed bicyclic imide was obtained whereas the other adducts were obtained as diastereomeric mixtures. In the case of trifluoroacetophenone, the diastereomeric 6-alkylated 1,6-dihydronicotinamides were formed as minor 1:1 adducts. The structure of each adduct determined by spectroscopic and X-ray crystallographic studies. The mechanism of the photosensitized reactions was discussed in terms of sequential indirect electron-proton transfer from BNAH to the carbonyl compounds followed by electron transfer or cross coupling between radical intermediates. On the other hand, thermal reactions of BNAH with the carbonyl compounds in the dark gave no adduct nor the half-oxidized dimers of BNAH but the alcohols. It is suggested that electron-transfer mechanisms are not responsible for the thermal reactions.

Chapter 3: Magnesium (II) ion catalyzes the photosensitized reduction of the carbon-carbon double bonds of dimethyl fumarate, derivatives of methyl cinnamate, and some other related olefins by BNAH. The metal ion forms a complex with BNAH in methanol as well as in 10:1 pyridine-methanol, leading to the retardation of electron transfer from BNAH to luminescent excited-state $Ru(bpy)_3^{2+}$. The net effects of the metal ion arise from the catalysis of both the first and second one-electron reduction processes.

Chapter 4: There were investigated photochemical behaviors of 4-alkylated 1-benzyl-1,4-dihydronicotinamides

($R^1R^2C(OH)$-BNA) (**a**: R^1 = Ph and R^2 = H; **b**: R^1 = Ph and R^2 = CF_3; **c**: R^1 = p-NC-C_6H_4 and R^2 = H). The direct photolysis of $R^1R^2C(OH)$-BNA gave R^1R^2CO and the dimers of the dihydronicotinamide fragment along with a minor amount of $[C_6H_5CH(OH)]_2$, being thus interpreted in terms of the homolysis between the $R^1R^2C(OH)$ and BNA moieties. In the $Ru(bpy)_3^{2+}$-photosensitized reactions, it is suggested that $[R^1R^2C(OH)\text{-BNA}]^{+\cdot}$ was generated as a key intermediate by electron transfer to excited $Ru(bpy)_3^{2+}$, undergoing a bond cleavage to give R^1R^2CO and the BNA$^{\cdot}$ dimers. In the case of **c**, however, $R^1R^2CH(OH)$ was formed, being attributed to a product from $[R^1R^2C(OH)\text{-BNA}]^{-\cdot}$ that formed by electron transfer from $Ru(bpy)_3^{+}$.

Chapter 5: The photosensitization by either fac-$Re(bpy)(CO_3)Br$ or $Ru(bpy)_3^{2+}$ resulted in the isomerization of the 1,1',4,4'-tetrahydro-4,4'-dimer of 1-benzylnicotinamide (4,4'-BNA_2) and the 1,1',4,6'-tetrahydro-4,6'-dimer (4,6'-BNA_2) to give a common mixture of 4,4'-BNA_2, 4,6'-BNA_2, and the diastereoisomer of 4,6'-BNA_2 in a 2:2:1 ratio at a photostationary state. The photosensitized isomerizations were discussed in terms of the following chemical sequences; (1) electon transfer from 4,4' and 4,6'-BNA_2 to the luminescent excited-state sensitizers, (2) bond cleavage of the cation radicals of 4,4' and 4,6'-BNA_2 to generate BNA$^{\cdot}$ and BNA^+, (3) back electron transfer from the one-electron reduced sensitizers to BNA^+, and (4) the free-radical dimerization of BNA$^{\cdot}$. On the other hand, either direct photoexcitation or thermal activation effected only the isomerization of 4,6'-BNA_2 to 4,4'-BNA_2 but not at all the retro isomerization, for which a 1,3-sigmatropic mechanism was suggested.

Chapter 6: fac-Re(bpy)$(CO)_3$Br photosensitizes reduction of 1-benzylnicotinamide (BNA^+) by triethylamine gave three diastereomeric half-reduced dimers of BNA^+. In the absence of BNA^+, photoalkylation of 2,2'-bipyridine ligand of the rhenium complex occurred by triethylamine.

Chapter 7 The photochemical coordination of a triethylamine molecule to the metal center of $Ru(bpy)_3^{2+}$ occures to generate a new complex capable of catalyzing a reaction of 1-benzylnicotinamide with methanol which gives a new compound, 1-benzyl-4-methoxy-1,4-dihydronicotinamide, as the primary product. This compound can reduce the nicotinamide to yield the 1,4-dihydronicotinamide in the dark.

ACKNOWLEDGEMENT

The author would like to express his sincere thanks to Professor Setsuo Takamuku and Associate Professor Shozo Yanagida for their kind guidance and helpful suggestions throughout this work.

The author is indebted to Dr. Chyongjin Pac for his invaluable assistance in accomplishing this work.

The author is also grateful to Professor Emeritus Hiroshi Sakurai for his warm-hearted encouragement.

Grateful acknowledgements are made to Mr. Mikio Ihama, Mr. Yoji Miyauchi, Mr. Yasunori Wada, Mr. Ken-Ichi Takada, and Mr. Ichiro Namura for their helpful collaboration in the course of experiments.

The author thanks Professor Kensuke Shima and Dr. Masahiko Yasuda at Miyazaki University for variable experiments about X-ray crystallographic analysis, Dr. Akito Ishida about CCPD measurements, and Dr. Shinobu Ito about FT-NMR measurements.

Further, much thanks is given to all members of Faculty of Chemical Process Engineering for their helpful assistance and friendship.

The author wishes to thank Professor Masaru Hojo, Associate Professor Ryo-Ichi Masuda, and Dr. Etsugi Okada at Kobe University, and Mr. Motofusa Taira who initiated the author into chemistry.

Finally, the author acknowledges heartwarming encouragement and assistance of his parents Takao and Kiyoko.